Natural Resources Canada / Ressources naturelles Canada

GEOLOGICAL SURVEY OF CANADA
OPEN FILE 8838

Understanding plateau and prairie landslides: annual report on landslide research in the Thompson River valley, British Columbia, and the Assiniboine River valley, Manitoba-Saskatchewan (2020-2021 to 2021-2022)

D. Huntley, D. Rotheram-Clarke, R. Cocking, J. Joseph, and P. Bobrowsky

2022

Canada

ISSN 2816-7155
ISBN 978-0-660-44150-4
Catalogue No. M183-2/8838E-PDF

GEOLOGICAL SURVEY OF CANADA
OPEN FILE 8838

Understanding plateau and prairie landslides: annual report on landslide research in the Thompson River valley, British Columbia, and the Assiniboine River valley, Manitoba-Saskatchewan (2020-2021 to 2021-2022)

D. Huntley[1], D. Rotheram-Clarke[1], R. Cocking[1], J. Joseph[1], and P. Bobrowsky[2]

[1]Geological Survey of Canada, 605 Robson Street, Vancouver, British Columbia
[2]Geological Survey of Canada, 9860 West Saanich Road, Sidney, British Columbia

2022

Permanent link: https://doi.org/10.4095/329205

This publication is available for free download through GEOSCAN (https://geoscan.nrcan.gc.ca).

Recommended citation

Huntley, D., Rotheram-Clarke, D., Cocking, R., Joseph, J., and Bobrowsky, P., 2022. Understanding plateau and prairie landslides: annual report on landslide research in the Thompson River valley, British Columbia, and the Assiniboine River valley, Manitoba-Saskatchewan (2020-2021 to 2021-2022); Geological Survey of Canada, Open File 8838, 73 p. https://doi.org/10.4095/329205

Publications in this series have not been edited; they are released as submitted by the author.

Table of Contents

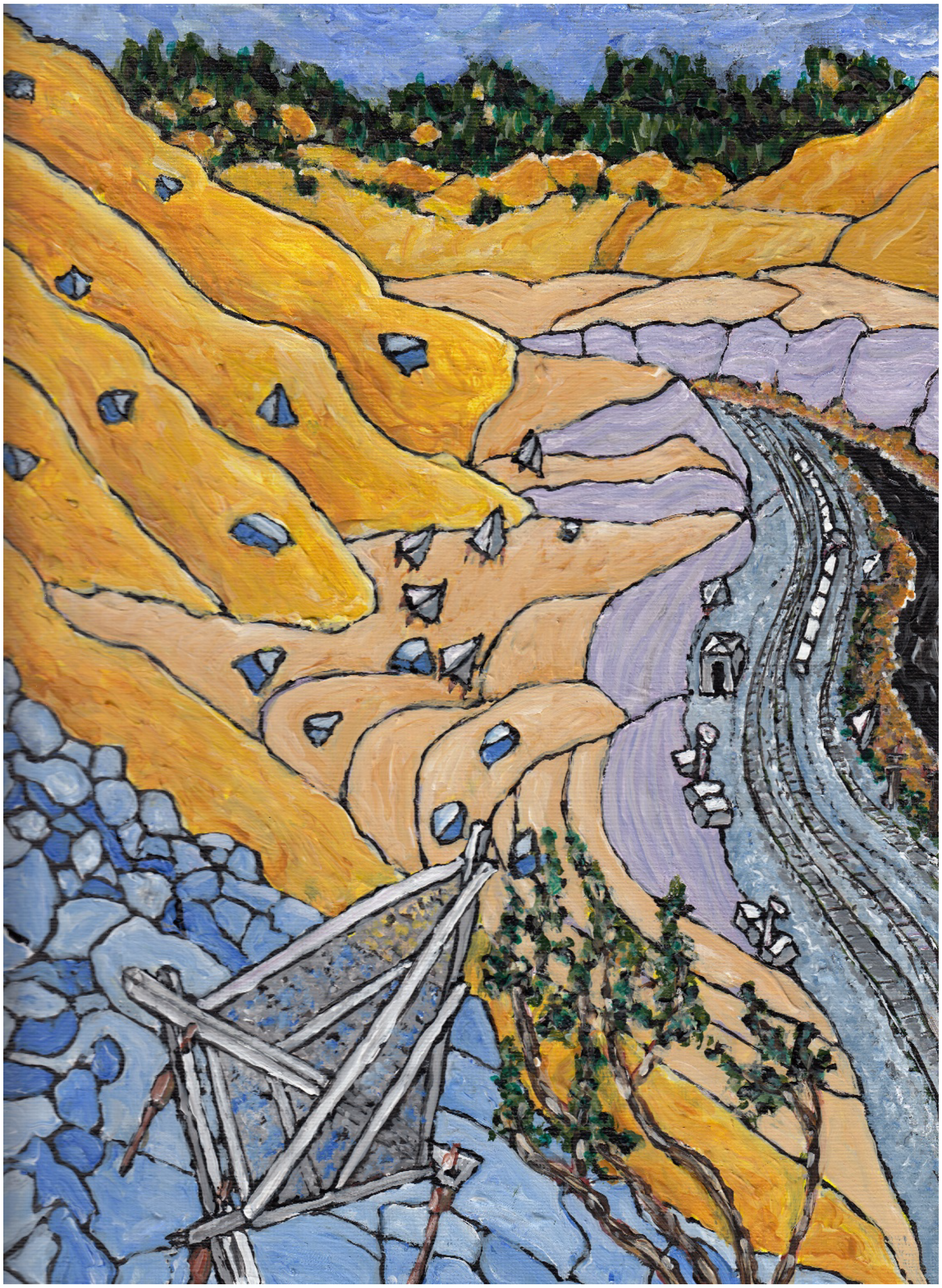

Corner Reflectorscape
Ripley Landslide, Thompson River valley, British Columbia
13 cm x 18 cm acrylic painting on cotton rag
Dr. David Huntley (Geological Survey of Canada)

Abstract
Open File 8838 is a publication of Interdepartmental Memorandum of Understanding (IMOU) 5170 between Natural Resources Canada (NRCAN), the Geological Survey of Canada (GSC), and Transport Canada Innovation Centre (TC-IC). IMOU 5107 aims to gain new insight into slow-moving landslides and the influence of climate changes through testing conventional and emerging monitoring technologies along strategically important sections of the national railway network in the Thompson River valley, British Columbia, and the Assiniboine River valley along the borders of Manitoba and Saskatchewan. The results of this research will be applicable to other sites in Canada, and elsewhere around the world where slow-moving landslides and climate change are adversely affecting critical socio-economic infrastructure.

Keywords
Geological Hazards, Climate Change, Landslide Monitoring, Railway Infrastructure, Geohazard Reduction, Thompson River, British Columbia, Assiniboine River, Manitoba-Saskatchewan

1. Introduction
Global socioeconomic recovery and rehabilitation will be strongly reliant upon transportation networks that are resilient to the adverse impacts of climate change and weather-driven geohazards (e.g., landslides, avalanches, floods and wildfires). For Canada, like many countries, national railway networks will be the dominant mode for transporting land-locked natural resources to, and from deep-water marine terminals, and commuters and tourists to, and from urban centres. Service efficiency and capacity are vital for a resilient national railway system transporting Canadian grain, coal, oil, potash and other natural resources to the global market. Railway transportation networks require sustainable, cost-effective management of service operations to meet future socioeconomic needs and ensure protection of the natural environment. Where transportation corridors traverse unstable terrain, critical rail infrastructure and safe operations are jeopardized, and presents potential local and national economic, social, and environmental challenges. The economic importance of national railway corridors, along with the need to understand and manage the safety issues related to landslides make on-site investigations a strategic priority for governments, the rail industry, and academia (Bobrowsky 2013; Bobrowsky 2016). Monitoring unstable slopes and vulnerable infrastructure is a cost-effective hazard management practice that also provides important geoscience information to help develop appropriate mitigation and adaptation measures (Bobrowsky 2018; Bobrowsky et al. 2018).

Sections of the Canadian National (CN) and Canadian Pacific (CP) railway corridors runs through the Thompson River valley between Ashcroft and Spences Bridge in southern British Columbia; and the Assiniboine and Qu'Appelle river valleys, southeastern Saskatchewan and southwestern Manitoba that have slopes particularly vulnerable to landslides (**Figure 1**). In both study areas, sections of rail track and other infrastructure traverse active landslides or active flood plains where gradual, continuous slope movements (and occasional rapid failures) affect safe and reliable operation. Historically, landslides and other geohazards (e.g., rock falls, debris flows, avalanches, floods, and wildfires) have resulted in train derailments and service disruptions in these areas. The economic importance of the Thompson, Assiniboine and Qu'Appelle transportation corridors make them strategic priorities for federal and provincial governments, as well as CN and CP, to understand and manage safety related to the landslides that threaten these routes.

Figure 1 The study areas. **a**) Rail transportation corridors in southwestern British Columbia with location of the Thompson River valley area of interest: **CN** - Canadian National Railways; **CP** - Canadian Pacific Railways; ***FR*** – Fraser River; ***TR*** - Thompson River. **b**) Landslides of the Thompson River valley, with location of Ashcroft, the railway transportation corridor and Ripley Landslide test site. **c**) Rail transportation corridors in southwestern Saskatchewan and southeastern Manitoba, showing railway routes and areas of interest to CN and CP; ***AR*** – Assiniboine River; ***QR*** – Qu'Appelle River (source DEM: SRTM). **d**) Worldview image for CN area of interest, Rivers Subdivision, Mile 184.4; A-A' geological cross-section, see **Figure 8** (base map source: arcgis.com). **e**) Worldview image for CP area of interest, Bredenbury Subdivision, Miles 82.6 and 86.5; B-B' and C-C' geological cross-sections (base map source: arcgis.com).

2. Research Objectives and Methods of Enquiry

Natural Resources Canada (NRCAN) through the Geological Survey of Canada (GSC), along with international and national partners, has pioneered innovative research and monitoring of landslides in the Thompson River valley since 2013. The following section summarizes the objectives, methods, and research activities carried out between 2020 and 2021 pertaining to this research program. (**Figure 2**).

2.1 Extreme weather, climate monitoring and geohazards

Over the next 50 years, measurable changes in temperature, precipitation, and other climatic factors are expected to display spatial variations across Canada (Weaver 2004; IPCC 2014). Depending on location, climate change will trigger positive or negative feedback in: groundwater recharge, river flow, flooding and stream erosion, the extent and duration of wildfires, the magnitude and frequency of landslides, the distribution of permafrost, and the distribution of wildlife and vegetation (Bruce and Cohen 2004; Smith and Burgess 2011; Weaver 2004; IPCC 2014). Increases in magnitude and frequency of landslides and other geohazards are expected as a response to rising precipitation amounts (as rain and snow), greater seasonal ranges in temperature and more extensive wildfires (cf. Heginbottom et al. 1995; Evans and Clague 1997; Geertsema et al. 2006; Couture and Evans 2006; Wang and Lesage 2007). Increased erosion rates of exposed sediments is likely if wind strength and duration increases due to changes in storm systems, air pressure gradients, loss of vegetation and wildfires (cf. Wolfe 1997; Wolfe 2001). Increasing precipitation, duration of rainfall, loss of vegetation, and wildfires will lead to an increase in magnitude and frequency of gully erosion on valley sidewalls (cf. Sauchyn and Nelson 1999; Valentin et al. 2005). In addition, rising flood magnitudes and frequency of events will contribute to increased erosion and deposition in rivers and streams adjacent to active landslides (cf. Knox 2000; Chen et al. 2006; St. George 2007; Chen and Grasby 2009).

Railway infrastructure and operations are expected to face unique challenges in design, monitoring, adaptation, mitigation, reclamation and restoration in a scenario of future extreme weather events and climate change. An understanding of the geographic distribution and temporal range of earth materials and geological hazards, and their potential responses to climate change is essential for a resilient and accessible transportation network, but also to protect the natural environment, local communities, land-use practices, and the national economy.

2.2 IMOU research objectives

IMOU-5170 aims to gain a better understanding of how extreme weather events and climate change influence landslide activity in the Thompson River valley, British Columbia, and the Assiniboine River valley, Saskatchewan-Manitoba. This fundamental geoscience information will contribute to more robust landslide hazard management strategies to maintain the resilience and accessibility of critical transportation infrastructure along strategically important sections of the national railway network, while also protecting the natural environment, community stakeholders, and Canadian economy.

Landslide monitoring technologies have been operational in the Thompson River Valley from 2013-2020, and have been installed at new sites in the Assiniboine River. The three primary research and development objectives include: 1) Better understand controls on landslide movement, and in particular, the impacts of extreme weather events and climate change. 2) Compare, evaluate, and identify the monitoring technologies which provide the most useful information on why, how, and when landslides move. 3) Help identify reliable real-time monitoring solutions for critical railway infrastructure (e.g., ballast, tracks, retaining walls, tunnels and bridges) able to withstand the harsh environmental conditions of Canada.

Figure 2 Contributions and interactions of key stakeholders in the Railway Ground Hazard Research Program, with funding structure.

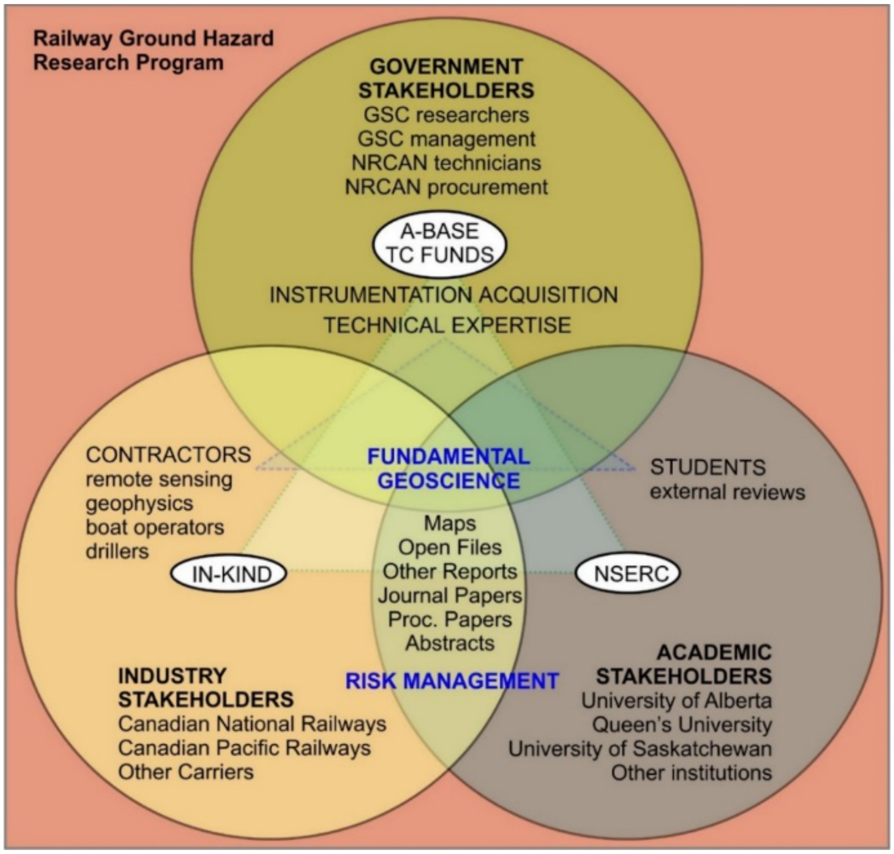

2.3 IMOU research methods overview

To better understand the impact of extreme weather and climate change on slope instability requires geospatial and temporal datasets that comprehensively describe landslide form, mechanism, and movement (**Table 1**; **Table 2**; **Table 3**; **Table 4**). We combine information from geological mapping (Huntley and Bobrowsky 2014; Huntley et al. 2020a) and geophysical surveys (e.g., Holmes et al. 2018; Huntley et al. 2018a; Huntley et al. 2019a, b; Holmes et al. 2020) with change-detection monitoring using remote sensing, global positioning, and borehole technologies (e.g., Macciotta et al. 2014; Hendry et al. 2015; Schafer et al. 2015; Journault et al. 2018). *Geohazard Mapping* captures information on landslide form, other geohazards and areas of concern, and conditions on adjacent stable slopes and water bodies. *Change Detection Monitoring* captures spatial and temporal variability in landslide movements using emerging airborne and spaceborne platforms, ground based RTK-GNSS systems, and climate variables. Geohazard mapping and change detection monitoring will be used to identify terrain units and slopes susceptible to landslides, floods, and other geohazards triggered by extreme weather events, changing climate (past, current and future), and additional factors (e.g., slope engineering and agricultural practices).

Table 1 Modified field and desktop methods employed in investigating unstable terrain in the Thompson River valley study sites for 2020-2021. UAV - unoccupied aerial vehicle; InSAR – synthetic aperture radar interferometry; RTK-GNSS – real-time kinematic global navigation satellite system.

Landslide study site	**Slope description**	**Geologic mapping methods** ***Field and desktop studies***	**Surface change detection** ***Field and desktop studies***			**Climate variables** ***Collected from Weather Station GSC-1*** ***Desktop studies***	**Discharge** ***Stage at Spences Bridge*** ***Desktop study***
			UAV	**InSAR**	**RTK-GNSS**		
Ripley Landslide	Both sides of valley unstable Embankments and retaining wall	Field studies Surficial Geology Bathymetry ERT Boreholes	RGB	RADARSAT SENTINEL	Annual surveys	Precipitation Temperature Wind	Annual discharge
North Slide (Solar Slump)	East side of valley unstable Embankments and retaining wall	Field studies Surficial Geology Bathymetry	RGB	RADARSAT SENTINEL	Annual surveys		

Table 2 Modified field and desktop methods in investigating unstable terrain at the St-Lazare (CN) and Harrowby (CP) study sites for 2020-2021. InSAR – synthetic aperture radar interferometry; UAV - unoccupied aerial vehicle; RTK-GNSS – real-time kinematic global navigation satellite system.

Landslide study site	**Slope description**	**Geologic mapping** ***Desktop study only***	**Surface change detection** ***Desktop studies only***		
			InSAR	**UAV**	**RTK-GNSS**
St-Lazare	Both sides of valley unstable Groundwater	Surficial Geology	RADARSAT SENTINEL	RGB	Annual surveys
Harrowby	Both sides of valley unstable	Surficial Geology	RADARSAT SENTINEL	RGB	Annual surveys

Table 3 Audit of IMOU activities affected by COVID-19 in 2020-2021.

Activity	Logistical, procurement and outreach plans	Operational status
Assiniboine valley *Geological mapping* *GNSS, UAV surveys*	1 Research scientist, 3 Physical scientists, 2 weeks	Cancelled: logistical challenges and prohibitions on inter-provincial travel
Thompson valley *Geological mapping* *GNSS, UAV surveys* *PRIME, Geocubes, weather station*	1 Research scientist, 3 Physical scientists, 4 weeks	Reduced activities: 1 Research Scientist, 1 Physical Scientist, 3 weeks
36th International Geological Congress *New Delhi, India*	1 Research scientist, 3 weeks, international travel	Postponed until 2022
Slope Stability 2020 *Perth, Australia*	1 Physical scientist, 1 week, international travel	Ran as a virtual conference
5th World Landslide Forum *Kyoto, Japan*	1 Research scientist, 2 weeks, international travel	Postponed until November 2021
American Geophysical Union *San Francisco, USA*	1 Research scientist, 1 week, continental travel	Ran as a virtual conference
Railway Ground Hazard Research Program Workshop *Edmonton, AB*	1 Research scientist, 3 days, inter-provincial travel	Ran as a virtual conference

Table 4 IMOU-5170 outreach: presentations and publications for 2020-2021.

Publication type, authors, and title, source
RGHRP Workshop Presentation
Huntley, D. 2020. COVID-19 landslide research in the Thompson River valley, British Columbia, and outlook for future work in the Assiniboine River valley, Saskatchewan-Manitoba, Canada. *RGHRP Annual Workshop (December)*, PowerPoint Presentation, 12 Slides, Virtual Presentation, North Vancouver
Conference Presentations
Holmes, J., Chambers, J., Wilkinson, P., Meldrum, P., Huntley, D., Boyd, J., Cimpoiasu, M, Sattler, K., Elwood, D., Bobrowsky, P. and Donohue, S. 2020. An assessment of landslide risk using 4-dimensional electrical resistivity tomography for monitoring an unstable slope that affects transport infrastructure in British Columbia, Canada. *American Geophysical Union*, Virtual Conference, iPosterSessions.com Rotheram-Clarke, D., Huntley, D., Bobrowsky, P., MacLeod, R., and Brillon, C. 2020. InSAR investigation of sackung-like features and debris flows in the vicinity of Hawkesbury Island and Hartley Bay, British Columbia, Canada: reducing landslide and tsunami risks for coastal communities and vulnerable infrastructure. *Slope Stability 2020,* Symposium Abstract, 1 narrated presentation, Virtual Conference Huntley, D., Rotheram-Clarke, D., MacLeod, R., Cocking, R., Joseph, J. and Bobrowsky, P. 2021a. Field testing innovative differential geospatial and photogrammetric monitoring of a slow-moving landslide, south-central British Columbia, Canada. *5th World Landslide Forum*, Abstracts Volume, 15 Slides, Kyoto, Japan. Postponed until further notice. Huntley, D., Bobrowsky, P., Holmes, J., Chambers, J., Meldrum, P., Wilkinson, and Donohue, S. 2022. Mapping and monitoring a very slow-moving landslide: Risk Reduction in the Thompson River valley, British Columbia, Canada. *36th International Geological Congress*, Abstracts Volume, 10 Slides, New Delhi, India. Postponed until further notice.
Open File Reports
Huntley, D., Bobrowsky, P., Rotheram-Clarke, D., Cocking, R., and Joseph, J. 2020. Understanding Prairie landslides: current research in the Assiniboine River valley, Manitoba-Saskatchewan (2019-2020). *Geological Survey of Canada*, Open File 8735, 26 pages, https://doi:10.4095/326821 Huntley, D., Bobrowsky, P., Rotheram-Clarke, D., MacLeod, R., Cocking, R., and Joseph, J. 2020. Understanding Plateau landslides: current research in the Thompson River valley, Interior Plateau, British Columbia (2013-2020); Geological Survey of Canada, Open File 8736, 60 pages, https://doi:10.4095/326830

Huntley, D., Bobrowsky, P., Cocking, R., Joseph, P., Neelands, N., MacLeod, R., Rotheram-Clarke, D., Usquin, R. and Verluise, F. 2020. Installation, operation and evaluation of an innovative global navigation satellite system monitoring technology at Ripley Landslide and South Slide, near Ashcroft, British Columbia; Geological Survey of Canada, Open File 8742, 36 pages

Huntley, D., Rotheram-Clarke, D., Cocking, R., Joseph, J. and Bobrowsky, P. 2020. Understanding Plateau and Prairie Landslides: research plans for the Thompson River valley, British Columbia, and the Assiniboine River valley, Manitoba-Saskatchewan (2020-2025); Geological Survey of Canada, Open File 8743, 25 pages

Book Chapters

Huntley, D., Rotheram-Clarke, D., Bobrowsky, P., MacLeod, R., and Brillon, C. 2020. InSAR investigation of sackung-like features and debris flows in the vicinity of Hawkesbury Island and Hartley Bay, British Columbia, Canada: reducing landslide and tsunami risks for coastal communities and vulnerable infrastructure. *Slope Stability 2020,* Symposium Special Volume, 10 Pages, https://doi.org/10.36487/ACG_repo/2025_09

Huntley, D., Bobrowsky, Rotheram-Clarke, D., MacLeod, R., Cocking, R., Joseph, J., Holmes, J., Donohue, S., Chambers, J., Meldrum, P., Wilkinson, P., Hendry, M. and Macciotta, R. 2021. Protecting Canada's railway network using remote sensing technologies. *Advances in Remote Sensing for Infrastructure*, 26 Pages, Springer International Publishing, https://doi:10.36487/AGC_repo/2025_09

Huntley, D., Rotheram-Clarke, D., Cocking, R., and Joseph, J. 2021. Landslide change detection monitoring with a benchmarked RADARSAT CONSTELLATION MISSION high temporal resolution dataset. Institute of Electrical and Electronic Engineers, *International Geoscience and Remote Sensing Symposium*, Special Volume, 4 pages, In review

Journal Papers

Holmes, J., Chambers, J., Meldrum, P., Wilkinson, B., Williamson, P., **Huntley, D.**, Sattler, K., Elwood., D., Sivakumar, V., Reeves, H. and Donohue, S. 2020. 4-Dimensional Electrical Resistivity Tomography for continuous, near-real time monitoring of a landslide affecting transport infrastructure in British Columbia, Canada. *Near Surface Geophysics*. 15 Pages, https://doi:10.1002/nsg.12102

Huntley, D., Holmes, J., Bobrowsky, P., Chambers, J., Meldrum, P., Wilkinson, P., Donohue, S., Hendry, M., Macciotta, R., Elwood, D., Sattler, K., and Roberts, N. 2020. Hydrogeological and geophysical properties of the very slow-moving Ripley Landslide, Thompson River valley, British Columbia. *Canadian Journal of Earth Sciences*, 21 Pages, https://www.nrcresearchpress.com/doi/10.1139/cjes-2019-0187#.X02CvO-SnD4

Sattler, K., Elwood, D., Hendry, M., Huntley, D., Holmes, J., and Wilkinson, P. 2020. Effect of pore-pressure dynamics on progressive failure in clay shale landslides. *Landslides*, 17 Pages, https://doi10.1007/s10346-020-01611-3

Huntley, D., Bobrowsky, P., MacLeod, R., Cocking, R., Joseph, J. and Rotheram-Clarke, D. 2021. Ensuring resilient socio-economic infrastructure: field testing innovative differential GNSS-InSAR-UAV monitoring technologies in mountainous terrain near Ashcroft, British Columbia, Canada. *Journal of Mountain Science*, Vol. 18 (1), pp. 1-20; https://doi.org/10.1007/s11629-020-6552-y

Huntley, D., Rotheram-Clarke, D., Pon, A., Tomaszewicz, A., Leighton, J., Cocking, R. and Joseph, J. 2021. Benchmarked RADARSAT-2, SENTINEL-1 and RADARSAT CONSTELLATION MISSION change detection monitoring at North Slide, Thompson River valley, British Columbia: implications for a landslide-resilient national railway network. *Canadian Journal of Remote Sensing.* https://doi.org/10.1080/07038992.2021.1937968

Sattler, K., Elwood, D., Hendry, M., Berscheid, B., Marcotte, B., Abdulrazagh, P. and Huntley, D. 2021. Field collection of geotechnical measurements for remote or low-cost data-logging requirements. *Geotechnical Testing Journal.* In press

3. METHODS, RESULTS, ANALYSIS AND DISCUSSION

This report builds upon the foundational work in the Thompson and Assiniboine river valleys presented in GSC Open Files 7531, 8548, 8735, 8736, 8742 and 8745 (Huntley and Bobrowsky 2014; Huntley et al. 2019c; Huntley et al. 2020b-e). Anticipating scenarios of future extreme weather events and climate change, geological hazard management solutions will require a clearer understanding of the form and function of landslides. Research and monitoring efforts will lead to: 1) Understanding the composition and internal structure of the landslide, including the range of earth materials and nature of failing rupture surfaces. 2) Delimiting the spatial extent of unstable parts of the slide body. 3) Establishing the timing, amount, direction, and rates of surface displacement from year to year. 4) Defining the interactions between climate-driven triggering mechanisms (e.g., groundwater pressure) and landslide activity.

3.1 Activity 1: Geohazard Mapping

Descriptions of local bathymetric, surficial and bedrock geological conditions, including earth materials, landforms and structures, and their hydrological properties are essential for understanding landslide composition, structures, and behaviours.

In this section, we describe field-based landslide mapping, and supporting desktop geospatial analyses undertaken at Ripley Landslide and North Slide in the Thompson valley railway corridor carried out in 2020 and 2021 (**Figure 1 a, b**). This description incorporates surficial geology observations and single-beam acoustic bathymetric surveys of Thompson River between Ashcroft and the Basque Slide (Huntley et al. 2019a; Huntley et al. 2021a; **Figure 1b**). Ten hydrogeological units were distinguished in surficial deposits and fractured bedrock through field mapping, exploratory drilling, and geophysical surveys (Huntley and Bobrowsky 2014; Huntley et al. 2017a; Huntley et al. 2019a-c; Holmes et al. 2020; Huntley et al. 2020a). Similar to surficial geological observations of landslides in the Thompson River valley, single-beam and multi-beam river surveys (Huntley et al. 2021a) reveal variations in channel bed composition, south of Ashcroft and north of Spences Bridge, ranging from sand and silt draping bedrock, to coarse gravel and boulders overlying clay-rich valley fill (**Figure 1b**). Shallow waters (riffles) with rapids lie adjacent to stable terrain, separated by deep scour pools (up to 5 m below river level) adjacent active slide toes (**Figure 1b**).

Geohazard mapping was limited to desktop terrain analysis in the Assiniboine study areas due to travel restrictions and logistical challenges resulting from COVID-19 (**Figure 1c-e**; **Table 5**).

3.1.1 Ripley Landslide

Ripley Landslide, 2.5 km south of Black Canyon, is a small, slow-moving (3 mm to 55 mm yr^{-1}) translational landslide: one of 14 active landslides along a 10 km stretch of the Thompson River valley south of Ashcroft, BC (**Figure 1a, b**). Intermittently active since the early 1950's (Bunce and Chadwick 2012), the landslide has been a geological and geophysical test site where insight is gained into the processes that result in slope failure along the transportation corridor (e.g., Huntley et al. 2014; Huntley et al. 2020a).

In 2020-2021, COVID-19 limited travel and site access to campaigns in September and November 2020, and March 2021. These visits were coincident with geotechnical investigations undertaken by CP and BGC Engineering Inc. (**Figure 3**). In 2019, CP senior management approved the provisional groundwork required to design and implement slope stabilization at the Ripley Landslide test site. Taking advantage of reduced traffic loads through the main national transportation corridor during the pandemic, CP and BGC Engineering Inc. began the first phase of this work in September 2020. This resulted in significant anthropogenic disturbance of the unstable slope. As a result, some of the GSC monitoring instrumentation installed at Ripley Landside will require the relocation or decommissioning. This includes InSAR corner reflectors, Geocube^{TM} stations (and coordinator), battery packs and solar panels, the Proactive Infrastructure Monitoring and Evaluation (PRIME) array, processor, modem and antennae, observation cameras, and soil moisture meters.

Figure 3 Overview of stakeholder geotechnical investigations at Ripley Landslide, September-October 2020: a) geotechnical borehole drilling undertaken by CP and BGC Engineering, using a sonic drill rig (NRCAN Photo 2021-495; b) core samples, collected and logged for geotechnical properties (NRCAN Photo 2021-496); c) boreholes and test pits excavated support findings of Huntley et al. (2020) (NRCAN Photo 2021-497).

In common with other landslide-prone areas with thick accumulations of Pleistocene deposits, unit/bed thicknesses, earth material textures, penetrative planar structures, and slopes strongly influence permeability, porosity, and drainage of hydrogeological units (cf. Porter et al. 2002; Clague and Evans 2003; Eshraghian et al. 2007, 2008; Bishop et al. 2008). These properties constrain the infiltration of precipitation, surface runoff and snowmelt, producing an increase in volumetric water content in pores and fractures, reduction of shear strength in the unsaturated slope, and displacement of landslide mass (Sattler et al. 2018; Sattler et al. 2020; Holmes et al. 2020). Four new exploratory boreholes (locations based on published GSC data) were drilled by BGC Engineering (**Figure 3**), yielding further corroborating evidence of earth materials at depth (**Figure 4**). These observations confirmed the landslide is failing along a sub-horizontal, weak, basal shear surface in plastic glacial clay beds infilling a bedrock basin (cf. Huntley and Bobrowsky 2014; Hendry et al. 2015; Schafer et al. 2015; Huntley et al. 2017a; Huntley et al. 2019a, b). Industry partners will monitor groundwater and subsurface displacement in these new boreholes until further slope remediation work is approved.

Figure 4 Lithostratigraphic logs of BGC boreholes (2005, 2013, 2015 and 2020, white circles) and test pits (2020, yellow circles), showing location of BGS geophysical test samples collected (light purple, orange and brown dots). Terrestrial ERT pseudosections (red transect lines A-D) (EBA-TetraTech, 2013), waterborne ERT pseudosections (yellow transect lines 2, 3, 4) (Advisian-Worley Parson Group, 2014) and PRIME installation (BGS, 2016-Present). Gamma radiation measured in counts per second (cps), induced conductivity measured in milliSiemens/m) (mS/m), and magnetic susceptibility in parts per thousand (ppt) (Frontier Geosciences Inc., 2015). Also shown are locations of elevated terrain conductivity readings on submerged slide toe. Landslide extent (approximate shown in dashed white line on oblique photo captured by a UAV in 2016 (after Huntley et al. 2017a; Huntley et al. 2019a, d).

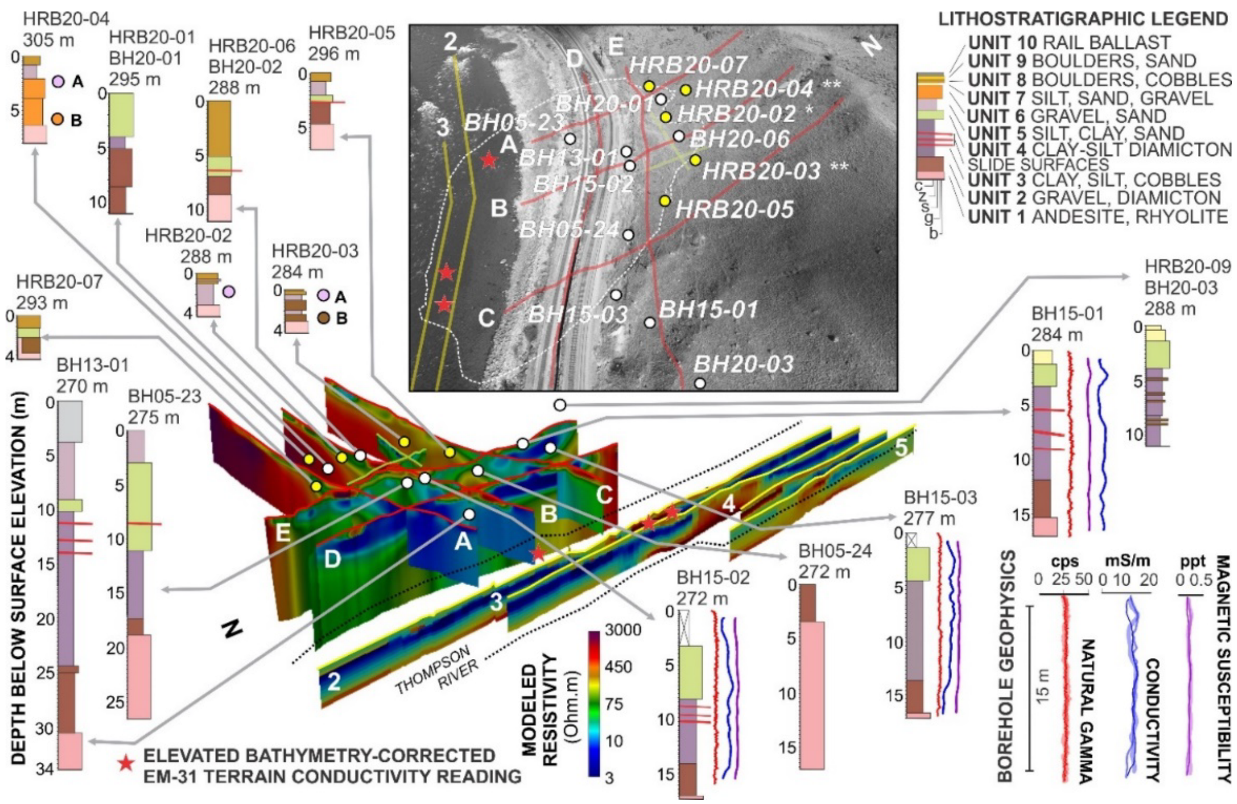

Electrical Resistivity Tomography (ERT), Ground Penetrating Radar (GPR), Fixed Frequency Electromagnetic Induction (FEM), Seismic Refraction, Multichannel Analysis of Surface Waves (MASW), and Acoustic Bathymetry results (Huntley et al. 2017a; Huntley et al. 2019a) have improved the understanding of the 3-D subsurface structure. The PRIME system installed on the head scarp in 2017 provides a more detailed insight into changing subsurface moisture conditions through time (Huntley et al. 2019c, d; Holmes et al. 2020). Differences in electrical resistivity of the units reflect hydrogeological conditions at the time of the survey. Resistive earth materials include dry glaciofluvial outwash and non-fractured bedrock; whereas glaciolacustrine clay and silt, water bearing fractured bedrock, and periodically saturated subglacial till and outwash are conductive (Huntley et al. 2019a; Huntley et al. 2020a). Dynamic, continuous real-time monitoring of electrical resistivity, now underway, will help characterize water-flow paths, and possible relationships to independently monitor pore pressures and slope creep. These new geophysical datasets enhance understanding of the composition and internal structure of this landslide (**Figure 4**), and provide important context to interpret multi-year slope stability monitoring ongoing in the valley.

Remote collaboration with the BGS and provincial and university partners continued to ensure semi-continuous geophysical mapping with a long-term aim of identifying precursors to movement to aid in the prediction of slope failure (**Table 5**). Despite sustaining damage during September ground investigations, the PRIME system will continue to collect electrical resistivity data beyond 2021 to provide a more refined picture of moisture-driven processes for landslides in this semi-arid terrain (e.g., Holmes et al. 2020; Huntley et al. 2020a; Sattler et al. 2020).

Table 5 Geohazard mapping activities matrix 2020-2021 for the Thompson River valley, BC (TRV), and the Assiniboine-Qu'Appelle river valleys, SK-MN (ARV).

Collaborating Institutions	**Personnel Requirements and Rôles**	**Activity Group 1 Objectives**	**Activity Outcomes**	**Dissemination (i.e., presentations, publications)**
Geological Survey of Canada	• 1 Research Scientist (Quaternary) • 2 Physical Scientists (Geophysics) • 1 GIS Technician	**Terrain mapping and fieldwork** **Geophysics (PRIME)** **Geoscience Outreach**	Logistical support for ground-truth fieldwork, and GNSS surveys In TRV (and ARV) Procurement of equipment and sample transfers, logistical support for systems maintenance, fieldwork (TRV and ARV) Logistical support for conferences, workshops, and publications that aimed to: • Characterized three-dimensional ground displacement patterns of discrete locations • Evaluated the utility of precipitation, ambient temperature, and soil moisture datasets • Predicted landslide activity based on comparison of geophysical results, meteorological records, and 3D-displacement measurements	**Conferences** **Journal Publication** **Government Documents** *Open File Reports* and Canadian Geoscience Series maps (GSC, BGS) **Academic Theses** Student M.Sc., Ph.D. theses and publications UA, USASK and UB senior authors
British Geological Survey	• 1 Research Scientist (Geophysics) • 2 Physical Scientist (Geophysics) • 1 Ph.D. student (University of Belfast [UB], Northern Ireland)			
Department of Civil Engineering, University of Alberta	• 3 Professors / Research Engineers • 1 M.Sc./Ph.D. Student			
College of Engineering, University of Saskatchewan				

3.1.2 North Slide

The North Slide, located 1.6 km northeast of the Black Canyon tunnel on the east bank of Thompson River (**Figure 1a, b**), is an ancient rotational-translational landslide in the Thompson River valley that was reactivated as a sudden onset, rapid retrogressive flow-slide on October 14, 1880, around 9 pm (Stanton 1898; Evans 1984; Clague and Evans 2003). In common with other 19th Century landslides in the valley (**Figure 1b**), it failed rapidly during, and after the summer months at a time when mid-slope terraces were intensively irrigated for agricultural land use, and toe slopes were incised and over-steepened during railway construction (Stanton 1898; Evans 1984; Clague and Evans 2003). The landslide blocked drainage of Thompson River for three days and impounded a lake that extended 14 km upstream and flooded Ashcroft. The landslide is divisible into four sectors (**Figure 5a**). I) An active slide toe (0.08 km^2) has sparse vegetation, active tension cracks, and steep scarp faces (active post-2000). II) The inactive slide main body and head scarp (0.55 km^2) exhibits sparse vegetation and subdued scarp faces and slide blocks (active ca. 1880). III) An ancient slide body (0.37 km^2) has established vegetation ground cover and subdued surface morphology (older than 300 years before present). IV) Stable upland terraces support irrigated crops and cattle pasture (**Figure 5b**).

Figure 5 The North Slide, Thompson River valley, British Columbia. **a)** Extent of active and inactive sectors of the landslide: **I**) an active slide toe (0.08 km^2) characterized by active tension cracks, sparse vegetation, and steep scarp faces (post 2000); **II**) inactive slide main body and headscarp (0.55 km^2), with sparse vegetation and subdued scarp faces and slide blocks (ca. 1880); **III**) inactive slide body (0.37 km^2) with established vegetation ground cover and subdued surface morphology (ancient, i.e., >300 year before present); **IV**) stable postglacial slopes and terraces supporting irrigated crops and cattle pasture. **CN** – Canadian National Railways; **CP** – Canadian Pacific Railways; ***TR*** – Thompson River. Base map merges ASTER DEM v2 worldwide elevation data (1 arc-second resolution) with WorldView Imagery in Global Mapper™ using a Universal Transverse Mercator projection with the Google Maps (sphere radius 6378137) datum. **A-A'** Line of section in **Figure 6.** Oblique aerial photograph of Thompson River, the Goddard, North and South slides impacting the CP track, and CN track crossing the CN54 Slide, view to the northeast. Note that the CN track crosses the river in Black Canyon (**Figure 1b**) to join the CP track on the east bank (pilot and photo credit, Drew Rotheram-Clarke; NRCAN photo # 2021-035).

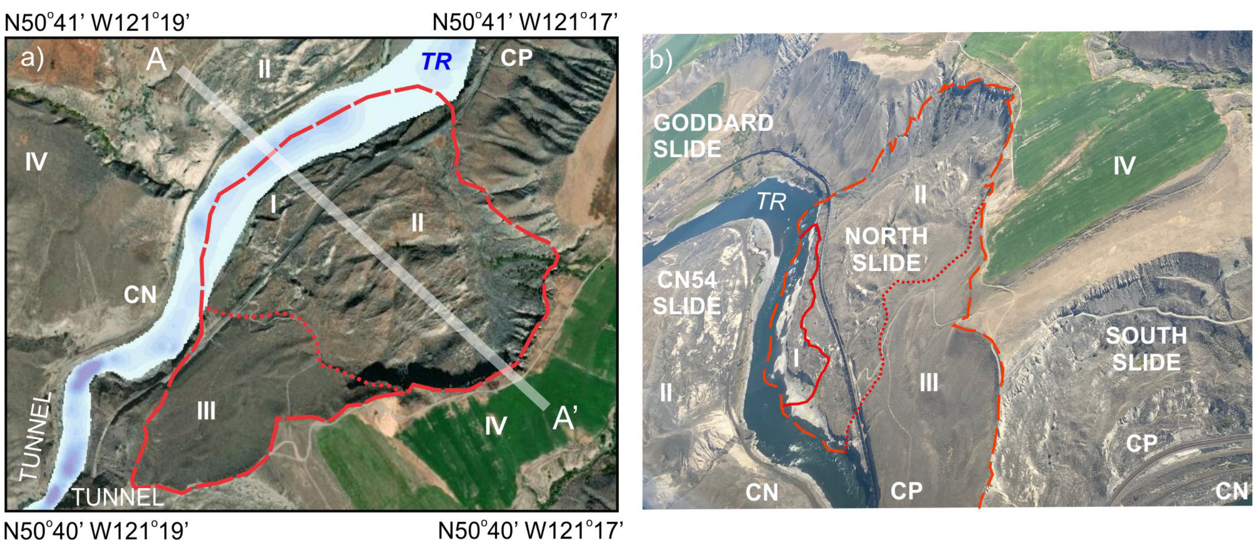

The landslide comprises glaciolacustrine sandy silt and sandy gravel outwash unconformably overlying silty till and glaciolacustrine silt and clay (**Figure 6**; Porter et al. 2002; Clague and Evans 2003; Eshraghian et al. 2007). Porter et al. (2002) reported that a prominent toe bulge (**Figure 7**) and rhythmically interbedded layers of soft brown clay, stiff, high plastic dark grey clay, and grey silt were exposed on the river floodplain. Borehole piezometer and inclinometer monitoring revealed preferential shearing in soft brown clay beds, with rupture zones at 264 and 269 m above sea level (asl), equivalent to 25 and 30 m below the CP rail grade. Piezometer data indicated hydrostatic conditions at depth below the track, and an upward gradient in the landslide toe (Porter et al. 2002).

Figure 6 Cross-section A to A' across North Slide modelled as a rotational-translational landslide in glacial deposits confined to a bedrock paleochannel or basin (after Porter et al 2002; Clague and Evans 2003; Eshraghian et al. 2007; Eshraghian et al. 2008). See **Figure 5** for location of cross-section.

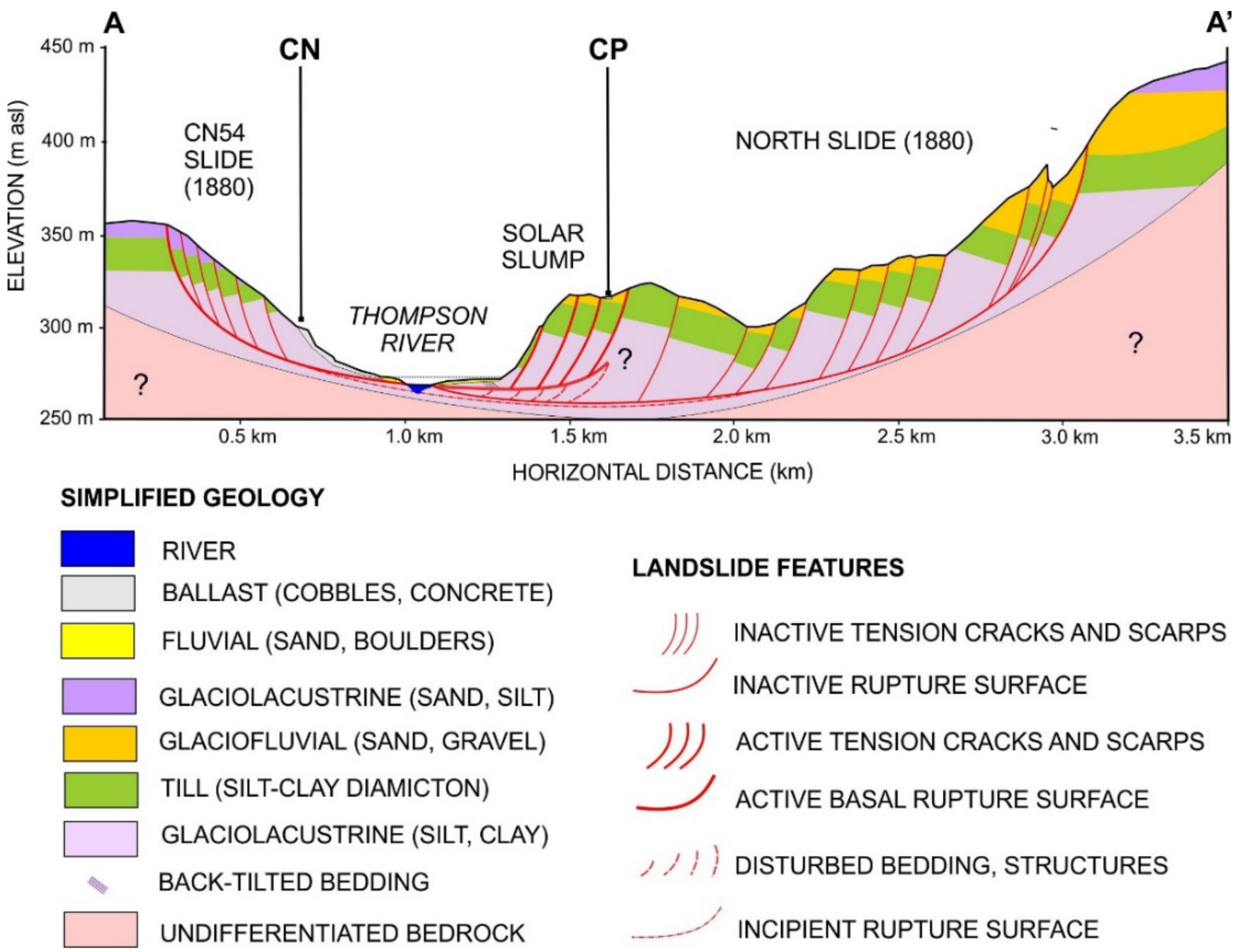

A comparison of air photos between 1928 and 1997 showed that the slope below the rail grade was being eroded by Thompson River, with historical bank erosion rates averaging 70 cm yr^{-1} (Porter et al. 2002). In October 2000, movement along 150 m of the toe of the North Slide (the "Solar Slump") resulted in between 5 and 15 cm of settlement at the CP grade. Peak observed movement rates were on the order of 15 cm yr^{-1} with an average rate of 3 cm yr^{-1} (Porter et al. 2002). Movement on the shallow rupture surface was measured at 5 cm to 11 cm yr^{-1}; while on the deeper slide surface, a movement rate of 3 cm to 4.5 cm yr^{-1} was recorded with borehole inclinometers (Porter et al. 2002). Mercury switch tip-over posts linked to rail signals were subsequently installed to monitor for ground displacement and reduce the chances of train derailment (**Figure 8**). Since 2001, movements at the rail grade have been managed through normal maintenance and track lifting operations. The slide toe remained active between 2013 and 2015 (Huntley et al. 2017b; Journault et al. 2018).

Figure 7 North Slide field observations: **a)** view north across the main slide body showing the active slide toe (I); inactive slide main body (II); and relict slide body (III) (NRCAN Photo 2021-036); **b)** prominent toe bulge in Thompson River floodplain (NRCAN Photo 2021-037); **c)** back-tilted rhythmite clay-silt beds exposed in the toe slope bulge (NRCAN Photo 2021-038).

Figure 8 North Slide "Solar Slump": **a)** an active slide toe characterized by sparse vegetation, fresh tension cracks, and steep scarp faces, view south (NRCAN Photo 2021-498); **b)** toe slope scarps and slide blocks, showing a power cable leading to a mercury switch tipping post, view north (NRCAN Photo 2021-499); **c)** solar panel array powering track signals and tipping posts (NRCAN Photo 2021-500); **d)** detail of installed mercury switch tipping posts (NRCAN Photo 2021-501).

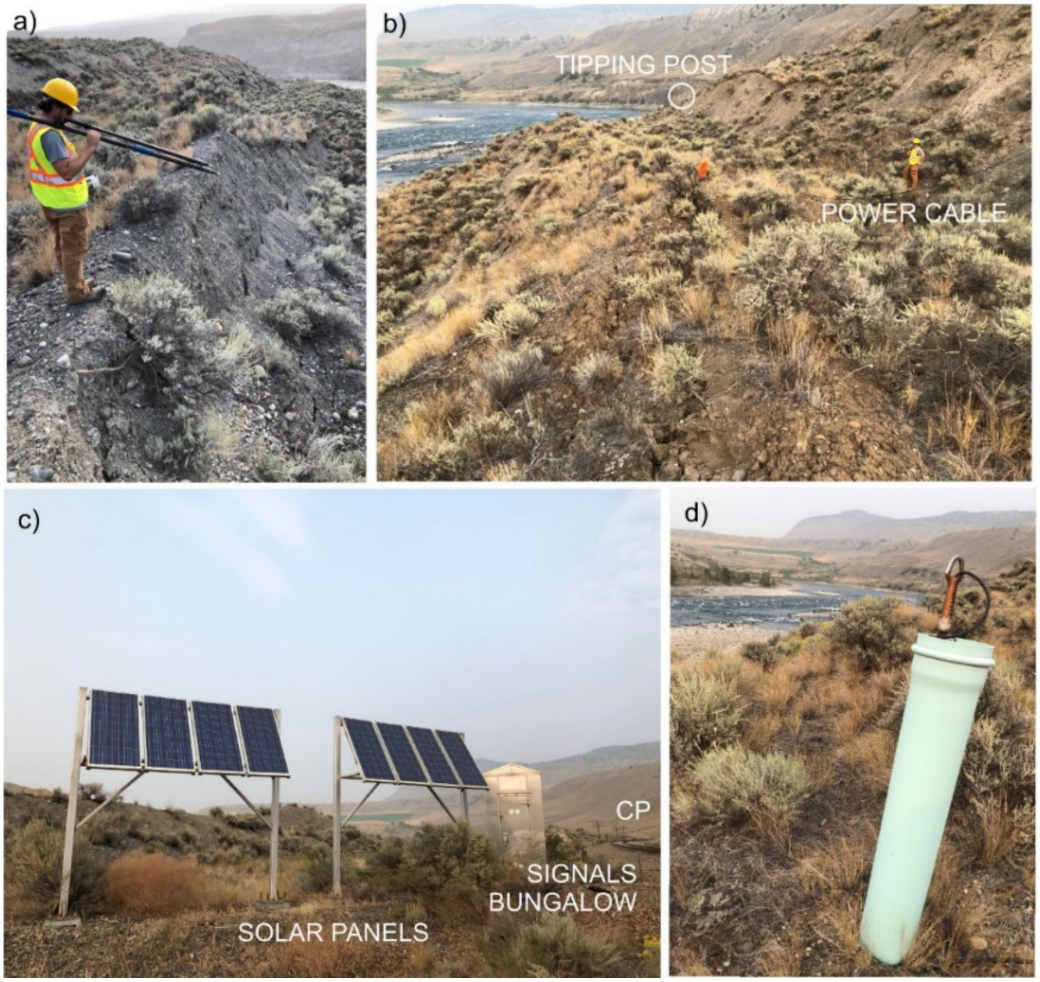

3.1.3 Assiniboine River Valley

Plans for ground-based work at the CN 184.4, and CP 86.5 and 82.6 study sites in the Assiniboine River valley, Manitoba (**Figure 1 c-e**) in 2020-2021 were abandoned due to COVID-19. This decision limited the acquisition of terrain information to remote sensing imagery and desktop analysis of benchmark GNSS and UAV datasets collected in 2019 (Huntley et al. 2020b; Huntley et al. 2020c; Huntley et al. 2020d). After processing, UAV imagery was sufficient to resolve vegetation type, cobble-sized boulders, and anthropogenic features (<5 cm across) at flight elevations of 50 m to 100 m above ground level. Desktop terrain analysis included visual interpretation of the processed 2019 UAV imagery for separate geological features. Conventional terrain classification systems were applied to allow comparison with landslides in the Thompson River valley and elsewhere (e.g., Resource Inventory Committee 1996; Howes and Kenk 1997; Huntley and Bobrowsky 2014; Deblonde et al. 2018). Hydrogeological units were defined by lithofacies and landform associations, unit thicknesses, earth material textures, degree of sorting, weathered and un-weathered colours, sedimentary structures and penetrative planar structures, degrees of consolidation, stratigraphic contact relationships, estimated geological age, and other distinguishing characteristics (**Figure 8**).

Figure 9 Cross-sections across the Assiniboine River valley in the vicinity of the landslide site at CN Rivers Mile 184, and CP Bredenbury Miles 82.6 and 86.5 (for locations, also see **Figure 1 c-e**). Terrain units: **Rd** – bedrock plain, drumlinized; **Rp-C** – bedrock plain, modified by meltwater erosion; **Tr-C** – corrugated till, modified by meltwater erosion; **GFp-C** – glaciofluvial outwash, modified by meltwater erosion and deposition; **Ap-M, Af** – alluvial floodplain and fan deposits, modified by meandering channels; **Cz-V, Fs, Fc** – undifferentiated colluvium, modified by gulley erosion, slow-moving rotational slumps in drift and shale, and soil creep on moderate to steep slopes (>18°). Simple stratigraphic model of the Assiniboine and Qu'Appelle river valleys showing hypothetical relationship of landslides to groundwater flow paths through earth materials in the study area (after Klassen 1972; Sauer 1978; Christiansen 1979; Mugridge et al. 1983; Young and Moore 1994; Blatz et al. 2004).

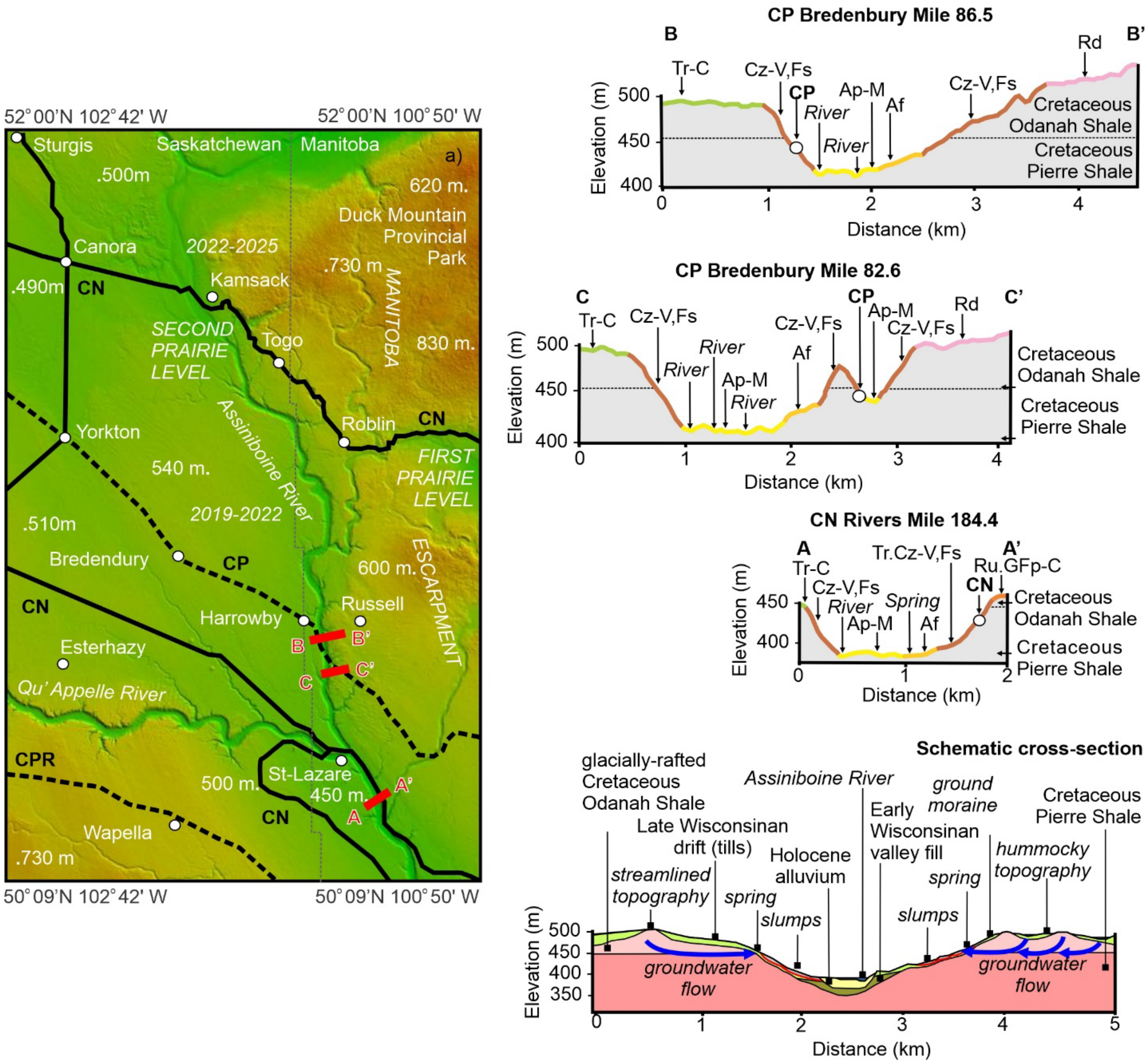

3.2 Activity 2: InSAR and RTK-GNSS Change Detection Monitoring

COVID-19 limited fieldwork for change detection monitoring activities to repeat RTK-GNSS and UAV surveys in the Thompson River valley. These data were employed to calibrate and benchmark desktop InSAR analyses performed by the GSC and 3vGeomatics Inc. (Pon et al. 2020). We demonstrate the applicability of interferometric analyses of RADARSAT-2 (RS2), SENTINEL-1 (S1) and RADARSAT

CONSTELLATION MISSION (RCM) datasets to characterize and monitor landslides in the Thompson River valley, BC and Assiniboine river valley, MN (**Table 6**).

Using RS2 and S1 SAR data acquired between 2013 and 2019, 3vGeomatics Inc. (Pon et al. 2020) applied proprietary advanced InSAR interpretation techniques to identify and measure locations experiencing ground displacement (**Figure 10**). From north to south along the railway transportation corridor, these include the following landslides with an average 1D line-of-sight (LoS) displacement greater than 3 cm yr^{-1}: Goddard Slide, North Slide, South Slide, Red Hill Slide and Ripley Landslide (**Figure 10**). Regions of highest activity correlate with cutbank erosion and channel bed scour on the outside bends of the river.

Table 6 Change detection activities matrix 2020-2021 for the Thompson River valley, BC (TRV), and the Assiniboine-Qu'Appelle river valleys, SK-MN (ARV).

<table>
<tr><th>Collaborating Institutions</th><th>Personnel Requirements and Rôles</th><th>Activity 2 Objectives</th><th>Projected Outcomes</th><th>Dissemination (i.e., presentations, publications)</th></tr>
<tr><td>Geological Survey of Canada

Canada Centre for Mapping and Earth Observation

Canadian Forest Services (Canadian Wood Fibre Centre)</td><td>• 1 Research Scientist (Quaternary)
• 2 Physical Scientist (Geophysics)
• 1 GIS Technicians</td><td rowspan="2">InSAR monitoring

GNSS monitoring

UAV change detection

Monitoring climate change variables</td><td rowspan="2">Logistical support for ground-truthing (TRV), procurement of corner reflectors (ARV)

Procurement of Geocube components from Ophelia (France) and GNSS components for in-house systems

Logistical support for systems maintenance, fieldwork (TRV and ARV)

Procurement of UAVs, software, components enabling optical, LiDAR and multispectral inventories

Logistical support for fieldwork (TRV and ARV)

Procurement of total weather station (air pressure, temperature, rain gauge, snow sensor, anemometer and wind vane; insolation), moisture meters

Procurement of soil moisture meters, supporting hardware, software, data loggers, batteries, solar panels and data communication components (ARV)</td><td rowspan="2">Conferences

Journal Publications

Government Documents
Open File Reports (GSC)

Academic Theses
Student theses and publications

UA and USASK senior authors

Continued over …</td></tr>
<tr><td>Department of Civil Engineering, University of Alberta</td><td>• 3 Professors / Research Engineers</td></tr>
</table>

College of Engineering, University of Saskatchewan	2 M.Sc./Ph.D. Students	 **Geoscience Outreach**	Logistical support for routine maintenance of equipment, replacement and new units (TRV) Logistical support for conferences, workshops, and publications that: • Characterized three-dimensional ground displacement patterns of discrete locations • Evaluated the utility of precipitation, ambient temperature, and soil moisture datasets • Predicted landslide activity based on comparison of geophysics results, meteorological records, and 3D-displacement measurements	

For InSAR analyses, the RS2 data stack consisted of 86 scenes with a descending (west-ranging) line-of-sight (LoS). It included 63 snow-free, useable scenes spanning the period of September 2013 to November 2019. Although RS2 had a repeat cycle of 24 days and a 3 m pixel ground resolution, the single look angle limited the quality of displacement to one-dimensional LoS measurements. Two S1 SAR stacks consisted of 90 ascending, and 111 descending scenes acquired between February 2015 and December 2019, respectively. Of these, 63 ascending (east-ranging LoS) scenes and 86 descending (westward LoS) scenes were snow-free and useable for analysis. With a 12-day repeat cycle and two look angles on ascending and descending orbital passes, two-dimensional displacement measurements were possible using the S1 stacks, although the 20 m pixel size limited the mapping resolution (Huntley et al. 2021a; Huntley et al. 2021b).

Underestimation occurs when there are insufficient samples to characterize the displacement gradient. Overestimating from unwrapping was not an issue (Pon et al. 2020). Gaps in the RS2 time-series (<40 days) due to missing acquisitions or masked aliased data in winter scenes were interpolated to minimize bias in down displacement measurements. There was no interpolation when gaps in interferograms were greater than 40 days (**Table 7**, e.g., winter of 2016-2017 and early 2019). For dual-look S1 data, missing data in one look-direction was partly corrected by interpolating with data from the opposite look-direction. With the single-look RS2 and S1 data, under- or overestimation of displacement occurs when there is a data gap with a significantly different rate from the surrounding periods (e.g., the snow-bound winter months). For the S1 2019 data gap, neither look-direction provided reliable measurements. Under- or overestimation due to unwrapping in interferograms was minimized by masking out bad branch cuts (Pon et al. 2020).

Table 7 Master interferogram stack date ranges for RS2, S1 and RCM scenes with number of used and unused images (italics) in each year indicated (Pon et al. 2020; Huntley et al. 2021b, c).

RADARSAT 2 Descending orbit (84 scenes acquired)	**SENTINEL-1 Descending orbit (113 scenes acquired)**	**SENTINEL-1 Ascending orbit (103 scenes acquired)**	**RADARSAT Constellation Mission Descending orbit (12 scenes acquired)**
2013 08-09 to 26-10 (3) *19-11 to 13-12 (2)*			
2014 19-03 to 14-11 (11) *06-01 to 23-02, 08-12 (4)*			
2015 07-04 to 09-11 (9) *01-01 to 14-03, 01-02 03-12 to 27-12 (6)*	**2015** 10-03 to 01-11 (14) *17-01 to 29-01, 25-11 to 19-12 (4)*	**2015** 27-03 to 10-11 (20) *14-01 to 07-02, 04-12 to 28-12 (4)*	
2016 25-03 to 03-11 (9) *13-02, 27-11 to 21-12 (3)*	**2016** 29-02 to 07-11 (10) *12-01 to 05-02, 01-12 to 25-12 (4)*	**2016** 07-02 to 10-11 (11) *04-12 to 28-12 (2)*	
2017 27-03 to 29-10 (10) *14-01 to 08-03, 22-11 to 16-12 (5)*	**2017** 13-03 to 27-10, 02-12 (17) *11-02 to 01-03, 08-11 to 26-12 (6)*	**2017** 03-04 to 24-10, 29-11 (18) *21-01 to 26-02, 05-11 to 23-12 (7)*	
2018 22-03 to 24-10 (10) *08-01 to 26-02, 17-11 to 11-12 (4)*	**2018** 20-03 to 27-11, 21-12 (23) *07-01 to 08-03, 09-12 (6)*	**2018** 17-03 to 13-09 (11) *04-01 to 05-03, 30-12 (6)*	
2019 17-03 to 12-11 (5) *04-01 to 24-02, 10-04 (3)*	**2019** 26-01, 15-03 to 04-12 (22) *02-01 to 03-03 (5)*	**2019** 12-03 to 19-11 (20) *11-01 to 23-01, 01-12 to 13-12 (4)*	
Total used = 57 images Total not used = 27 images	**2020** 17-08 to 29-08 (2) Total used = 88 images Total not used = 25 images	Total used = 80 images Total not used = 23 images	**2020** 27-06 to 28-12 (12) Total used = 12 images

Average LoS displacement measurements were selected within the more active areas of the landslides of concern. These measurement points are indicated with grey triangles on figures below. For RS2 interferograms, average displacement is scaled with respect to the descending (westward) LoS, with negative values (red) representing movement away from the satellite and positive values (blue) capturing movement to toward the satellite (**Figure 10**). For S1 data, ascending and descending stacks were combined, and then relative phase measurements were geocoded onto a common spatial grid to derive displacement directions in the east-west-up-down plane (Pon et al. 2020). Multi-master interferograms were created (minus winter scenes) with atmospheric effects removed, and signal enhancement including pixel searching and adaptive filtering (Pon et al. 2020).

Figure 10 InSAR results for the Thompson River valley showing landslides of concern and the CN and CP tracks (solid black lines). Raster comparisons of 1D line-of-sight (LoS) time-series for descending orbits of RS2 and S1. Point coverage for time-series based on displacing areas defined by the signal-to-noise ratio for each pixel (Pon et al. 2020). **a)** RS2 average linear displacement rate rastered at 3 cm yr^{-1}, with purple polygons delimiting 4-sigma confidence levels. **b)** S1 average linear displacement rate, rastered at 3 cm yr^{-1}, with purple polygon delimiting 4-sigma confidence levels. Data acquired and processed by 3vGeomatics Inc. (Pon et al. 2020).

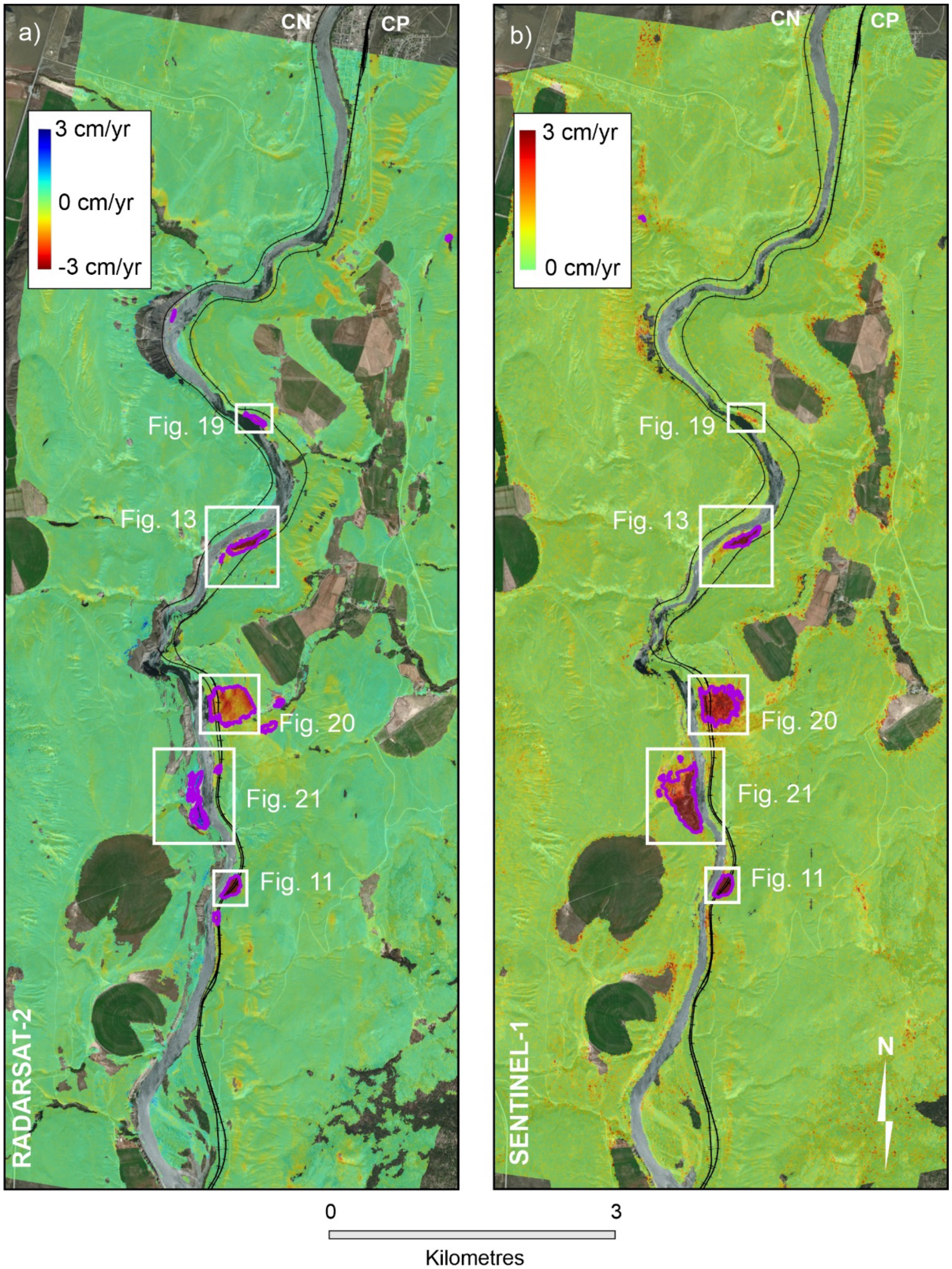

Interferometric analyses of RS2 and S1 C-band InSAR imagery from 2014-2020 acquired, processed, and provisionally interpreted by 3vGeomatics (**Figure 10**) were compared with RCM data collected from August to December 2020 acquired and processed by the GSC (Huntley et al. 2021b). These satellite InSAR datasets were applied to landslide mapping, modelling, and back-analysis of deformation velocities, and long-term deformation trends (e.g., Macciotta et al. 2014; Journault et al. 2016; Huntley et al. 2017b; Bobrowsky et al. 2018; Journault et al. 2018).

Spaceborne InSAR results were benchmarked with ground-based RTK-GNSS measurements and UAV photogrammetry collected in September 2019 and November 2020. These terrestrial surveys confirm that westward average LoS SAR vectors are not parallel to the average GNSS slope displacement vector.

3.2.1 Ripley Landslide

Persistent scatter InSAR results from monitoring of the Ripley Landslide between 2013 and 2019 indicate ground movement is concentrated within the centre of the sliding mass and averages 3.9 cm/year. The fastest displacements are detected upslope from the railway tracks, and on the southern flank of the landslide (**Figure 10**; **Figure 11a**). Displacement is captured at the 4-sigma level in both RS2 and S1 data in a 150 m x 250 m area (**Figure 11b, c**), indicating there is strong evidence for slope displacement compared to InSAR data noise. Most areas within the landslide boundary on surface experience average and maximum line of sight (LoS) displacement rates (equivalent to the downslope direction for the west-facing test site) of InSAR corner reflectors and other coherent targets (e.g., buildings, large boulders) between 2.5 cm and 7.5 cm yr^{-1} (cf. Journault et al. 2016; Huntley et al. 2017b; Journault et al. 2018).

The time series and corresponding instantaneous displacement rates shown in **Figure 11** (**d, e**) are taken from the centre of the slide mass, in a 40 m^2 area covering both rail lines between KYL 00029 and KYL-00037 (**Figure 11b, c**). RS2 velocity values were calculated from 12 days of displacement before and after each image acquisition; S1 values were derived from 6 days of displacement before and after acquisition. Ripley Landslide shows significant year-to-year variability, with 2017 and 2018 showing the most displacement within the monitoring record, and 2016 and 2019 having relatively little displacement within the record. The slide is much more active in winters than the summer, with minimal displacement occurring in the early summer. The S1 data indicates the displacement is downslope, with the east-west displacement twice the vertical displacement (Pon et al. 2020).

As with the North Slide (next section), the high level of temporal variability and localized periods of fast displacement resulted in complex interferograms that could not be unwrapped properly, thereby underestimating the displacement rate. For example, complexities in the 2016-2017 winter interferograms are indicative of high levels of displacement. The 4-month 2016-2017 cross-winter RS2 interferogram has at least three fringes (possibly >6), suggesting 15 cm of displacement during this interval. In the S1 descending data, two 12-day interferograms in March 2017 show one or two fringes, which would imply displacement rates approaching 100 cm yr^{-1}.

These results corroborate the datasets from PRIME monitoring and indicates fluctuations in precipitation over the winter months may contribute to intervals of landslide activity. Similar magnitudes and spatial-temporal patterns of displacement were also recorded by GNSS and UAV surveys between September 2019 and September 2020 (**Figure 12**; Huntley et al. 2017b; Journault et al. 2018; Huntley et al. 2021c).

Figure 11 RS2 and S1 InSAR results for Ripley Landslide. **a)** Ripley Landslide and adjacent active landslides (red dashed lines delimit extent of displaced ground). Cumulative 1D line-of-sight (LoS) displacement rates, scaled at 7 cm yr^{-1} over Ripley Landslide based on RS2 **(b)** and S1 **(c)** data. The RS2 rate is LoS, while the absolute S1 rate is in the east-west-up-down plane. Grey triangle indicates where LoS measurements were calculated; Purple polygons defines areas with displacement at the 4-sigma level. Cumulative displacement time series from the centre of Ripley Landslide (thin red line), based on RS2 **(d)** and S1 **(e)** data, with peak ground velocities (red arrows). The location of of the RTK-GNSS Geocubes ™ are shown as black triangles.

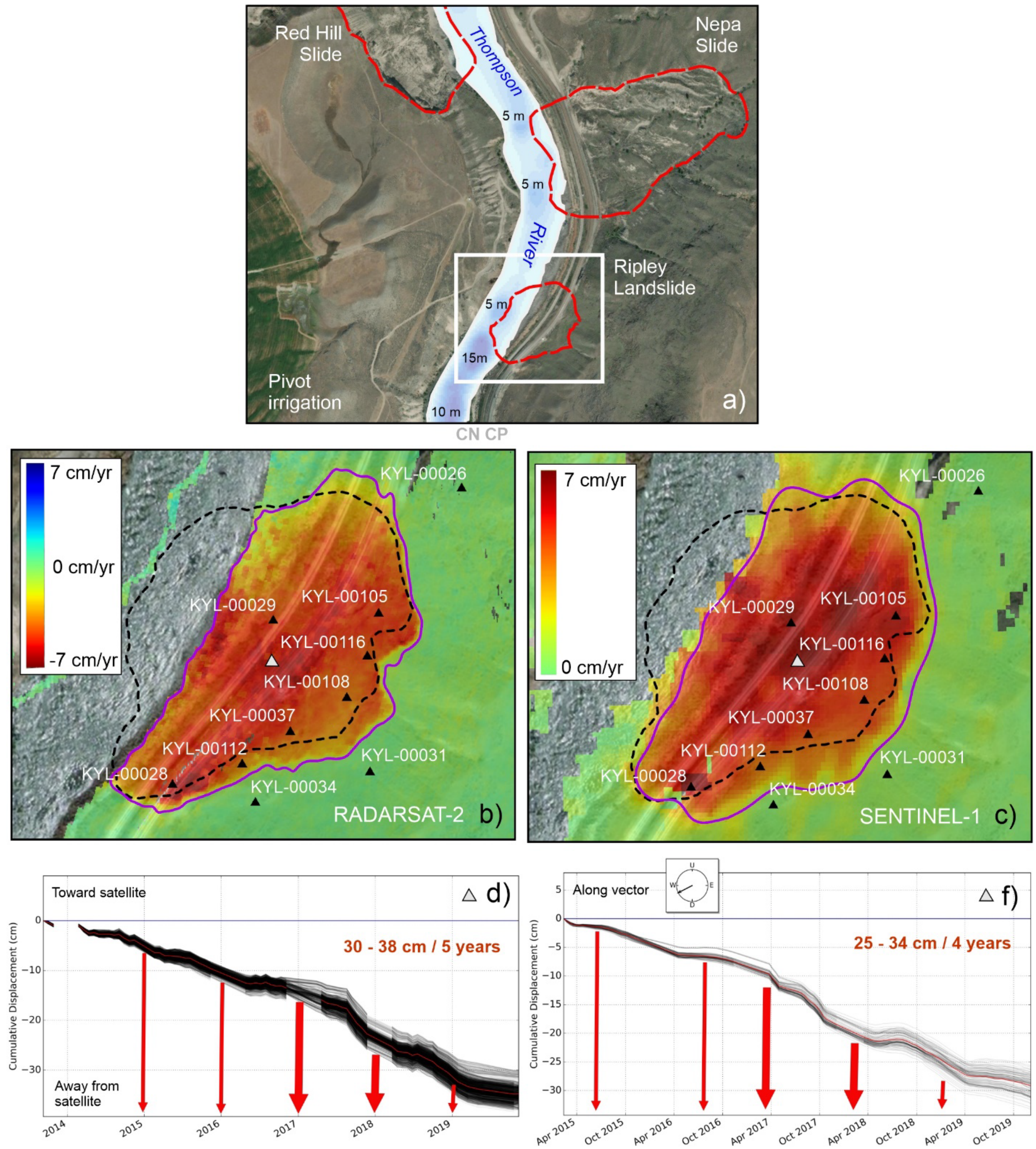

From south to north across the main slide body east of the CN and CP tracks annual cumulative displacements and surface displacement vectors for 2019-2020 vary from 6.8 cm yr^{-1} WNW (GCP-12) to 8.2 cm yr^{-1} NW (GCP-10) (**Figure 12**). West of the railway right-of-way, across the slide toe, greatest amount of annual cumulative displacement, 7.4 cm yr^{-1}, occurs in the middle of the toe slope (GCP-9) with a surface vector to the NW. At the southern flank of the slide toe, adjacent to a 15 m-deep depression interpreted as a scour pool (Huntley et al. 2021c), the toe slope is moving at 6.7 cm yr^{-1} NW. This displacement is contributing to sagging and deformation of the CP lock-block retaining wall 10 m to the

SE of GCP 9. At the northern limit of the toe slope, the annual cumulative displacement is 6.8 cm yr^{-1} and NW surface displacement vector (**Figure 12**). A 21.4 cm yr^{-1} displacement to the SE recorded at GCP-14 is attributed to disturbance of the GCP during routine track maintenance (e.g., addition of ballast and track realignment). Comparing GNSS displacement vectors with RS2 and S1 LoS vectors shows that east- and west-ranging satellites capture only a component of true slope displacement, however that the measured displacement rates along comparable displacement vectors is comparable.

3.2.2 North Slide

As an active landform (**Figure 10**; **Figure 13a**), the North Slide "Solar Slump" offers an ideal case study for assessing the improved operational capabilities of SAR technology, and for testing whether satellite InSAR can be effectively employed for the rapid identification of changes in landslide activity and deformation trends. Persistent scatterer interferometry of RS2 image stacks from 2013 to 2015 coarsely defined the area of displacement, and identified displacement of coherent targets indicating LoS deformation rates in excess of 5 cm yr^{-1} (Journault et al. 2016; Huntley et al. 2017b; Journault et al. 2018).

Change detection with RS2 and S1

The "Solar Slump" is clearly visible on RS2 and S1 processed deformation rate maps, scaled at 3 cm and 15 cm yr^{-1} (**Figure 13b-d**). Purple contours denote areas with significant displacement detected at the 4-sigma level. Most of the toe slope is detected at 4-sigma significance in both data sets (Pon et al. 2020). A 400 m long and 75 m wide section of the toe slope is observed to be undergoing displacement, with 4-sigma confidence, in both the RS2 and S1 data. The mean cumulative displacement rate in this area ranges from 7 to 15 cm yr^{-1}. An additional 200 m long section of the toe slope, located further to the south west, is detected displacing at 1 to 2 cm yr^{-1} at the 4-sigma level in the RS2 data.

Interferograms of the North Slide toe slope are highly complex, and show significant temporal variability (Pon et al. 2020). Displacement rates are likely underestimated due to aliasing in the 12-day to 24-day interferograms. There are periods of slower displacement where the short-term interferograms are not aliased. RS2 and S1 average displacement rates are likely greater than 15 cm yr^{-1}. In addition, displacement missed during data gaps >40 days influence the final derived cumulative rates (**Figure 13e, f**). Although rates can be much higher for smaller portions of time, average S1 displacement does not exceed 10 cm yr^{-1} (**Figure 13b**); whereas the maximum RS2 displacement rate is 15 cm yr^{-1} (**Figure 13d**). The S1 data indicate toe slope displacement is more westward than vertical. The floodplain toe bulge does not show significant displacement in either data set.

The "Solar Slump" time-series for the RS2 and S1 data reveal seasonal patterns to displacement and rates of movement (**Figure 13e, f**). The RS2 data show that the toe slope was particularly active in 2014 from July to November, with displacement rates exceeding 40 cm yr^{-1}. August to October 2017 also showed increased displacement in the RS2 and S1 data, with rates exceeding 40 cm yr^{-1} and 20 cm yr^{-1}. A sustained period of displacement, with rates approaching 30 cm yr^{-1} in the RS2 data and 20 cm yr^{-1} in the S1 data is observed from June 2018 and March 2019. Displacement rates increased to 15 cm yr^{-1} between July and November 2019. When combined with the mean monthly discharge values for Thompson River measured at Spences Bridge (**Figure 1a**; https://wateroffice.ec.gc.ca/ [URL 2020]), a strong correlation between the timing and amount of ground movement and river level becomes apparent (**Figure 14a, b**).

Figure 12 RTK-GNSS change detection of ground control points (GCPs) across Ripley Landslide from September 2019 to September 2020.

The RS2 data in 2014 measured an interval of increased displacement from May to November (**Figure 14a, b**), with a peak displacement velocity of 42 cm yr^{-1} occurring in August (**Figure 14a**). For 2015, RS2 recorded increased displacement between January and November, spanning the rising and falling river levels (**Figure 14a**). In April, a peak displacement velocity of 24 cm yr^{-1} occurred as water rose 1 m above the March low discharge level. An interval of increased ground movement, up to 22 cm yr^{-1}, is recorded between August and September (**Figure 13a**) as discharge falls (**Figure 14a**).

The S1 data indicate increased displacement from May to November, with peaks in displacement velocity at 10 cm yr^{-1} coincident with high water levels in June, and in October as discharge falls (**Figure 14a**). RS2 data in 2016 record increased displacement from April to November, with a peak ground velocity of 30 cm yr^{-1} occurring in August (**Figure 13c, e**). For S1 data, increased displacement rates occur between May and December, with an August peak displacement estimated at 9 cm yr^{-1} (**Figure 13b, f**).

Figure 13 RS2 and S1 InSAR results for the North Slide "Solar Slump". **a)** Thompson River valley showing extent of the North Slide (dashed red lines line). **b)** S1 average linear displacement rate over the North Slide, scaled at 3 cm yr^{-1}, with purple polygon delimiting 4-sigma confidence levels; showing extent of the North Slide (dashed black lines line), CN and CP tracks (solid black lines). **c)** RS2 average linear displacement rate rastered at 3 cm yr^{-1}, with purple polygon delimiting 4-sigma confidence levels. **d)** RS2 cumulative displacement rates rastered at 10 cm yr^{-1}, with purple polygon delimiting 4-sigma confidence levels. White boxes delimit the area of comparison between RS2, S1 and RCM datasets. **e)** RS2 LoS average cumulative displacement time series (thin red line) with peak ground velocities (red arrows). **f)** S1 average cumulative displacement time series in the east-west, up-down plane (thin red line) with peak ground velocities (red arrows); inset box shows direction of motion derived from the S1 dual look InSAR analysis. Data processed by 3vGeomatics (Pon et al. 2020).

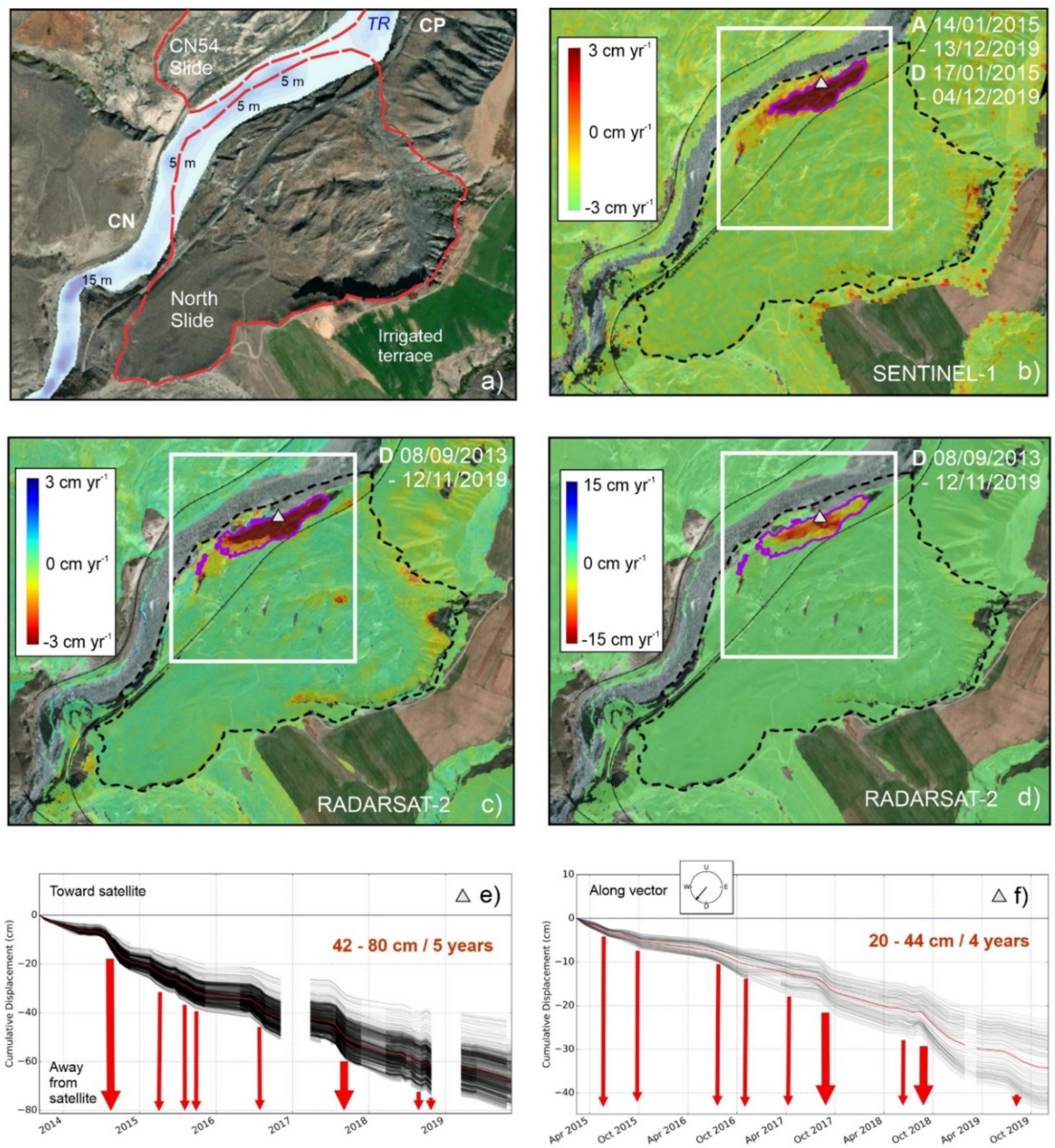

For 2017, RS2 data record increased displacement from May to November, whereas two intervals of increased displacement are resolved in the S1 data from April to June, and August to November. Both the RS2 and S1 data show a larger peak in ground displacement velocity occurring in September (**Figure 13e, f**; **Figure 14a**). The RS2 and S1 data both record two peaks in displacement velocity in 2018: in September and October/November (**Figure 13e, f**) as river stage falls (**Figure 14a**).

Change detection with RCM

Data quality was influenced by changes in vegetation, agriculture, water, rail tracks, sand and snow, especially when there were gaps of months between scenes in the time-series. RS2 and S1 images exhibited similar seasonal effects. Ice and snow cover caused spurious signals in the InSAR data, producing false positives and limiting the detection of real displacement. Scenes with >20% snow coverage were excluded from analysis. The useable, snow-free dates for useful imagery typically ranged between early March and late November. Data gaps in **Figure 13** and **Figure 14** are not just instances of missing data and snow; others are created from strong aliasing. For example, RS2 and descending S1 interferograms for winter and spring months of 2013-2014 (120 days), 2016-2017 (144 and 24 days [RS2]; 126 and 12 days [S1]) were masked because they had strong displacement. Some areas in the RS2 data showed rates up to 60 cm yr^{-1} at points in the time-series (Pon et al. 2020).

Sampling issues were solved with higher resolution (temporal and spatial) data from RCM (cf. Samsonov et al. 2017; Dudley et al. 2020). A small RCM stack from the end of August to early December 2020 was acquired. These images are acquired in both ascending and descending orbit passes (east and west-ranging) at a nominal ground resolution of 3 m with an ideal revisit frequency of 4 days. The combination of relatively high spatial and temporal resolution has the potential to resolve high rates of movement over smaller areas which would otherwise be aliased by the coarse spatial resolution of S1 or the coarse temporal resolution of RS2. For GSC-processed RCM scenes, displacement is scaled in radians (**Figure 15a, b**; **Figure 16a-d**).

RCM InSAR results reveals relatively high deformation at the North Slide from the end of August to middle September 2020. The RCM 4-day interferogram between 2020/08/26 – 2020/08/30 shows nearly a full fringe cycle (**Figure 15a b),** indicating a rapid and complex deformation pattern. This interferogram is the only system with such a short revisit time. Maximum deformation over this 4-day period is estimated to be ~2.5 cm, corresponding to a rate >200 cm yr^{-1}. Several fringes indicate movement of approximately 2 cm to 5 cm over 28-day (**Figure 16a**) and 16-day periods, indicating a rapid and complex deformation pattern in the most affected zones that might not be adequately captured by RS2, S1 and RCM. RCM interferograms shown were corrected for atmospheric phase variations.

The zone of maximum displacement on the RCM, RS2 and S1 interferograms occurs less than 100 m west and northwest of the CP tracks (**Figure 15**; **Figure 16a-d**). The upslope limit of deformation extends to the CP tracks along a 100 m section in the northeast portion of the interferograms (**Figure 15**; **Figure 16a-d**). This displacement could overtime debuttress upslope slide blocks near the active track, and reactivate pre-existing failure surfaces. Continued InSAR monitoring can detect potential future activity.

Figure 14 Comparing RS2 and S1 InSAR results with Thompson River discharge time series. **a)** Discharge values for Thompson River at Spences Bridge (station 08LF051, N50º12’16” W121º23’37’), gross drainage area 55,400 km^2 (https://wateroffice.ec.gc.ca/ [URL accessed November 2020]); months spanning peak displacement period on top axis; RS2 average peak ground velocities (grey arrows); S1 average peak ground velocities (blue arrows); bold years on bottom axis indicate annual cumulative displacement >10 cm yr^{-1} in the RS2 data. **b)** RS2 cumulative displacement curve (red line), months spanning peak displacement period on top axis, RS2 average peak velocities (grey arrows), and S1 average peak ground velocities (blue arrows); plotted with yearly mean discharges (green dots), mean discharge (green line), and trend line for 2013 to 2019 (green dotted line); bold years on bottom axis indicate annual cumulative displacement >10 cm yr^{-1} in the RS2 data.

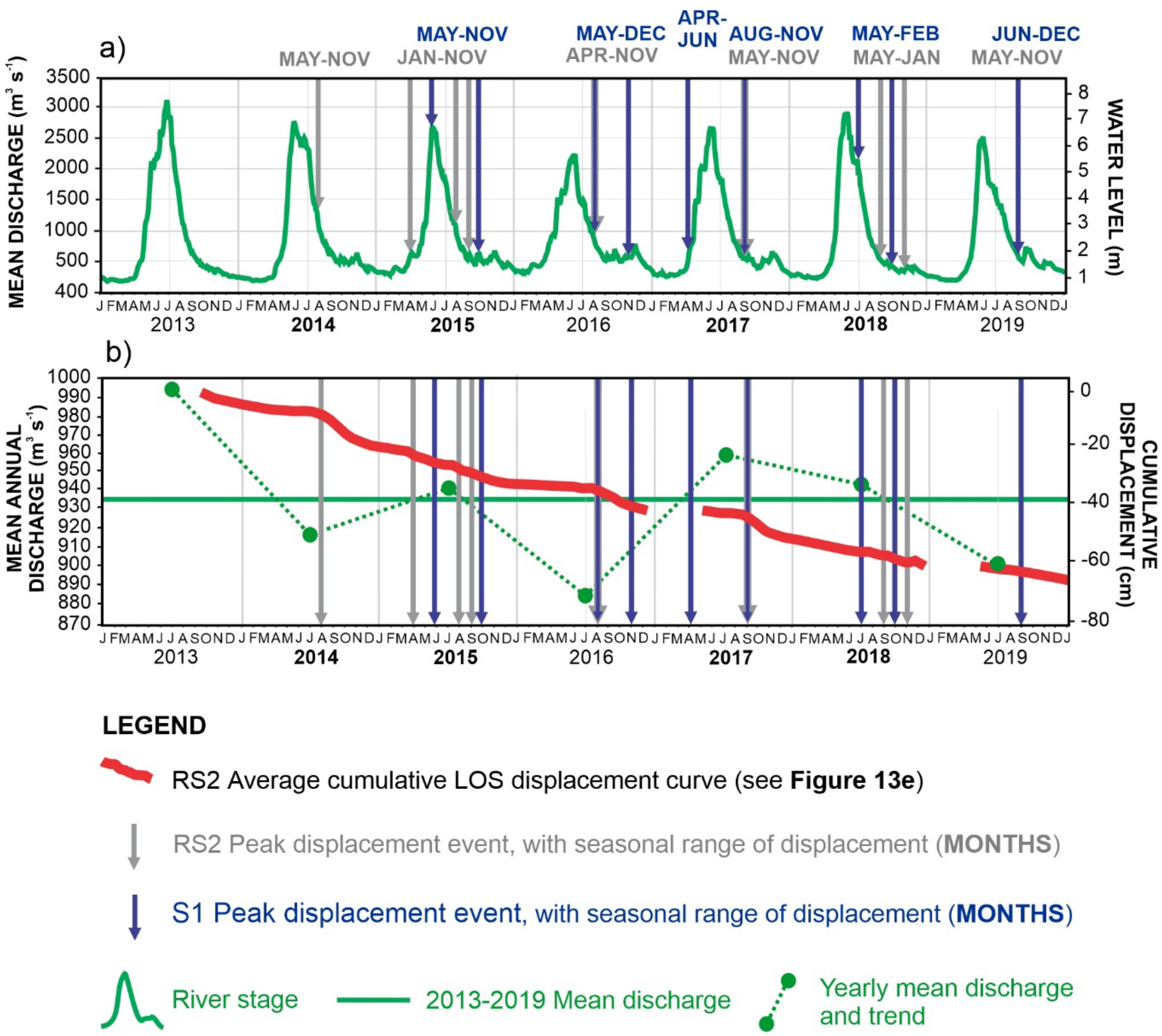

Figure 15 North Slide: **a**) extent and sectors of the landslide (see **Figure 5** for legend), showing the area of coverage by RCM discussed in text (white box). **b**) RCM 4-day interferogram showing phase change between 2020/08/26 – 2020/08/30 (4 days) with UAV derived SFM-DSM overlayed at 50% transparency for context. Interferogram shown has not been corrected for atmospheric phase variations.

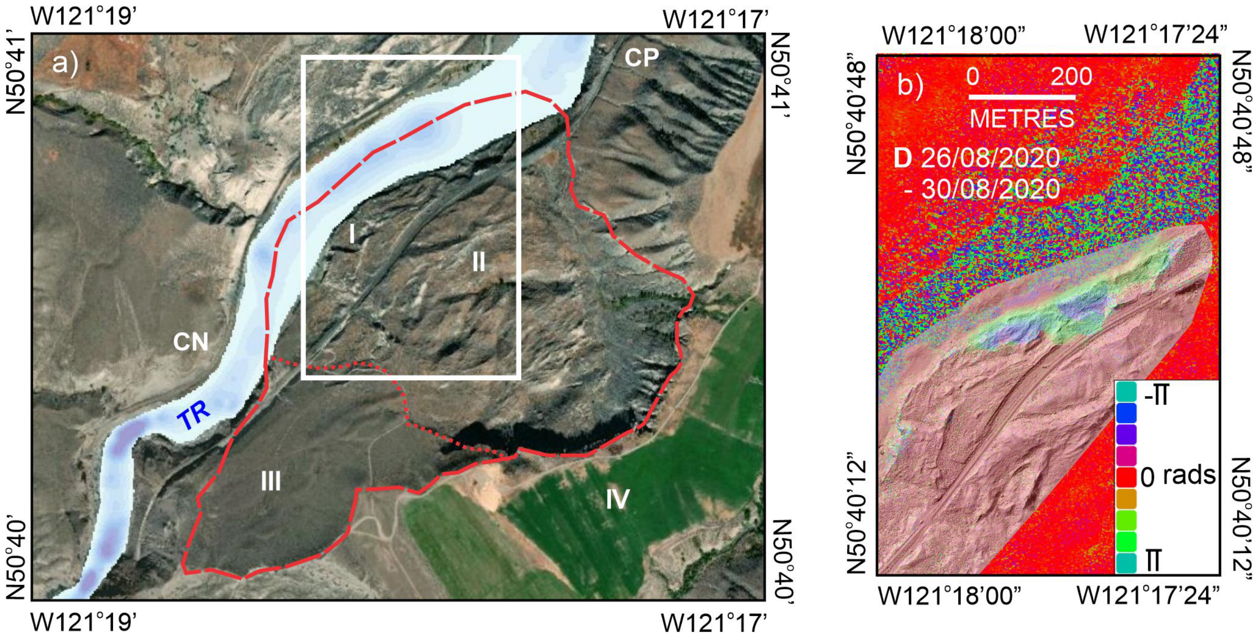

Figure 16 Comparison of RCM, RS2, and S1 interferograms. **a)** RCM 28-day interferogram, showing phase change between 2020/08/30 – 2020/09/11 (28 days), **b**) RS2 interferogram showing phase change between 2018/08/10 – 2018/09/03 (24 days). **c**) RCM interferograms showing phase change between 2020/08/14 – 2020/08/30 (16 days). **d**) S1 interferogram showing phase change between 2020/08/17 – 2020/08/29 (12 days). The UAV-derived SFM-DSM is overlayed at 50% transparency for context. Interferograms shown have not been corrected for atmospheric phase variations.

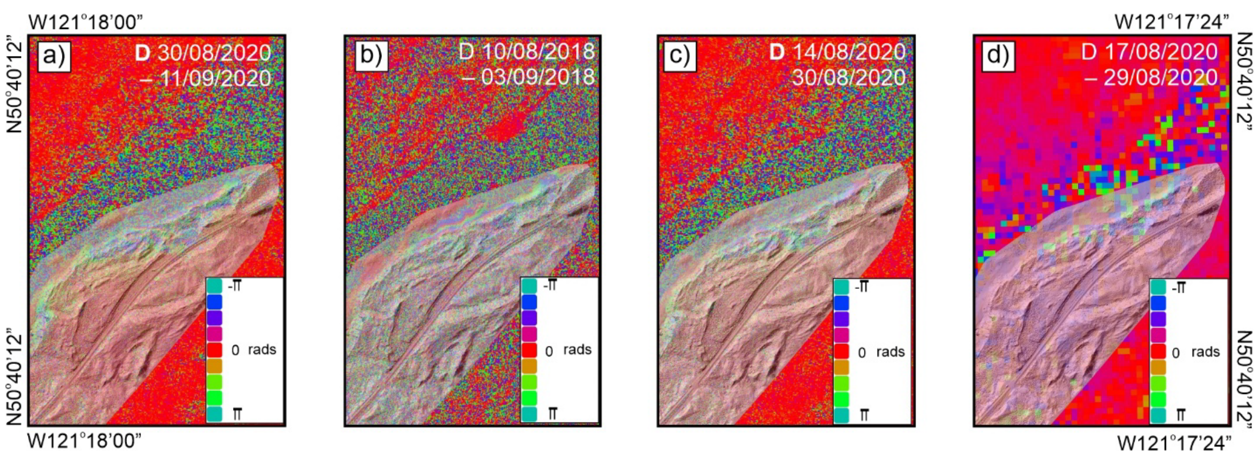

Benchmark Surveys

Bathymetric survey: The March 2015 single-beam river survey revealed variations in channel bed composition ranging from sand and silt draping bedrock to coarse gravel and boulders overlying clay-rich valley fill adjacent to the toe slope of North Slide. Shallow waters (riffles) with rapids lie adjacent to stable terrain, separated by deep scour pools (up to 5 m below river level) incised adjacent to the active slide toe (**Figure 17**).

RTK-GNSS survey: A total of twelve GCPs are positioned on stable boulders across the North Slide toe slope and active floodplain (**Table 8**; **Figure 17**). Measurement precision and accuracy discounts points showing <3 cm yr^{-1} or less movement (NS-1, NS-2, NS-3, NS-4, NS-5, NS-6, NS-10 and NS-11). Between 2019 and 2020, NS-3 moved 3 cm to the southwest. This unusual vector is attributed to displacement of the GCP at the crest of a gully by wildlife. In contrast, those GCPs with annual differences of ≥3 cm yr^{-1} are considered robust measurements, as this is the precision limit for RTK-GNSS monitoring. GCPs NS-7, NS-8 and NS-9 show displacement vectors to the north-northwest. Maximum annual displacement values of 15.77 cm yr^{-1} (NS-8) and 20.40 cm yr^{-1} (NS-7) are very similar to the estimates from RS2 and S1 InSAR datasets (see above). Significantly, the displacement vectors indicate movement toward the scour pools lying adjacent to the "Solar Slump" (**Figure 17**). Although these values are a little higher than typically seen with InSAR, this is understandable since the RTK-GNSS shows significant northward motion that is only partly captured by up/down/E/W sensitive InSAR.

Table 8 North Slide ground control points (WGS84 datum, Universal Transverse Mercator projection) for September 2019 and September 2020. *NS-12 location added in 2020 to capture displacement of the river toe bulge.

GCP number	September 2019			GCP number	September 2020		
	Easting	Northing	Elevation		Easting	Northing	Elevation
NS-1	5614632.796	619972.723	304.106	NS-1	5614632.779	619972.734	304.468
NS-2	5614778.667	620066.501	305.014	NS-2	5614778.665	620066.508	305.376
NS-3	5614884.893	620151.243	308.377	NS-3	5614884.875	620151.219	308.725
NS-4	5614950.7	620196.822	308.029	NS-4	5614950.702	620196.826	308.382
NS-5	5615032.301	620198.938	300.447	NS-5	5615032.3	620198.95	300.794
NS-6	5615062.16	620202.244	297.91	NS-6	5615062.171	620202.259	298.251
NS-7	5615088.67	620186.019	291.501	NS-7	5615088.853	620185.929	291.645
NS-8	5615068.315	620127.335	287.554	NS-8	5615068.467	620127.293	287.702
NS-9	5615052.564	620072.899	286.149	NS-9	5615052.597	620072.89	286.497
NS-10	5614968.184	620042.442	293.253	NS-10	5614968.186	620042.443	293.606
NS-11	5615005.536	620092.757	296.681	NS-11	5615005.542	620092.765	297.035
				NS-12*	5615146.213	620138.065	276.785

UAV survey: The merged mosaic and DSM captures the surface condition of the North Slide, including the "Solar Slump", and the extent of bare earth and vegetation growth (e.g., grasses, shrubs, and trees) in September 2019. Metre-scale anthropogenic features (e.g., train tracks, signals bungalow, solar panel array) are resolvable in high resolution raster imagery (**Figure 18a, b**). Relevant geomorphic features visible in the 2019 UAV oblique aerial photogram include: terraces at an elevation of 300 m asl, with steep river-cut scarps; ephemeral gullies draining the inactive 19th Century slide surface; active slide scarps across the "Solar Slump"; and the landslide toe bulge in the active floodplain of Thompson River (**Figure 18a**). These features are provisionally mapped in plan along with the location of the GCPs in **Figure 18b**. Southeast and upslope of the CP tracks, retrogressive translational back-rotated slide blocks and scarps from the 1880 landslide are now subdued features due to 140 years of wind deflation, soil creep, and surface runoff. Slopes ≥12^{o} are draped in a veneer of colluvium derived from till and glaciolacustrine sediments. The historical landslide and active "Solar Slump" are gullied by ephemeral streams, and drain to a coarse alluvial fan prograding into Thompson River along the western margin of the toe slope (**Figure 18a**).

Figure 17 Location and vectors of North Slide GCPs. GCPs with significant annual displacement (≥3.00 cm y^{-1}) are indicated. March 2015 bathymetric survey data (Huntley et al. 2018b) merged with hill-shaded ASTER GDEM v2 worldwide elevation data (1 arc-second resolution) with Worldview Imagery in Global Mapper ™.

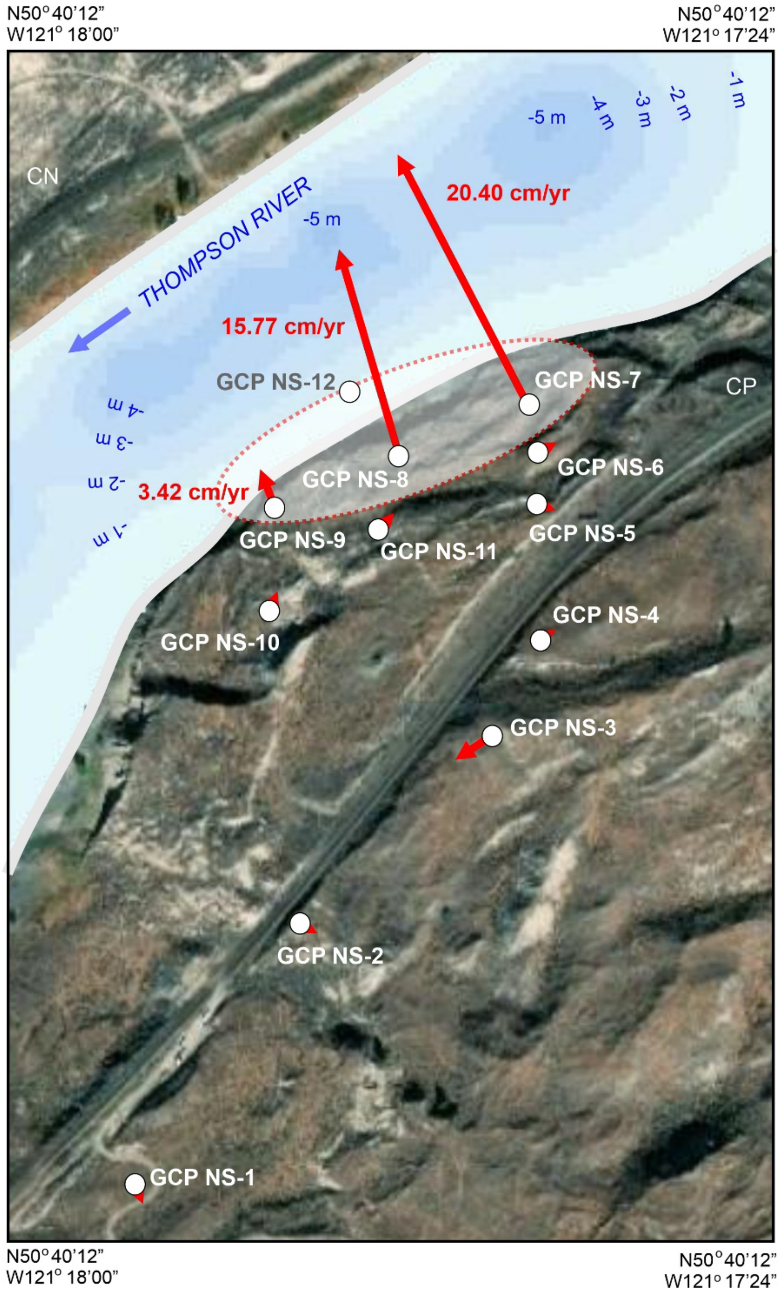

The DSM clearly shows that across the "Solar Slump", landslide scarps form subparallel to the orientation of the river channel (**Figure 18b**). In the north, cutbank erosion along a 200 m section of Thompson River has exposed and triggered a series of slumps in terraced glaciolacustrine and till deposits below 280 m asl. These small slumps (⩽ 50 m^2) are not directly impacting railway infrastructure, but are contributing to slope unloading. In the northwest, landslide scarps follow the arc of relict back-rotated slide blocks (GCPs NS-5, NS-6, NS-10, NS-11), and increase in size and activity toward the river (GCPs NS-7, NS-8 and NS-

9). Monitoring stations in the vicinity of the railway track (i.e. GCPs NS-3, NS-4, NS-5, NS-6, NS-11) show ⩽ 3 cm yr^{-1} of movement (**Figure 18b**). Landslide back scarps and tension cracks on the DSM are extrapolated beneath railway ballast close to the solar panel array and signals bungalow (between GCPs NS-4 and NS-5).

Figure 18 Baseline September 2019 UAV results. **a)** Oblique UAV photo mosaic generated with Pix4D Mapper structure from motion (SfM) software. **b)** Plan view of the "Solar Slump" showing distribution of terrace and landslide scarps, ephemeral gullies, and GCPs across the slide toe. Inset map shows location of the "Solar Slump" with respect to the North Slide main body and head scarp (outlined in red dashed line).

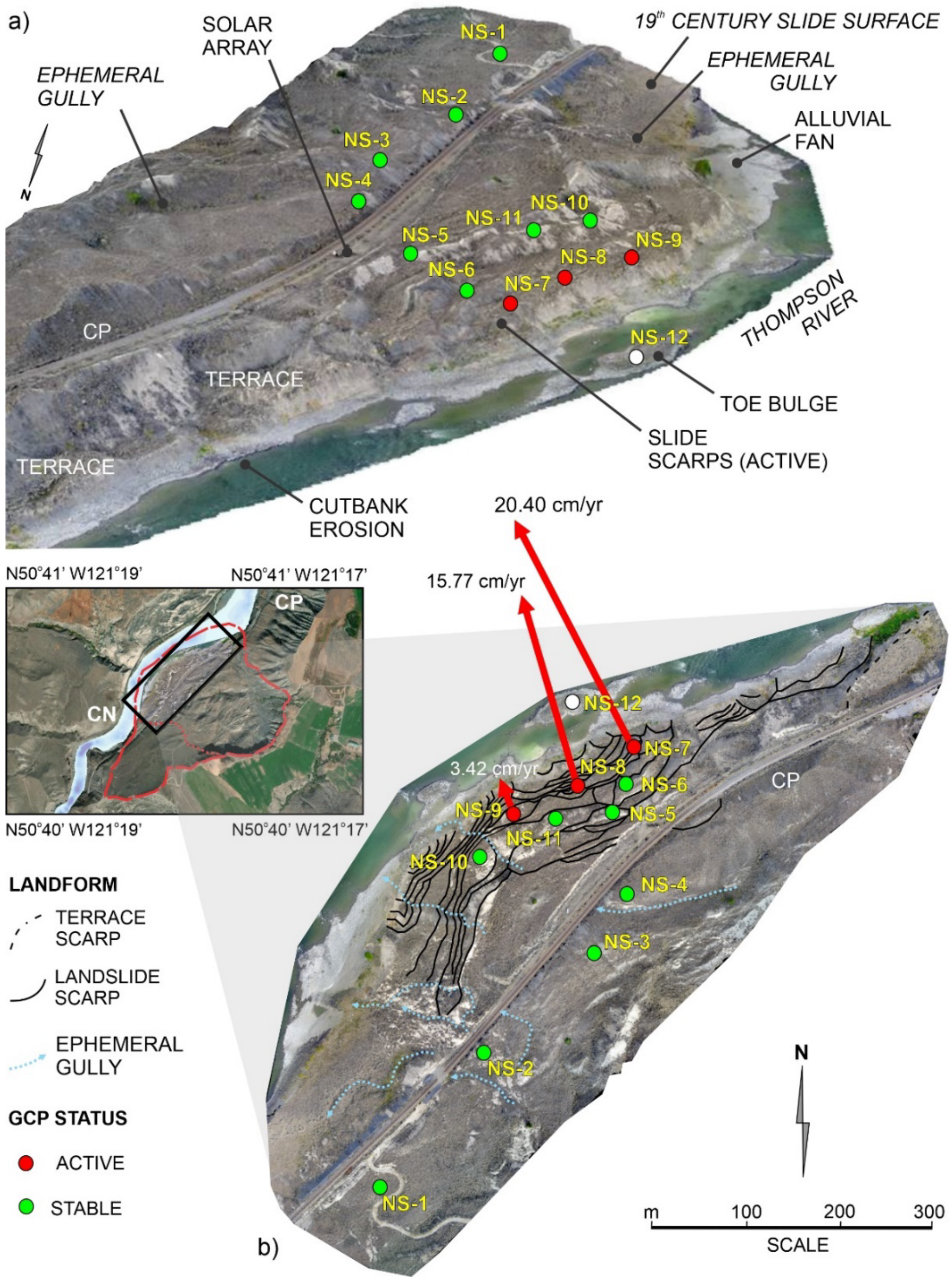

InSAR raster images and UAV DSMs (**Figures 13 to 18**) all show significant displacement encroaching on rail infrastructure less than 100 m downslope of the CP tracks. No significant movement is indicated between these GCPs between the 2019 and 2020 RTK-GNSS measurements (**Figure 17**; **Figure 18**), suggesting the zone of potential displacement does not extend more than 50 m upslope of the tracks. Indistinct slide scarps extending across the western toe slope correspond to the narrow zones of high LoS displacement in the RS2, S1 and RCM SAR datasets (**Figures 13-18**).

3.2.3 Other Thompson River Valley Landslides

Goddard Slide

Active slope movement is observed along the Goddard Slide toe slope, and this movement is adjacent to a 15 m-deep depression in Thompson River interpreted as a scour pool (**Figure 10**; **Figure 19**). The remaining areas of the slide show no evidence of significant displacement relative to data noise. For the area of activity, RS2 and S1 datasets show a seasonal fluctuation in displacement rate with accelerated movement from late summer through to early winter. For RS2, the average linear displacement rate from 2014-2019 ranged from 2.8 cm yr^{-1} to 7.6 cm yr^{-1}. Lower displacement values were derived from S1 datasets, ranging from 1.0 cm yr^{-1} to 2.7 cm yr^{-1} (Pon et al. 2020).

Figure 19 Goddard Slide: average 1D line-of-sight (LoS) linear displacement scaled at 3 cm yr^{-1}; grey triangle indicates where LoS measurements were calculated; purple polygon delimits significant displacement (>3 cm yr^{-1}) at the 4-sigma confidence level (Pon et al. 2020). Bathymetric data (Huntley et al. 2018b) merged with Worldview image in Global Mapper ™.

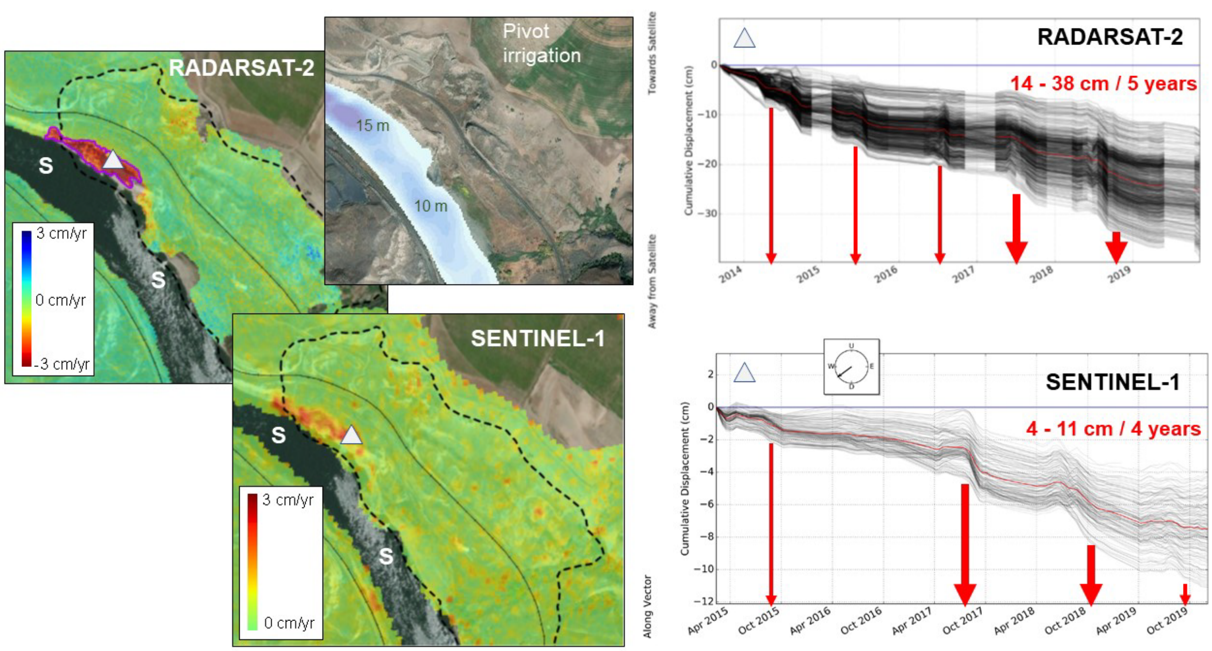

South Slide

Northern portions of the South Slide show no evidence of significant slope displacement relative to data noise. However, the South Slide south extension (area delineated in purple in **Figure 20**), which includes a reactivated portion of an ancient feature, displays a linear displacement trend. For RS2, the average linear displacement rate from 2014-2019 ranged between 2.4 cm yr^{-1} and 4.2 cm yr^{-1}; similarly, S1 linear displacement values ranged from 3 cm yr^{-1} to 4 cm yr^{-1} (Pon et al. 2020).

Figure 20 South Slide south extension: average 1D line-of-sight (LoS) linear displacement scaled at 3 cm yr^{-1}; grey triangle indicates where LoS measurements were calculated; purple polygon delimits significant displacement (>3 cm yr^{-1}) at the 4-sigma confidence level (Pon et al. 2020). Bathymetric data (Huntley et al. 2018b) merged with Worldview image in Global Mapper ™.

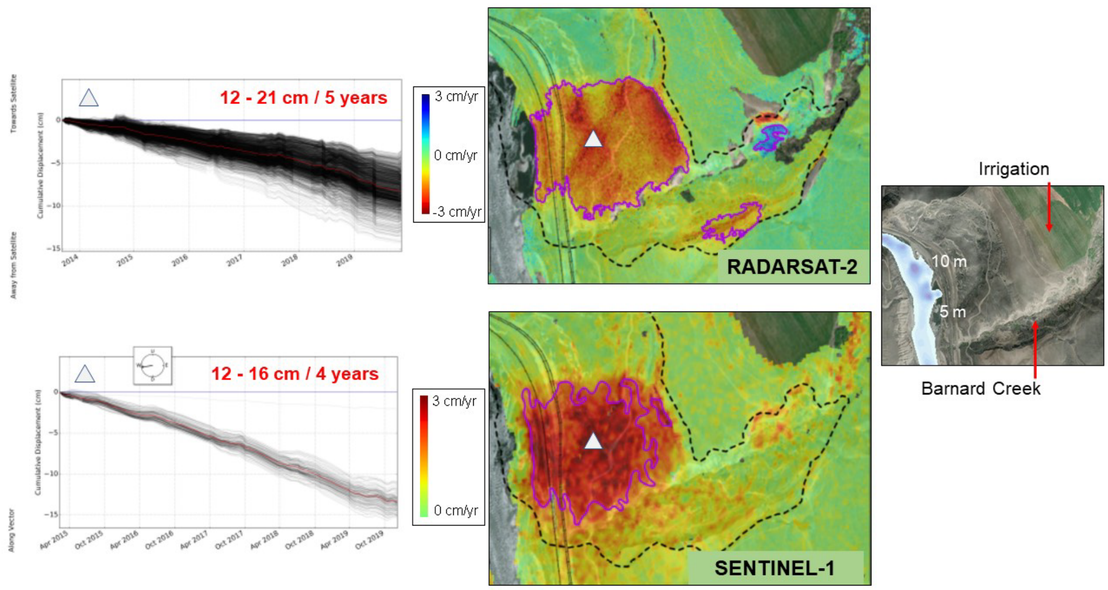

Red Hill Slide

The Red Hill Slide is the most active landslide in the Thompson River valley and displays a linear displacement trend over a large portion of the landslide from 2014-2019 (**Figure 21**). For RS2, the average linear displacement rate from 2014-2019 ranged from 6.8 cm yr^{-1} to 10.4 cm yr^{-1}. Higher displacement values ranging from 9.7 cm yr^{-1} to 13.5 cm yr^{-1} were derived from S1 datasets (Pon et al. 2020).

3.2.4 Assiniboine River Valley

Ground-based studies were abandoned in 2020-2021, limiting the acquisition of landslide information to remote sensing platforms and desktop analysis of benchmark GNSS and UAV datasets collected in 2019. RCM has been tasked to collect C-band SAR as the satellite passes over the Assiniboine River valley.

A 12-day interferogram of the Miniota, MN area (**Figure 1d**) from February 7th to 19th 2021 is shown in **Figure 22**. Most of the phase anomalies are surrounding bodies of water confined to meltwater spillways on the prairie plains, springs rising along valley and coulee sidewalls, or on the Assiniboine River floodplain. Given the time of year (winter), these anomalies are likely caused by freezing action rather than ground deformation (**Figure 22**). Phase anomalies along the crest of the Assiniboine River valley east of the CN track are associated with dense stands of oak, birch, and aspen. These deciduous wooded areas were likely accumulating snow over the period of the interferogram. Come spring, snowmelt along the crest and upper valley slopes will contribute to saturated ground conditions, surface runoff, gulley flow, and increase spring discharge adjacent to the CN track. At this point, no information on landslide activity has been captured.

Figure 21 Red Hill (1928) Slide: average 1D line-of-sight (LoS) linear displacement scaled at 3 cm yr^{-1}; grey triangle indicates where LoS measurements were calculated; purple polygon delimits significant displacement (>3 cm yr^{-1}) at the 4-sigma confidence level (Pon et al. 2020). Bathymetric data (Huntley et al. 2018b) merged with Worldview image in Global Mapper ™.

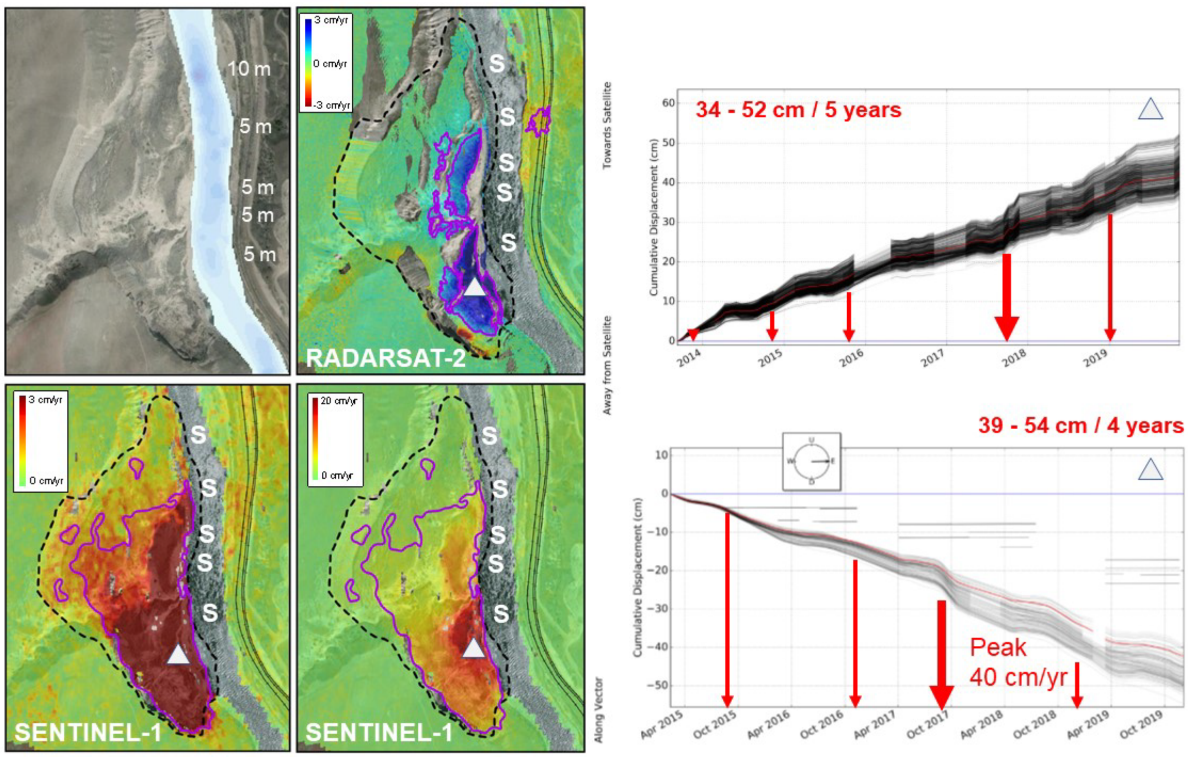

Figure 22 RCM 12-day interferogram of the Miniota, MN area (07-02-21 to 19-02-21), merged with ASTER GDEM v2 worldwide elevation data (1 arc-second resolution) and Worldview Imagery in Global Mapper ™ using a Universal Transverse Mercator projection with the Google Maps (sphere radius 6378137) datum.

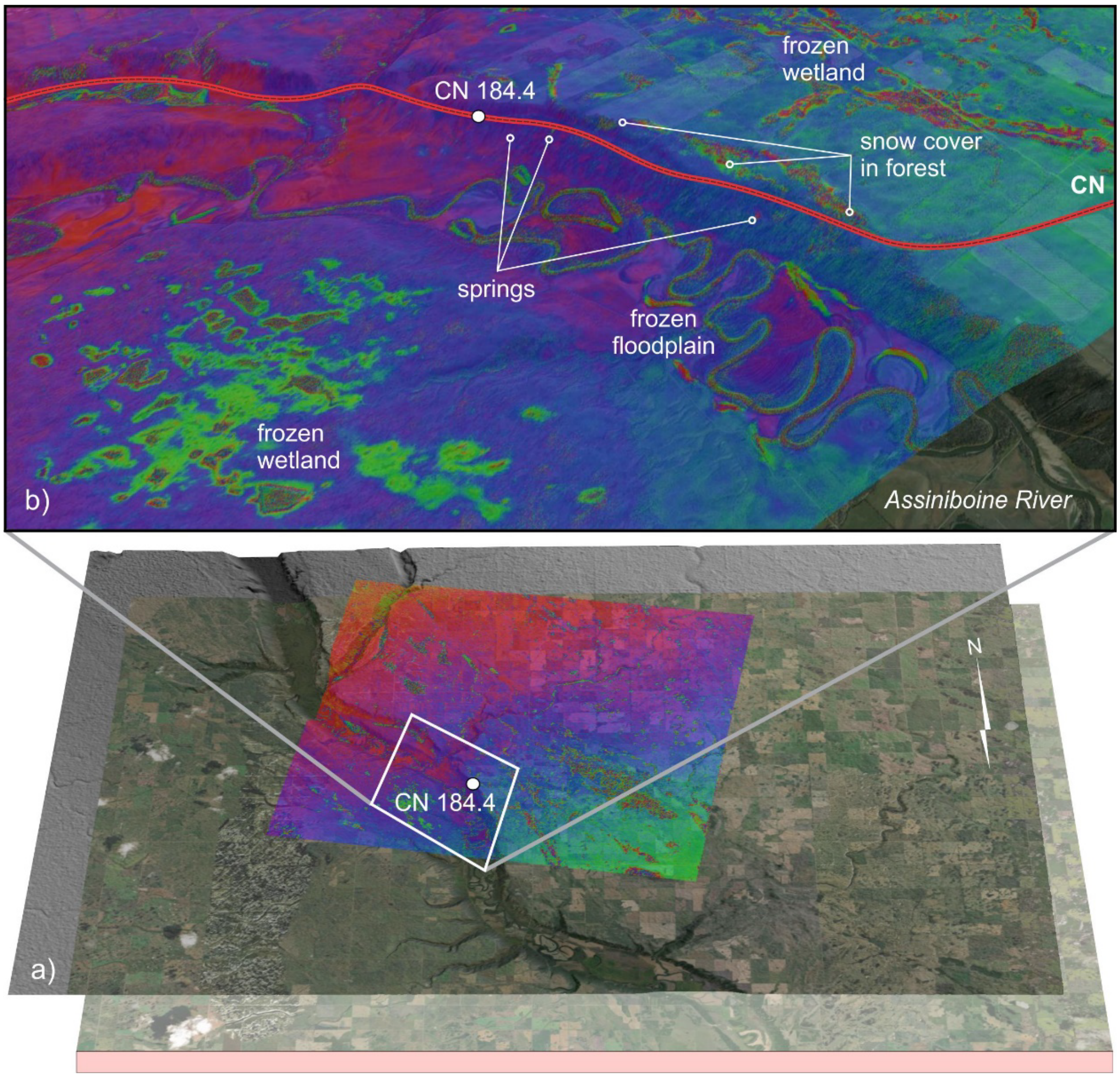

4. SYNTHESIS: GEOHAZARD MODEL

GNSS-benchmarked InSAR results for Ripley Landslide and North Slide provide foundational insight for understanding past and current behaviour, and predicting future activity of landslides in the Thompson River transportation corridor. Knowledge of the geographic distribution and temporal range of earth materials, geological hazards, and their potential responses to climate change are essential to minimize hazards and ensure a resilient railway transportation network, protection of natural resources and the environment, the safety and security of local communities, land-use practices, and the national economy. Research by the GSC as part of IMOU-5170 and ICL-IPL Project 202 focuses on assessing innovative methods for monitoring landslides.

4.1 Landslide monitoring

This study improves the spatial and temporal resolution of displacement of landslides in the Thompson River railway transportation corridor (**Figure 1a, b**). Our research and development demonstrates that spaceborne InSAR methods can effectively identify and monitor creeping slopes that stakeholders (e.g., CN, CP and TC) should be watching. Processed InSAR datasets, benchmarked against ground-based RTK-GNSS measurements and UAV photogrammetry, once incorporated in geohazard reduction tools, can alert stakeholders of landslide displacement events that could unacceptably damage track and stop train service. In addition, these datasets can be related to other monitoring information (e.g. precipitation, groundwater), and provides a basis for understanding landslide mechanisms.

The remote monitoring approaches generally agreed in terms of measured creep rates, indicating confidence in these approaches for landslide monitoring. The resolution of InSAR monitoring (cm yr^{-1}) and areal coverage makes it very useful for widespread surface monitoring of creeping landslides. This approach is of particular importance for management of linear infrastructures, which can often span multiple slopes. LiDAR change detection has error typically in the range of decimeters, which precludes this approach from detecting landslides moving at creep rates over sub-annual time-scales. Slope Inclinometers or extensometers are really the only other strategies that have the potential to measure creeping landslides at these time scales, but are costly to install and operate, only cover a point location on surface, and are subject to damage (e.g. shearing).

Peak surface displacement values strongly correspond to changes in river surface elevation (and water depth) over the submerged toe slope, active flood plain, and along steep channel banks. For the 2013-2019 InSAR and GNSS time-series, ground displacement events occur while river levels are at their lowest between February and March, but before rising to peak in June; or after July until November while storm-fed river levels progressively fall until the next winter minimum (**Figure 14**; **Figure 18**). Small surface displacements occur when average annual discharge is $\leq$900 m^3 s^{-1}. Increased surface displacement occurs when average annual discharges are well above 900 m^3 s^{-1} (**Figure 18e, f**).

These results confirm the suitability of RS2 and S1 InSAR time-series analyses for historical and active displacement monitoring of landslide hazards. There are limitations to change detection monitoring of landslides with spaceborne platforms. InSAR does not perform well in snow, so the quality of monitoring is subject to local weather conditions. For the Thompson River valley, the GSC weather station provides important climate data to calibrate InSAR and other monitoring tools. Ripley Landslide (**Figure 11**), North Slide (**Figure 13**), Goddard Slide (**Figure 19**), South Slide (**Figure 20**) and Red Hill Slide (**Figure 21**) all exhibit seasonal intervals when surface displacement is too fast relative to the frequency of measurement. How quickly landslides transition from a creep state to a higher velocity is unknown, and given the RS2 and S1 return times, spaceborne InSAR monitoring could very well miss the transition on landslides of concern (**Figure 10**). In this context, RCM with operational 3-day to 4-day return times for scene acquisition, combined with automated image processing (cf. Samsonov et al. 2017; Dudley and Samsonov 2020) will be a powerful tool for change detection monitoring in the Thompson River valley, and elsewhere along national railway transportation corridors (e.g., Assiniboine River valley, Manitoba).

4.2 Landslide mechanisms

For landslides impacting critical railway infrastructure in the Thompson River valley, slope reactivation is partly related to a drawdown response to overpressure in the slope during drops in water level after high summer flow (i.e. rapid drawdown conditions), or by erosion of channel banks during flood events. Based on our current understanding, there are three slope failure scenarios for reactivated landslides along the Thompson River valley depending on geological and environmental conditions and anthropogenic activities. 1) Rapid to very rapid movement resulting from retrogressive growth along existing rupture surfaces. 2) Retrogression by sliding on rupture surfaces exposed during river incision. 3) Very slow to slow reactivation (creep) of a slide on previously developed rupture surfaces without retrogression (cf. Clague and Evans 2003; Eshraghian et al. 2007; Eshraghian et al. 2008; Hendry et al. 2015).

Annually, reactivation occurs along deep-seated rupture surfaces, and is triggered by cutbank erosion and slope unloading as the river level falls from summer peak discharge (cf. Porter et al. 2003; Eshraghian 2007; Eshraghian et al. 2008). Each year, through the peak flow period, Thompson River is continually removing colluvium from the toe slope, while high pore pressures are generated where porous glacial deposits overlie less permeable clay-rich sediments in the discharge zone at the base of the slope. River and groundwater level fluctuations (>5.6 m) between winter minimum flows to summer peak discharge change the supporting (buttressing) pressure on the slide toe slope. An increase in sustained high-volume flows through summer and fall also contributes to further incision of scour pools and channel bank erosion, exposing deeper rupture surfaces and altering the geometry of the slide toe (cf. Eshraghian et al. 2007; Eshraghian et al. 2008).

Scour holes observed in bathymetry adjacent to landslide slopes along the Thompson River Valley (**Figure 1 b**; **Figure 9**) are evidence of active channel incision. Scour holes exposing clay-rich rupture surfaces further reduce the margin of stability (cf. Eshraghian et al. 2008; Huntley et al. 2021c). Hydraulic connectivity between the river and groundwater in the toe slope is suggested by seasonal changes in discharge and pore water pressures, and upward hydraulic gradients measured in borehole piezometers (Porter et al. 2003; Eshraghian 2007; Eshraghian et al. 2008). Instability is triggered when falling river levels cause groundwater drawdown in the toe slope blocks. Acceleration begins when the river level and groundwater head on the rupture surfaces fall after mid-summer peak discharge (**Figure 6e**).

4.3 Potential landslide impacts

Conventionally, geohazard risks are defined in terms of the probability for loss, where losses can include casualties, damage to infrastructure and property, economic losses, and environmental degradation due to recurring landslides (cf. Fell 1994; Hermanns et al. 2016). The consequences of ground movement of active landslides along the Thompson River depend on the scale and rate of movement, and temporal occurrence between train passage and landslide activity. Small, incremental surface displacements, if left unfixed, contribute to track misalignment requiring short-term (seasonal) reorganization of train schedules to allow ground crews to safely add ballast and adjust the track positions. In contrast, frequent, rapid, large and widespread ground movements are a concern for railway companies, government agencies, and local communities. Larger surface displacements have the potential to cause major track misalignment, train derailment, and considerable local environmental damage. Substantial channel and slope remediation following a major retrogressive failure will require costly reorganization of transportation and shipping schedules, leading to national socioeconomic losses from service disruption.

Occurrence of rapid retrogressive landslides similar to the 19th Century North Slide event has the potential to compromise the safe and secure transport of intermodal goods through the Thompson River valley, with negative socioeconomic and environmental consequences. For example, such a landslide would destroy track infrastructure, require considerable mitigation costs, and has the potential to cause upstream flooding or a landslide-generated wave that could impact the community of Ashcroft depending on the level of river blockage or velocity of the landslide. Negative environmental consequences would include the loss of natural resources, including pink salmon runs, wildfowl, game animals, cattle and crops, and potable water for communities. Future climate warming and extreme weather events are anticipated to trigger dramatic changes in the landscape through increased slope instability, river erosion and floods (cf. Evans and Clague 1997; Sauchyn and Nelson 1999; Couture and Evans 2006; Geertsema et al. 2006; St. George 2007; Chen and Grasby 2009). Climate-driven geomorphological processes will challenge the integrity and resilience of transportation infrastructure and local communities. Although there was no clear relationship between movement events and average annual precipitation through the 20th Century (Porter et al. 2002; Tappenden 2016), an increase in frequency and magnitude of rainfall and snow fall events in response to future climate variation may change this. Increasing precipitation and higher sustained river flows will change groundwater pressures on slide rupture surfaces extending below the river.

4.4 Landslide geohazard reduction

Geotechnical solutions in the Thompson River valley railway corridor have aimed to minimize the effects of river erosion, while also preventing the development of new tension cracks. InSAR datasets show that river berm construction was only partly successful at the CN50.9 Slide, Goddard Slide, CN54 Slide, South Slide and Nepa Slide (Journault et al. 2018; Pon et al. 2020; **Figure 1b**). Construction of mitigation measures for large slow-moving slopes, such as river berms, lock-block retaining walls, or engineered slopes can have significant economic costs. Monitoring and early warning for maintenance and cautionary speed enforcement can be effective strategies for management and mitigation of landslide hazard where the cost of slope mitigation is grossly disproportional to the risk reduction benefit (cf. Bunce and Chadwick 2012; Huntley et al. 2021c). GPS monuments (Ripley Landslide) and mercury switch tip-over posts (North Slide) maintained by CP are linked to rail signals as reactive, precautionary measures to slow or stop trains. The rail grade is managed through routine maintenance and track lifting operations.

Our studies show that satellite InSAR platforms with repeat visit times of weeks (e.g., RS2 and S1) to days (e.g., RCM) provide landslide monitoring capability with cm-scale precision and accuracy when periodically benchmarked with ground-based RTK-GNSS measurements and UAV photogrammetry. This approach can be an effective tool to detect and monitor landslides across broad areas; however is subject to some limitations depending on site conditions (Section 4.1). Additional monitoring techniques (e.g slope inclinometers) can be implemented to overcome potential limitations, and build a robust monitoring and early warning system.

5. FURTHER RESEARCH PLANS (2021-2022)

Given the current trajectory of the pandemic, COVID-19 will influence the scope of research activities for the duration of IMOU-5170 (until 2025). This realignment of priorities requires an amendment to the projected activities outlined in IMOU-5170 (Huntley et al. 2020e). For 2021-2022, research activities will rely on desktop terrain analysis and remote change detection monitoring and limited on-site work in the Thompson River valley, BC, and the Assiniboine River valley, MN-SK. Going forward, geohazard mapping and change detection monitoring will rely on cloud-based high-performance computer processing of large InSAR, GNSS and other datasets (e.g., climate variables, ground moisture, borehole inclinometry, electrical resistivity) to reduce in-house computational time. Although current research is focused on test sites in the Thompson and Assiniboine river valleys, the scope of activities will be expanded into other regions of interest where critical socioeconomic infrastructure are vulnerable to geohazards and climate change (**Table 9**).

Through 2021-2022, NRCan-GSC and TC-IC will examine the impact of past and future extreme weather and climate change, while also providing new information on landslide hazards in a timely manner to ICL-IPL Project 2020 and Railway Ground Hazard Research Program (RGHRP) stakeholders (e.g., TC-IC, CN, CP, and UA). From our understanding of the behaviour of Ripley Landslide, where increases in slope activity seem to correlate with the times of the year with increased rainfall and snowmelt, future geospatial and temporal analyses will incorporate rainfall and snow melt data from the GSC weather station (**Figure 1b**). The fundamental geoscience knowledge generated through the proposed research will allow key industry stakeholders (e.g., CN and CP) and university partners (e.g., UA and USASK) to develop robust solutions to measure, manage, and mitigate landslide geohazards and their consequences.

IMOU-5170 research will have six objectives. 1) Acquisition of air photographs, satellite imagery, and other geospatial datasets for both study areas (and additional sites if necessary). 2) Developing in-house (or at-home) functionality and capability using cloud storage and processing services. 3) Developing desktop remote mapping protocols and data analyses, combining terrain studies with geospatial datasets to meet the IMOU mandate. 4) Acquisition (and installation) of climate station components (e.g., tipping-bucket rain gauge, air temperature sensor, snow depth gauge, anemometer and wind vane), borehole instruments (e.g., piezometers, inclinometers), optical, LiDAR, and hyperspectral UAV sensors, and InSAR corner reflectors. 5) Stability modelling to forecast how climate-forced changes in river levels and groundwater contribute to slope stability and potential activation of upslope blocks, and to establish thresholds for extreme river flow and associated scour. 6) Communicating research results through conferences, workshops, and publications (e.g. **Table 4**).

5.1 Remote predictive geohazard mapping

Damaging landslides caused by extreme weather, climate change, earthquakes, or anthropogenic activities can occur in all regions of Canada. With pandemic travel restrictions in place for the near future, on-site geological investigations will be limited in duration, geographic extent, and detail. Strategic selection of ground observations in BC, SK and MN in the coming years will be driven by the need to benchmark remote sensing results and site-specific monitoring datasets (e.g., boreholes and RTK-GNSS surveys). Predicting the distribution of terrain adversely impacted by landslides and other geological hazards as climate changes across Canada will greatly reduce the risks to socioeconomic recovery.

Anticipating limited field access for traditional ground-based geological and geomorphic observations, remote predictive mapping (RPM) techniques will be a research focus beginning in 2021. RPM is an efficient and cost-effective paradigm for mapping large regions in short time spans (e.g., Schetselaar et al. 2007; Behnia et al. 2012; Campbell et al. 2013; Harris and Grunsky 2015). This technique involves the compilation, iterative revision, and interpretation of multiple geoscience datasets in a geographic information system (GIS) to produce predictive geological maps.

RPM differs from traditional ground-based mapping because the compilation of map units away from control points (i.e., field observations and sample sites) is repeatedly objectively tested and calibrated against remote sensing imagery. Predictive maps *do not* represent “geological truth”, rather a best estimate of what an area represents on the ground based on interpretation of spectral signatures on different satellite imagery (Harris and Grunsky 2015). To this end, bedrock units, surficial deposits and landforms described on the ground may not correspond with their classification on predictive maps derived from satellite imagery and air photos. The volume, range, accuracy, precision of geoscience data and experience of mappers are key factors in how closely the predictive map corresponds to geological patterns obtained by field mapping.

RPM will employ machine-learning algorithms applied to high spatial resolution optical and multi/hyperspectral satellite imagery. Like traditional field mapping, the successful recognition and extraction of geological information is a learning process based on experience in interpreting image data in a variety of physiographic and geological settings. The RCM process uses an algorithm that randomly and repeatedly samples training areas (or regions of interest), then cross-validates the classification results.

5.1.1 RPM approach

RPM requires the acquisition, processing, and geological interpretation of available remotely sensed data sets, in addition to legacy geological and topographic data compiled in a GIS (cf. Schetselaar et al. 2007; Behnia et al. 2012; Campbell et al. 2013; Harris and Grunsky 2015). Predictive maps would be generated by combining enhanced and fused remotely sensed data with expert interpretation of field–based observations and samples, and visually extracted geological information from printed hard copy maps. Commercially available image processing and analysis software packages (e.g., ArcMap™ and ENVI™) would be employed to produce *unsupervised* remote predictive maps by repetitive sampling of satellite image files. When software and statistical analyses are used in consort with expert input from geologists, more reliable *supervised* remote predictive maps are produced.

5.1.2 Landslide susceptibility mapping

An updated 1:20,000,000-scale map landslide-susceptibility map (cf. Bobrowsky, and Dominguez 2012) could be derived from the RPM activity and reclassification of GSC Map 1880A (Fulton, 1995) using the new GSC surficial geology data model (Deblonde et al. 2018). To create landslide susceptibility units of a size appropriate for publication, adjacent similar polygons would be merged in ArcGIS™. The result digital map product would be a tool to be used to guide researcher interpretations of national scale DInSAR monitoring results (see below); and for risk managers to use to help minimize damage to critical infrastructure and injury or loss of life resulting from landslides and related geological hazards.

5.1.3 Ground studies

An accurate and precise supervised remote predictive geohazard map using a robust classification algorithm requires training areas be carefully selected to be as spectrally homogenous as possible. However, at regional scales of mapping, many earth materials can experience wide ranges in moisture saturation, temperature, vegetation cover, bedrock geology, and other factors that can result in spectral heterogeneity on different satellite images and stereo-pair air photos taken over several years and at different seasons.

Landforms and surficial deposits with similar textures and clast contents but quite different depositional environments can appear spectrally similar on individual images. Determining a genetic origin for earth material deposits from the spectral signatures of satellite images, stereo-pair air photos, or UAV DSMs alone is not possible. Corroborating ground-based benchmark observations of earth material textures and composition, associated landforms, and vegetation cover are essential to robust RPM (**Table 9**).

Table 9 Geohazard mapping activities of IMOU-5170: RPM, field studies, and procurements planned for 2021-2022. GSC-WS1, GSC-WS2 and GSC-WS3 are total weather stations.

Transportation Corridor	Landslide Hazards	Vulnerable Infrastructure	RPM Datasets	Field Activities
CN and CP corridor, Thompson River valley, BC	Large, slow landslides Small rapid debris flows Small rapid rock falls	Railways Highways Agriculture Potable water	LANDSAT SPOT Other imagery	*Field observations of:* Bedrock lithologies Geological structure Surficial deposits Landform inventory Soil moisture Groundwater Geophysics (ERT)
CN and CP corridors, Assiniboine River valley, MN-SK	Large, slow landslides Small rapid debris flows	Railways Highways Pipelines Power lines Reservoirs Agriculture		*Field observations of:* Bedrock lithologies Geological structure Surficial deposits Landform inventory Soil moisture Groundwater *Procurement of* ERT system
CN/CP spur lines, Kelowna and Okanagan Valley, BC	Large, slow landslides Small rapid debris flows Small rapid rock falls	Railways Highways Pipelines Powerlines Reservoirs Urban land use Agriculture Light industry		*Field observations of:* Bedrock lithologies Geological structure Surficial deposits Landform inventory Soil moisture Groundwater Geophysical (seismic)
Kitimat-Terrace-Prince Rupert Corridor	Small rapid landslides Large rapid rock falls Large debris torrents Tsunamis	Railways Highways Pipelines Powerlines Urban land use Heavy industry Marine uses		*Field observations of:* Bedrock lithologies Geological structure Surficial deposits Landform inventory Soil moisture Geophysical (seismic)

5.2 Change detection monitoring

5.2.1 InSAR monitoring

With future climate change, railway infrastructure and operations are expected to face unique challenges in design, monitoring, adaptation, mitigation, reclamation, and restoration. Satellite SAR change detection monitoring and early warning for maintenance and cautionary speed enforcement are considered effective strategies for hazard management given the economic costs, and environmental consequences of attempting to stabilize active slopes (**Table 10**).

Highly accurate cumulative deformation and rate measurements cannot be determined from the analysis of single interferograms. The combination of relatively high spatial and temporal resolution offered by RCM resolves rapid movement over small areas that would otherwise be aliased by the coarser spatial and temporal resolution of RS2 and S1. In this context, RCM with operational 3 to 4-day return times for scene acquisition, combined with automated image processing (cf. Samsonov et al. 2017; Dudley et al. 2020) will be a powerful tool for change detection monitoring in the Thompson River valley, BC (**Figure 19**; **Figure 20**) and elsewhere along national railway transportation corridors (e.g., Prince Rupert-Kitimat-Terrace and Okanagan Valley), and the Assiniboine River valley, MN-SK (**Figure 23**),

Research with InSAR specialists at 3v Geomatics and TRE-Altamira in Vancouver, BC, will continue through 2021-2022. This collaboration is examining the feasibility of merging national-scale surficial geology and landslide susceptibility maps with regional-scale InSAR monitoring. Beginning in 2022, the GSC will begin fostering remote sensing research with the Canada Centre for Mapping and Earth Observation, Canada Space Agency (CSA) and Japanese National Institute of Advanced Science and Technology (AIST). This collaboration will focus on comparing landslide change detection capabilities of Canada's RCM and Japan Aerospace Exploration Agency (JAXA) ALOS 1 and 2 satellite L-band SAR and Hyperspectral Image Suite (HISUI) imagery. A goal of this collaboration is to develop machine-learning capabilities and artificial intelligence-based landslide analyses. These results will be compared with and build upon legacy benchmarked RCM, RS2 and S1 differential SAR interferometric time-series datasets (e.g., **Figure 9**; **Figure 20**).

<u>Thompson River valley, BC</u>

Understanding the temporal relationship between slope displacement and river discharge levels is crucial for effective management of landslide risk in the Thompson River railway transportation corridor. The continued acquisition of RS2, S1 and RCM SAR imagery and time-series analyses will ensure long-term landslide monitoring adjacent to critical rail infrastructure (Bobrowsky and Sladen 2013; Huntley et al. 2017; Huntley et al. 2021c). For the Thompson River valley, the primary research objective is to determine whether displacement and peak ground movement toward the river detected by RTK-GNSS benchmarked SAR datasets can be definitively linked to large changes in river level between spring, summer and fall; or when river levels are elevated above or slightly below average flow (cf. **Figure 14**; **Figure 18**).

<u>Assiniboine River valley, MN-SK</u>

Trihedral aluminium corner reflectors with snow covers procured from MacDonald Dettwiler Associates (MDA) in 2021 (**Table 3**) will be stored at GSC-Vancouver until trans-Canada travel and fieldwork is logistically possible in 2022-2023. Installation will face numerous logistical challenges from 2021 to 2023.

To ensure timely arrival at remote farmland sites in the Assiniboine River valley, corner reflectors will be transported from Vancouver by road and delivered in a GSC vehicle. To avoid anomalous displacement measurements during winter months attributed to frost heave cycles in soils and bedrock, corner reflectors must be mounted on posts seated up to 3 m below surface. A power auger and drill extensions purchased in 2020 will be deployed to drill post-holes through clay-rich soil, till and bedrock at CN Rivers Mile 184, and CP Bredenbury Miles 82.6 and 86.5 (**Figure 1 c-e**). Location of corner reflectors must also be cognizant and respectful of local First Nations land claims, family farms, and other landowners in the Assiniboine River valley.

Once installed and georeferenced using RTK-GNSS, these permanent coherent artificial InSAR targets will greatly improve the precision and accuracy of backscatter and interferometric processing of RS2, S1 and RCM C-band SAR datasets in the Assiniboine River valley. Corner reflectors can be located on the RCM (and older) imagery based on their precise geospatial coordinates and their backscattering characteristics. As demonstrated at Ripley Landslide, georeferenced corner reflectors can be readily identified in stacks of SAR imagery by examining the degree of phase stability over time for every resolution cell within the study area (Journault et al. 2016; Huntley et al. 2017b; Journault et al. 2018).

RS2, S1, RCM and ALOS SAR scenes will be acquired with left- and, or right-looking line-of-sight geometries from ascending and descending orbital passes. By considering only targets with persistent scatterer characteristics and correcting for phase change contributions caused by orbital position errors, topography and atmospheric effects, a time-series of deformation for each target can be recovered with measurement accuracies of several mm (Huntley et al. 2020f). Backscatter amplitude characteristics will be analysed through the image stack to identify and remove any unreliable corner reflector measurements from processing of time-series profiles. Low backscatter amplitude of corner reflectors over the winter months attributed to snow cover (cf. Huntley et al. 2020f; Pon et al. 2020) will be avoided by using the bespoke MDA corner reflector design incorporating the Perspex snow shed. This will ensure that slope monitoring occurs throughout the year. Multi-temporal averaging of stacks of SAR scenes reduces speckle on baseline imagery (Huntley et al. 2020f).

GAMMA Software (Wegmüller et al. 2019) will be used to create a dual-look multi-temporal interferogram network stacks consisting of independent interferometric measurements at corner reflectors and other persistent scatterers (e.g., buildings and other infrastructure). This highly redundant network will be used to create a deformation time-series for each corner reflector using a multi-baseline approach. GAMMA software will also used to create interferogram maps from pairs of SAR images. Interferograms will be corrected for a mean phase bias (i.e., a first order atmospheric correction).

Kelowna, Okanagan Valley, interior BC

RCM stacks will be acquired in both ascending and descending orbit passes (east and west-ranging) at a nominal ground resolution of 3 m with an ideal revisit frequency of 4 days. The combination of relatively high spatial and temporal resolution has the potential to resolve high rates of movement over smaller areas which would otherwise be aliased by the coarse spatial resolution of S1 or the coarse temporal resolution of RS2 (Huntley et al. 2021a, b).

Data quality will be influenced by changes in vegetation, urban land use, agricultural practices, water management, highways and rail tracks, sand and snow; especially when there were gaps of months between scenes in the time-series. RS2 S1 and RCM images all exhibited similar seasonal effects. The performance of ALOS remains to be evaluated. Ice and snow cover causes spurious signals in the InSAR data, producing false positives and limiting the detection of real displacement. Scenes with >20% snow coverage are typically excluded from analysis (Pon et al. 2020). For most parts of Canada, the useable, snow-free dates for useful imagery will typically range between early March and late November.

Kitimat-Terrace-Prince Rupert, coastal BC

Future development in coastal northwest BC requires safe, secure locations for infrastructure installations and communities. The challenge for managing environmental and infrastructure protection and site reclamation will be to accommodate future extreme weather events, climate change, and damage from earthquakes, landslides and tsunamis. New insights into the terrestrial and marine geohazards offered by our work in this region will help reduce the future development risks to governments, resource industries, communities and the environment.

We demonstrated the ability of georeferenced, orthorectified, averaged, and resampled multi-look intensity (backscatter) RS2 imagery to capture debris flow and flooding events in the vicinity of remote communities and marine infrastructure following major storm events (Huntley et al. 2020f). An on-going program to detect debris flows, landslides, and other geohazards using RS2 and RCM datasets will help local First Nation villages determine the extent to which identified debris flows impact local watersheds. To this end, GSC 1:50,000-scale surficial geology and landslide hazard maps (Blais-Stevens et al. 2016; Maynard et al. 2018) will also provide useful information to guide geohazard management decisions.

Deep-seated bedrock fractures on fjord walls flank, formed by stress release during ice retreat from the fjord, glacio-isostatic crustal rebound, neo-tectonic faulting, and permafrost loss during deglaciation. Past failures of large bedrock masses along similar bedrock lineaments, suggest fractured fjord sidewalls may be prone to failure. Displacement waves generated by a large volume slope failure could have severe socioeconomic consequences for local coastal infrastructure, resource industries and remote communities.

Huntley et al. (2020f) created a single-look multi-temporal interferogram network stack consisting of independent interferometric measurements at five corner reflectors installed on the western flank of Hawkesbury Island. This highly redundant network was used to create corner reflector deformation time-series using a multi-baseline approach (Huntley et al. 2020f). The results of a 2017-2019 InSAR analysis suggested that, at least on short time scales (< 2 years), the western flank of Hawkesbury Island is not rapidly deforming (Huntley et al. 2020f).

However, a longer change detection time-series, and subsequent landslide/landslide generated wave hazard analysis, is required to establish whether fjord side walls are stable and do not represent a geological hazard to fjord-bound communities, coastal infrastructure, and natural resource activities. Trihedral corner reflectors installed on the western flank of Hawkesbury Island will continue to perform for long-term high precision DInSAR monitoring with C-band and L-band satellites. The application of GAMMA software (Wegmüller et al. 2019), advanced InSAR processing techniques incorporating both persistent scatterer targets and distributed targets (e.g., corner reflectors) will greatly improve the spatial density of displacement records. Analysis of the vertical and horizontal deformation components would combine ascending and descending acquisition geometries of satellite data. Integration of historical SAR datasets with GNSS and UAV data collected will improve knowledge of the behaviour and characteristics of landslides in the Kitimat-Terrace-Prince Rupert transportation corridor. This fundamental geoscience knowledge will help define a sequence of thresholds representative of increasing states of activity to better manage landslides and other geohazards.

5.2.2 GNSS monitoring

RTK-GNSS change detection monitoring in the Thompson River valley has provided insight on the rates and spatial pattern of creep as well as the timing, and possibly precursors of changes in creep behaviour (Ripley Landslide and North Slide). This new knowledge will help to characterize landslide hazard, and ultimately reduce landslide risk. The locations of highest creep rates (e.g., **Figure 11**; **Figure 13**) will help identify where track damage can be expected if creep is continuous. Spatial variability in landslide motion will help inform the mechanism of the monitored landslides, such as whether failure involves complex interactions between structurally separate blocks, thus improving landslide characterization and mitigation efforts (**Table 10**).

Comparing displacement trends with proxy records of possible landslide drivers – including temperature, precipitation, river level and irrigation will help stakeholders establish landslide-warning thresholds based on antecedent and current environmental conditions. Such comparisons will include detailed analysis of GNSS displacement histories spanning acceleration periods indicated by the CP GNSS markers (at Ripley Landslide) to identify possible environmental triggers. If gradual acceleration is found to precede failure events, future RTK-GNSS and Geocube™-measured accelerated creep can be used to forecast impending failures.

<u>Thompson River valley, BC</u>

Unfortunately, broken Geocube™ networks on both Ripley Landslide and South Slide have remained unrepaired due to COVID-19 restrictions. For 2021-2022, time will be spent developing reliable power supplies (batteries and solar panels), establishing the functionality of Geocube™ units, and restoring survey networks through a combination of home-office research and in-field installation activities (cf. Huntley et al. 2020b, e). As the restored Geocube™ networks stabilize through 2022 and beyond, data collected (remotely and on-site, respectively) will be processed and presented to graphically show: 1) displacement trends; 2) 3D displacement (mm) -vs- date (month, year); 3) surface angle of movement (angle, degrees) -vs- date (month, year); 4) precipitation (mm) and 3D displacement (mm) -vs- date (month, year); and 5) temperature (^{o} C) and 3D displacement (mm) -vs- date (day, month, year).

Seasonal RTK-GNSS surveys (March, July, September, November) will help to improve characterization of slope activity by combining three-dimensional displacement measurements with more spatially detailed line-on-sight displacements measured by, for example InSAR or UAV photogrammetry. In addition, networked RTK-GNSS data will help evaluate the utility of precipitation, ambient temperature, and soil moisture in predicting landslide activity based on comparison of three-dimensional displacement measurements with geophysical results and meteorological records (cf. Holmes et al. 2020; Sattler et al. 2021).

Table 10 Change detection activities to monitor landslide hazards as part of IMOU-5170: InSAR, RTK-GNSS, UAV, Climatic Variables, and procurements planned for 2021-2022. GSC-WS1, GSC-WS2 and GSC-WS3 are total weather stations.

Transportation Corridor	Landslide Hazards	Infrastructure at Risk	Satellite SAR Activities	RTK-GNSS Activities	UAV Activities	Climate Monitoring
CN and CP corridor, Thompson River valley, BC	Large, slow landslides Small rapid debris flows Small rapid rock falls	Railways Highways Agriculture Potable water	*C-band* *L-band* SAR image interpretation Interferometry Cumulative displacement time-series	Maintenance of Geocube™ networks (continuous) Repeat RTK-GNSS surveys of GCPs (seasonal)	*RTK-300 Matrice* RGB LiDAR DJI Phantom 4 RGB SfM DSMs (seasonal)	*Maintenance of:* GSC-WS1 Rainfall Snowfall Temperature Wind
CN and CP corridors, Assiniboine River valley, MN-SK	Large, slow landslides Small rapid debris flows	Railways Highways Pipelines Power lines Reservoirs Agriculture	*C-band* SAR image interpretation Interferometry Cumulative displacement time-series Installation of corner reflectors	Lab testing of Geocube™ units and power supply RTK-GNSS and GCPs (seasonal)	*RTK-300 Matrice* RGB LiDAR *DJI Phantom 4* RGB SfM DSMs (seasonal) *Sky Canoe* Hyperspectral SAR LiDAR	*Procurement of:* GSC-WS2 Rainfall Snowfall Temperature Wind *Installation* 2022-2023
CN/CP spur lines, Kelowna and Okanagan Valley, BC	Large, slow landslides Small rapid debris flows Small rapid rock falls	Railways Highways Pipelines Powerlines Reservoirs Urban land use Agriculture Light industry	*C-band* SAR image interpretation Interferometry Cumulative displacement time-series Installation of corner reflectors	RTK-GNSS and GCPs (baseline data acquisition)	*RTK-300 Matrice* RGB LiDAR *DJI Phantom 4* RGB SfM DSMs (seasonal)	Data mining Regional weather station databases
Kitimat-Terrace-Prince Rupert Corridor	Small rapid landslides Large rapid rock falls Large debris torrents Tsunamis	Railways Highways Pipelines Powerlines Urban land use Heavy industry Marine uses	*C-band* *L-band* SAR image interpretation Interferometry Cumulative displacement time-series Installation of corner reflectors	Logistical planning for 2022-2023 fieldwork	*RTK-300 Matrice* RGB LiDAR *DJI Phantom 4* RGB SfM DSMs (seasonal) *Sky Canoe* Hyperspectral SAR	*Procurement of:* GSC-WS3 Rainfall Snowfall Temperature Wind *Installation* 2022-2023

Assiniboine River valley, MN-SK

Given the logistical complexities of installation outlined in Huntley et al. (2020b), Geocubes™ will not be installed by the GSC at CN Rivers Sub-division Mile 184, CP Bredenbury Sub-division Mile 82.6 and CP Mile 86.5 until at least the summer or fall of 2022. Installation of new GCPs and repeat RTK-GNSS surveys of GCPs established in 2019 will be similarly postponed.

5.2.3 UAV Change Detection

When combined with high-resolution (millimetric) RTK-GNSS measurements of GCPs, UAV photogrammetry is the most time efficient and cost-effective field method to delimit the spatial and temporal distribution of movement and displacement across unstable slopes from year to year. UAV photogrammetric surveys generate high-quality repeat DSMs that can be compared to characterize surface change of active landslides along the transportation corridor (Huntley et al. 2021c; **Table 10**; **Figure 22**).

In addition to COVID-19, several other issues may delay the addressing of activity objectives in the coming years. Other project commitments limit access time for the GSC technical support to fly UAVs, survey terrain, and process data using ArcGIS and other software packages. In-house computing abilities are limited by stock computers and software, and limited data storage capabilities provided by Shared Services Canada. Aviation regulations are strictly enforced near railway property, requiring personnel with a flying license and controlled traverses avoiding the railway right-of-way. This has been partly addressed by having GSC staff complete advanced UAV training in 2021. Lastly, wildfires and extremely poor air conditions, like those experienced during the 2017 and 2018 field seasons, will prevent flight and survey objectives. With changing climate and weather conditions, poor air quality may limit sortie times and ranges in the future.

Applications for Remotely Piloted Aircraft Systems

Photogrammetric and LiDAR change detection with the DJI Phantom 4 and 300RTK Matrice UAVs are most cost- and time-effective for landslides under 3 km^2 (Huntley et al. 2021c). Battery power and visual line of sight flight restrictions limit the usefulness of UAVs in regional landslide and geohazard inventories and change detection monitoring along linear infrastructure corridors (e.g., railways, highways, and pipelines). Aerial photography with greater spatial coverage is possible from fixed wing aircraft and helicopters but is more costly and lacks the precision georeferencing of RTK-UAV photogrammetry. Additionally, conventional aircraft and UAVs cannot fly in poor weather or low light conditions.

Remotely piloted aircraft systems (RPAS) capable of carrying payloads >10 kg that can be operated beyond visual line of sight (BVLOS) are an emerging airborne remote sensing tool. Autonomous vertical liftoff and landing (VTOL) aircraft with radar, gas-electric hybrid propulsion, and discrete frequency communications (e.g. skycanoe.ca). With a payload capability up to 100 kg, and an effective range of 500 km per charge, VTOL RPAS aircraft could be the ideal platform to undertake regional landslide and geohazard inventories and change detection monitoring (**Table 10**). Optical, LiDAR and hyperspectral (e.g., infrared) sensors and software mounted to the 300RTK Matrice, or an RPAS, will greatly expand the geospatial information collected along linear infrastructure corridors.

Thompson River valley, BC: Repeat UAV surveys of Ripley Landslide, North Landslide and other landslides of concern will be conducted in 2021-2022 (**Figure 9**). Comparison of these subsequent surveys with legacy surveys (2016-2020) are expected to allow exceptionally precise quantification of points and rates of movement. Geo-referenced UAV overflights are planned for summer, fall and winter of 2021-2022 to capture changes between the surface models, and comparison with DSMs generated in 2016, 2017, 2018, and 2019. These additional surveys will enable comparison of landslide motion over multiple periods, thus providing a further means to evaluate creep acceleration measured by CPR's GNSS markers. The 2021 overflights, and in future years, will be conducted using the GSC's DJI Phantom 4 and DJI Matrice RTK300 hexacopter. The reliable Phantom unit, with a weight of 1.4 kg, includes a fixed payload consisting of a 12.4 MB RGB camera. The larger Matrice weighs 9.5 kg (operating empty weight) and will carry a 6 kg payload consisting of a Velodyne VLP-16 Puck LiDAR (16 channels, 300,000 points/second) and Zenmuse X3 RGB camera.

The primary research objective is to compare and evaluate change detection datasets acquired during UAV photogrammetric and LiDAR surveys. A secondary objective will be to establish whether high resolution hyperspectral UAV imaging can be used to remotely map the distribution and activity of landslides in the Thompson River valley (e.g., delimiting soil moisture and colluvial sediments with distinctive spectral signatures).

Kelowna-Okanagan Valley, BC: Photogrammetric and LiDAR change detection with UAVs is ineffective for mapping areas of interest greater 3 km^2. Operational base maps will blend detailed RTK-UAV surveys of key sites of interest with broader, lower resolution satellite imagery (e.g., Worldview and Aster datasets) covering the urban limits of Kelowna.

Kitimat-Terrace-Prince Rupert, BC: Mountainous terrain and poor weather conditions are challenge for landslide monitoring in north coastal BC using conventional aircraft and UAVs. Test flights of the Sky Canoe with mounted optical, LiDAR and, or hyperspectral sensors would occur over First Nations traditional lands with critical socioeconomic infrastructure. These datasets will provide insights into the terrestrial and marine geohazards to help reduce the future development risks to governments, natural resource industries, communities, and the environment.

Assiniboine River valley, MN-SK: RTK-GNSS-UAV surveys in 2019 have captured the baseline georeferenced imagery of landslide morphology at the CN 184.4, and CP 86.5 and 82.6 sites in the Assiniboine River valley (Huntley et al. 2020d). The resulting centimetre-resolution DSMs generated from the UAV surveys show metre-scale features (e.g., boulders, corner reflectors) on the wooded valley slopes. COVID-19 travel prohibitions will prevent the GSC from undertaking UAV or Sky Canoe overflights in the Assiniboine River valley until the summer of 2022 (at least). Eventually, these surveys will extend surface-change characterization of the very slow-moving landslides in the Assiniboine and Qu'Appelle river valleys. Like the activity goal in the Thompson River valley, comparison of these subsequent surveys, especially employing LiDAR, will allow exceptionally precise quantification of points and rates of movement.

5.2.4 Climate change detection

A key research objective of IMOU-5170 is to determine the degree to which climate variables influence groundwater conditions and landslide activity (cf. Schafer et al. 2015; Holmes et al. 2020; Sattler et al. 2021). Fluctuations in temperature over the winter months may also contribute to intervals of ground thaw, changes in porewater pressures and landslide activity. These relationships will be tested over the coming years through validation of landslide deformation records (e.g., RTK-GNSS, Geocubes™, UAV, and InSAR change detection monitoring) correlated to climate variables in the Thompson River valley, Assiniboine River valley, and other landslide test sites.

Thompson River valley, BC

In the Thompson River valley, a climate monitoring station has collected valuable data on precipitation, snowfall, air temperature since 2016, and from 2019, wind speed and wind direction. Beginning in 2020-2021, this multi-year climate-series will be compared with borehole monitoring results of groundwater levels and subsurface displacement, GNSS, UAV, and InSAR to investigate inter-annual variation in seasonal displacement rates. A research goal will be to establish the degree to which the amount and duration of precipitation (as snow and rain) events, and air temperature are important controls on ground displacement at the start of melt season in late winter-early spring (cf. Sattler et al. 2018; Holmes et al. 2020; Sattler et al. 2020).

Kelowna-Okanagan Valley, BC

Long-term climate data for the Kelowna region are available at https://climate.weather.gc.ca/ so a GSC weather station installation is not required in this study area. Statistical time-series analyses will better define long-term trends in precipitation, temperature, and other climate variables for comparison with changes in landslide activity on natural and modified urban slopes. These data would be evaluated against observations of groundwater levels in wells, and surface runoff measured at stream gauging stations.

Kitimat-Terrace-Prince Rupert, BC

Similarly, long-term climate data for the Kitimat-Terrace-Prince Rupert region are available at: https://climate.weather.gc.ca/. The strategic location of a GSC weather station in the First Nations community of Hartley Bay will capture the local variability of weather conditions in the north coastal mountains and serve as a community outreach activity. Statistical time-series analyses from climate stations will better define long-term trends in precipitation, temperature, and other climate variables for comparison with changes in landslide activity on natural and anthropogenically modified slopes. Again, climate datasets would be evaluated against observations of groundwater levels in wells, and surface runoff measured at stream gauging stations.

Assiniboine River valley, MN-SK

The goal for 2020-2021 will the procurement and testing of components for a climate monitoring station (rainfall, snow, air temperature, wind speed and direction). Installation in the Assiniboine River valley will likely take place in 2022-2023, after which it will be possible to test whether a component of landslide movement can be attributed to local weather conditions (e.g., precipitation, air temperature, wind, barometric pressure).

6. CONCLUDING REMARKS

Research plans, equipment procurement, and geoscientific outreach were significantly impacted by COVID-19 in 2020-2021 (**Table 3; Appendix A**). Dramatic changes in operational processes challenged and realigned productivity goals for team members and stakeholders. Travel prohibitions limited access to conferences and field sites. Collaboration with the TC-IC, CN, CP, BGS, UA, USASK and other stakeholders was maintained through a blend of virtual meetings with more traditional modes of communication. NRCan-GSC, TC-IC, and collaborators began to address outstanding questions on the impact of past and future extreme weather and climate change on landslide activity in the Thompson River valley, BC and Assiniboine River valley MN-SK (**Figure 1**). New information on landslide hazards published in national and international journals, as textbook chapters, and presented at virtual conferences (**Table 4**) are summarized in this open file report. These publications provide fundamental geoscience knowledge to help key industry stakeholders (e.g., CN and CP) and university partners (e.g., UA and USASK) measure, manage, and mitigate landslide geohazards and their consequences.

For 2021-2022, research activities will cover terrain analysis (desktop studies and fieldwork) and change detection monitoring (remote and on-site/in situ) in the Thompson and Assiniboine river valleys, in addition to expanding to other parts of British Columbia where railway infrastructure is vulnerable to landslide activity (**Table 9**; **Table 10**). For the immediate future, the research focus on five objectives. 1) Acquisition of air photographs, satellite imagery, and other geospatial datasets for study areas. 2) Developing in-house (or at-home) functionality and capability using cloud storage and processing services. 3) Developing desktop remote mapping protocols and data analyses, combining terrain studies with geospatial datasets to meet the IMOU mandate. 4) Acquisition of climate station components (e.g., tipping-bucket rain gauge, air temperature sensor, snow depth gauge, anemometer and wind vane), borehole instrumentation and drilling requirements (e.g., piezometers, inclinometers), and InSAR corner reflectors. 5) Communicating R&D through conferences, workshops, and publications (**Table 9**; **Table 10**).

6.1 Acknowledgements

Field studies were made possible through the support of Danny Wong (Canadian Pacific Railways, Calgary, Alberta) and Trevor Evans (Canadian National Railways, Kamloops, BC). Philip LeSueur (P.Geo.) provided an internal Geological Survey of Canada critical peer review of the draft manuscript.

7. REFERENCES

Behnia, P., Harris, J., Rainbird, R., Williamson, M. and Sheshpari, M. 2012. Remote predictive mapping of bedrock using image classification of Landsat and SPOT data, western Minto Inlier, Victoria Island, Northwest Territories, Canada, International Journal of Remote Sensing, Vol 33 (21) pp. 6876-6903, https://doi.org/10.1080/01431161.2012.693219

Blais-Stevens, A., Maynard, D., Weiland, I., Geertsema, M. and Behnia, P. 2016. Surficial geology and landslide inventory in Douglas Channel fjord, northwest British Columbia', GeoVancouver, Canadian Geotechnical Society, 7 p.

Blatz, J. A., Ferreira, N.J. and Graham, J. 2004. Effects of near-surface environmental conditions on instability of an unsaturated soil slope. Canadian Geotechnical Journal, Vol. 41, pp. 1111-1126

Bobrowsky, P.T. and Dominguez, M.J. 2012. Landslide Susceptibility Map of Canada. Geological Survey of Canada, Open File 7228, 1 sheet

Bobrowsky, P. 2013. Recent advances in landslide monitoring. Paper presented at CIRiDe-International Congress on Disaster Risk and Sustainable Development, Catamarca, Argentina, 1 p.

Bobrowsky, P. 2016. Ripley Landslide: a Canadian test site for landslide investigation and monitoring. International Consortium on Landslides, Technical Presentation, ICL Board Meeting, Paris, 1 page

Bobrowsky, P. 2018. IPL-202 Ripley Landslide Monitoring Project (Ashcroft, B.C., Canada). International Programme on Landslides, Unpublished Annual Report, 1 p.

Bobrowsky, P. and Sladen, W. 2013. Installing Fibre Optics with the China Geological Survey. NRCAN-ESS S&T Newsletter, Issue #21 (NRCan Wiki online digital version only)

Bobrowsky, P., MacLeod, R., Huntley, D., Niemann, O., Hendry, M., Macciotta, R. 2018. Ensuring Resource Safety: Monitoring Critical Infrastructure with UAV Technology. Resources for Future Generations, Conference Abstracts Volume, Vancouver, Canada, 1 p.

Bruce, J.P. and Cohen, S.J. 2004. Impacts of climate change in Canada (Chapter 4). In Coward, H. and Weaver, A.J. (editors); Hard Choices: climate change in Canada; Wilfred Laurier Press, 273 pages, ISBN 0-88920-442-X

Bunce C. and Chadwick, I. 2012. GPS monitoring of a landslide for railways. In Landslides and Engineered Slopes - Protecting Society through Improved Understanding, pp. 1373-1379

Campbell, J.E., Harris, J.R., Huntley, D.H., McMartin, I., Wityk, U., Dredge, L.A., and Eagles, S., 2013. Remote Predictive Mapping of Surficial Earth Materials: Wager Bay North Area, Nunavut - NTS 46-E (N), 46-K (SW), 46-L, 46-M (SW), 56-H (N), 56-I and 56-J (S); Geological Survey of Canada, Open File 7118. doi:10.4095/293158

Chen, Z. and Grasby, S.E. 2009. Detection of decadal and interdecadal oscillations and temporal trend analysis of climate and hydrological time-series, Canadian Prairies. Geological Survey of Canada Open File 5782, 13 p.

Chen, Z, Grasby, S. E., Osadetz, K.G., Fesko, P. 2006. Historical climate and stream flow trends and future water demand analysis in the Calgary region, Canada. Water Science and Technology, Vol. 53, no. 10, pp. 1-11

Christiansen, E. 1979. The Wisconsinan deglaciation of southern Saskatchewan and adjacent areas. Canadian Journal of Earth Sciences, Vol. 16 (4), pp. 913-938

Clague, J.J. and Evans, S.G. 2003. Geologic framework of large historic landslides in Thompson River valley, British Columbia. Environmental & Engineering Geoscience, Vol. 9, pp. 201–212

Couture, R. and Evans, S. 2006. Slow-moving disintegrating rockslides on mountain slopes. In Landslides from massive rock slope failure: proceedings of the NATO Advanced Research Workshop on Massive Rock Slope Failure: New Models for Hazard Assessment. In Evans, S.G., Scarascia Mugnozza, G., Strom, A and Hermanns, R.L. (editors); NATO Science Series, Sub-Series IV: Earth and Environmental Sciences, Vol. 49, pp. 377-393

Deblonde, C. Cocking, R.B., Kerr, D.E., Campbell, J.E., Eagles, S., Everett, D., Huntley, D. H., Inglis, E., Parent, M., Plouffe, A., Robertson, L., Smith, I.R. and Weatherston, A. 2018. Science Language for an Integrated Geological Survey of Canada Data Model for Surficial Geology Maps (Version 2.3.14), Geological Survey of Canada, Open File 8236, 50 pages (2 sheets)

Dudley J.P. and Samsonov S.V. 2020. The Government of Canada automated processing system for change detection and ground deformation analysis from RADARSAT-2 and RADARSAT Constellation Mission Synthetic Aperture Radar data: description and user guide; Geomatics Canada, Open File 63, 65 p. https://doi.org/10.4095/327790

Eshraghian, A., Martin, C. and Cruden, D. 2007. Complex earth slides in the Thompson River Valley, Ashcroft, British Columbia. Environmental and Engineering Geoscience, Vol. XIII, pp. 161-181

Eshraghian, A., Martin, C. and Morgenstern, N. 2008. Movement triggers and mechanisms of two earth slides in the Thompson River Valley, British Columbia, Canada. Canadian Geotechnical Journal, Vol. 45, pp. 1189-1209

Evans, S.G. 1984. The 1880 landslide dam on Thompson River, near Ashcroft, British Columbia. In: Current Research, Part A: Geological Survey of Canada Paper 84-1A, pp. 655–658

Evans, S.G. and Clague, J.J. 1997. The impact of climate change on catastrophic geomorphic processes in the mountains of British Columbia, Yukon, and Alberta. In: Responding to global climate change in British Columbia and Yukon, Vol I of the Canada Country Study: Climate Impacts and Adaptation, edited by E. Taylor and B. Taylor, Chapter 7, 16 p.

Fell, R. 1994. Landslide risk assessment and acceptable risk. Canadian Geotechnical Journal, Vol. 31, pp. 261–272

Fulton, R.J. 1995. Surficial Earth Materials of Canada. Geological Survey of Canada Map 1880A; 1:5,000,000

Geertsema, M., Schwab, J.W. and Blais-Stevens, A. 2006. Landslides impacting linear infrastructure in west-central British Columbia. In Proceedings of the 1st Specialty Conference on Disaster Mitigation, pp. DM 1- 10

Harris, J., and Grunsky, E. 2015. Predictive lithological mapping of Canada's North using Random Forest classification applied to geophysical and geochemical data. Computers and Geosciences, Vol. 80, pp. 9-25

Heginbottom, J.A., Dubreuil, M.A., Harker, P.T., Caron, A. Paul, P. and Rose, I. 1995. Canada Permafrost; National Atlas of Canada, 5th Edition, Scale 1:7 500 000

Hendry, M., Macciotta, R. and Martin, D. 2015. Effect of Thompson River elevation on velocity and instability of Ripley Slide. Canadian Geotechnical Journal, Vol. 52(3), pp. 257-267

Hermanns, R., Oppikofer, T., Böhme, M., Dehls, J., Yugsi Molina, F. and Penna, I. 2016. Rock slope instabilities in Norway: first systematic hazard and risk classification of 22 unstable rock slopes from northern, western and southern Norway. Landslides and Engineered Slopes. Experience, Theory and Practice, pp. 1107–1114

Holmes, J., Chambers, J., Donohue, S., Huntley, D., Bobrowsky, P., Meldrum, P. Uhlemann, S., Wilkinson, P. and Swift, R. 2018. The Use of Near Surface Geophysical Methods for Assessing the Condition of Transport Infrastructure. Civil Engineering Research Association, Special Issue on Structural Integrity of Civil Engineering Infrastructure, Journal of Structural Integrity and Maintenance, 6 p.

Holmes, J., Chambers, J., Meldrum, P., Wilkinson, B., Williamson, P., Huntley, D., Sattler, K., Elwood., D., Sivakumar, V., Reeves, H. and Donohue, S. 2020. 4-Dimensional electrical resistivity tomography for continuous, near-real time monitoring of a landslide affecting transport infrastructure in British Columbia, Canada. Near Surface Geophysics, 15 p., doi.org/10.1002/nsg.12102

Howes, D.E. and Kenk, E. 1997. Terrain classification system for British Columbia (revised edition): a system for the classification of surficial materials, landforms and geological processes of British Columbia. B.C. Ministry of Environment Manual 10, 90 p.

Huntley, D. and Bobrowsky, P. 2014. Surficial geology and monitoring of the Ripley Slide, near Ashcroft, British Columbia, Canada; Geological Survey of Canada, Open File 7531, 21 p.

Huntley, D., Bobrowsky, P., Parry, N., Bauman, P., Candy, C. and Best, M. 2017a. Ripley Landslide: the geophysical structure of a slow-moving landslide near Ashcroft, British Columbia, Canada. Geological Survey of Canada, Open File 8062, 59 p.

Huntley, D., Bobrowsky, P., Charbonneau, F., Journault, J. and Hendry, M. 2017b. Innovative landslide change detection monitoring: application of spaceborne InSAR techniques in the Thompson River valley, British Columbia, Canada. In: Landslide Research and Risk Reduction for Advancing Culture and Living with Natural Hazards, Volume 3, 4th World Landslide Forum (ICL-IPL), Ljubljana, Slovenia 29- May – 2 June 2017, Springer Nature, 13 p.

Huntley, D., Bobrowsky, P., Hendry, M., Macciotta, R., Elwood, D., Sattler, K., Reeves, H., Chambers, J., Meldrum, P. Holmes, J. and Wilkinson, P. 2018a. Using multi-dimensional ERT modelling to provide new insight into the hydrogeological structure of a very slow-moving landslide in glacial sediments, Thompson River valley, British Columbia, Canada. Geological Society of America Annual Meeting, Session T65, Abstract Volume, 1 p.

Huntley, D., Bobrowsky, P., MacLeod, R. and Roberts, N. 2018b. New insights into form and function of very slow-moving landslides from bathymetric surveys of Thompson River, British Columbia Geological Society of America Annual Meeting, Session T53, Abstract Volume, 1 p.

Huntley, D., Bobrowsky, P., Hendry, M., Macciotta, R. and Best, M. 2019a. Multi-technique geophysical investigation of a very slow-moving landslide near Ashcroft, British Columbia, Canada. Journal of Environmental and Engineering Geophysics; Volume 24 (1) pp. 85-108

Huntley, D., Bobrowsky, P., Sattler, K., Elwood, D., Holmes, J., Chambers, J., Meldrum, P. Holmes, J. and Wilkinson, P. Hendry, M. and Macciotta, R. 2019b. PRIME installation in Canada: protecting national railway infrastructure by monitoring moisture in an active landslide near Ashcroft, British Columbia. 32nd SAGEEP, Environmental and Engineering Geophysical Society. Proceedings Volume of the Annual Meeting, Portland, Oregon, USA, 1 p.

Huntley, D., Bobrowsky, P., MacLeod, R., Cocking, R., Joseph, J., Sattler, K., Elwood, D., Holmes, J., Chambers, J., Meldrum, P., Wilkinson, P., Hendry, M., Macciotta, R. 2019c. Geological Survey of Canada, Open File 8548, 1 sheet, https://doi.org/10.4095/314548

Huntley, D., Bobrowsky, P., Hendry, M., Macciotta, R., Elwood, D., Sattler, K., Chambers, J., and Meldrum, P. 2019d. Application of multi-dimensional electrical resistivity tomography datasets to investigate a very slow-moving landslide near Ashcroft, British Columbia, Canada. Landslides, Vol. 16, pp. 1033-1042, https://doi.org/10.1007/s10346-019-01147-1

Huntley, D., Holmes, J., Bobrowsky, Chambers, J., Meldrum, P., Wilkinson, P., Elwood, D., Sattler, K., Hendry, M. and Macciotta, R. 2020a. Hydrogeological and geophysical properties of the very slow-moving Ripley Landslide, Thompson River valley, British Columbia. Canadian Journal of Earth Sciences, 21 pages, doi.org/10.1139/cjes-2019-0187

Huntley, D., Bobrowsky, P., Cocking, R., Joseph, P., Neelands, N., MacLeod, R., Rotheram-Clarke, D., Usquin, R. and Verluise, F. 2020b. Installation, operation and evaluation of an innovative global navigation satellite system monitoring technology at Ripley Landslide and South Slide, near Ashcroft, British Columbia; Geological Survey of Canada, Open File 8742, 36 p.

Huntley, D., Bobrowsky, P., Rotheram-Clarke, D., MacLeod, R., Cocking, R., and Joseph, J. 2020c. Understanding Plateau landslides: current research in the Thompson River valley, Interior Plateau, British Columbia (2013-2020); Geological Survey of Canada, Open File 8736, 60 p., https://doi:10.4095/326830

Huntley, D., Bobrowsky, P., Rotheram-Clarke, D., Cocking, R., and Joseph, J. 2020d. Understanding Prairie landslides: current research in the Assiniboine River valley, Manitoba-Saskatchewan (2019-2020). Geological Survey of Canada, Open File 8735, 26 p., https://doi:10.4095/326821

Huntley, D., Rotheram-Clarke, D., Cocking, R., Joseph, J. and Bobrowsky, P. 2020e. Understanding Plateau and Prairie Landslides: research plans for the Thompson River valley, British Columbia, and the Assiniboine River valley, Manitoba-Saskatchewan (2020-2025); Geological Survey of Canada, Open File 8743, 25 p.

Huntley, D., Rotheram-Clarke, D., Bobrowsky, P., MacLeod, R., and Brillon, C. 2020f. InSAR investigation of sackung-like features and debris flows in the vicinity of Hawkesbury Island and Hartley Bay, British Columbia, Canada: reducing landslide and tsunami risks for coastal communities and vulnerable infrastructure. Slope Stability 2020, Symposium Special Volume, 10 p., https://doi.org/10.36487/ACG_repo/2025_09

Huntley, D., Rotheram-Clarke, D., Cocking, R., and Joseph, J. 2021a. Landslide change detection monitoring with a benchmarked RADARSAT CONSTELLATION MISSION high temporal resolution dataset. Institute of Electrical and Electronic Engineers, International Geoscience and Remote Sensing Symposium, Special Volume, 4 p.

Huntley, D., Rotheram-Clarke, D., Pon, A., Tomaszewicz, A., Leighton, J., Cocking, R. and Joseph, J. 2021b. Benchmarked RADARSAT-2, SENTINEL-1 and RADARSAT CONSTELLATION MISSION change detection monitoring at North Slide, Thompson River valley, British Columbia: implications for a landslide-resilient national railway network. Canadian Journal of Remote Sensing. https://doi.org/10.1080/07038992.2021.1937968

Huntley, D., Bobrowsky, Rotheram-Clarke, D., MacLeod, R., Cocking, R., Joseph, J., Holmes, J., Donohue, S., Chambers, J., Meldrum, P., Wilkinson, P., Hendry, M. and Macciotta, R. 2021c. Protecting Canada's railway network using remote sensing technologies. Advances in Remote Sensing for Infrastructure, 26 Pages, Springer International Publishing, https://doi:10.36487/AGC_repo/2025_09

Intergovernmental Panel on Climate Change 2014. Working Group II Report: Climate Change 2014 Impacts, Adaptation and Vulnerability. IPCC 5th Assessment Report; https://www.archive.ipcc.ch/

Journault, J., Macciotta, R., Hendry, M., Charbonneau, F., Bobrowsky, P., Huntley, D., Bunce, C., and Edwards, T. 2016. Identification and quantification of concentrated movement zones within the Thompson River valley using satellite borne InSAR. Canadian Geotechnical Society, Proceedings Volume of GeoVancouver2016 Annual Meeting, 13 p.

Journault, J. Macciotta, R., Hendry, M., Charbonneau, F., Huntley, D. and Bobrowsky, P. 2018. Measuring displacements of the Thompson River valley landslides, south of Ashcroft, B.C., Canada, using satellite InSAR. Landslides. Volume 15 (4), pp. 621-636, DOI 10.1007/s10346-017-0900-1

Klassen, R. 1972. Wisconsin events and the Assiniboine and Qu'Appelle valleys of Manitoba and Saskatchewan. Canadian Journal of Earth Sciences, Vol. 9 (5), pp. 544-560

Knox, J.C. 2000. Sensitivity of modern and Holocene floods to climate change. Quaternary Science Reviews, Vol. 19, pp. 439-457

Lonergan, S. 2004. The human challenges of climate change (Chapter 3). In Coward, H. and Weaver, A.J. (editors); Hard Choices: climate change in Canada; Wilfred Laurier Press, 273 pages, ISBN 0-88920-442-X

Macciotta, R., Hendry, M., Martin, D., Elwood, D, Lan, H., Huntley, D., Bobrowsky, P., Sladen, W, Bunce C., Choi, E and Edwards, T. 2014. Monitoring of the Ripley Slide in the Thompson River Valley, B.C. Geohazards 6 Symposium, Proceedings Volume, Kingston, Ontario, Canada

Maynard, D., Weiland, I., Blais-Stevens, A. and Geertsema, M. 2017. Surficial geology, Hartley Bay, Douglas Channel area, British Columbia, parts of NTS 103-H/6 and 11. Geological Survey of Canada, Natural Resources Canada, https://doi.org/10.4095/299824

Mugridge, S-J. and Young, R. 1983. Disintegration of shale by cyclic wetting and drying and frost action. Canadian Journal of Earth Sciences, Vol. 20 (4), pp. 568-576

Resource Inventory Committee 1996. Terrain stability mapping in British Columbia: a review and suggested methods for landslide hazard and risk mapping. Resource Inventory Committee Publications, www.publications.gov.bc.ca (URL 2011)

Pon, A., Tomaszewicz, A., and Leighton, J. 2020. Monitoring of Thompson River Valley, BC, Canada. Geological Survey of Canada, Unpublished Technical Report and Supplementary Database, 61 p.

Porter, M., Savigny, K., Keegan, T., Bunce, C. and MacKay, C. 2002. Controls on stability of the Thompson River landslides. In: Proceedings of the 55th Canadian Geotechnical Conference: Ground and Water – Theory to Practice, Canadian Geotechnical Society, pp. 1393-1400

Samsonov, S.V., Feng, W. and Short, N. 2017. DInSAR products and applications for the RADARSAT Constellation Mission. Geomatics Canada, Open File 37, 19 p.

Sattler, K., Elwood, D., Hendry, M, Macciotta, R., Huntley, D., Bobrowsky, P. and Meldrum, P. 2018. Real-time monitoring of soil water content and suction in slow-moving landslide. GeoEdmonton 2018, Proceedings Paper, 8 p.

Sattler, K., Elwood, D., Hendry, M., Huntley, D., Holmes, J., and Wilkinson, P. 2020. Effect of pore-pressure dynamics on progressive failure in clay shale landslides. Landslides, 17 p.

Sauchyn, D.J. and Nelson, H.L. 1999. Origin and erosion of the Police Point landslide, Cypress Hills, Alberta. In Holocene climate and environmental change in the Palliser Triangle: a geoscientific context for evaluation the impacts of climate change on the southern Canadian prairies; Lemmen, D.S. and Vance, R.E. (editors); Geological Survey of Canada, Bulletin 534, 1999; pp. 257-265

Sauer, K. 1978. The engineering significance of glacier ice-thrusting. Canadian Geotechnical Journal, Vol. 15 (4), pp. 457-472

Schafer, M., Macciotta, R., Hendry, M., Martin, D., Bobrowsky, P., Huntley, D., Bunce, C. and Edwards, T. 2015. Instrumenting and Monitoring a Slow Moving Landslide. GeoQuebec 2015 Paper, 7 p.

Schetselaar, E., Harris, J., Lynds, T. and de Kemp, E. 2007. Remote Predictive Mapping 1. Remote Predictive Mapping (RPM): A Strategy for Geological Mapping of Canada's North. Geoscience Canada, Vol. 34 (3/4), pp 93-111

Smith, S.L. and Burgess, M.M. 2011. Permafrost and Climate Interactions. In Singh, V. P. and Singh, P. and Haritashya, U.K. (editors); Encyclopedia of Earth Sciences, Vol. 46, Pt. 15, pp. 852-857

Stanton, R.B. 1898. The great land-slides on the Canadian Pacific Railway in British Columbia. Proceedings of Civil Engineers, **132** (2), pp. 1–48

St. George., S. 2007. Stream flow in the Winnipeg River basin, Canada: trends, extremes and climate linkages. Journal of Hydrology, Vol. 332, pp. 396-411

Tappenden, K.M. 2016. Impact of Climate Variability on Landslide Activity in the Thompson River Valley Near Ashcroft, B.C. In: Proceedings of the 69th Canadian Geotechnical Conference, October 2-5, 2016, Vancouver, Canada

Valentin, C., Poesen, J. and Li, Y. 2005. Gully erosion: impacts, factors and control. Cantena; Vol. 63, pp. 132-153

Wang, B. and Lesage, K. 2007. Impact of climate change on slope stability in permafrost regions. Proceedings of the 8th International Symposium on Cold Region Development,11 p.

Weaver, A.J. 2004. The Science of Climate Change (Chapter 2). In Coward, H. and Weaver, A.J. (editors); Hard Choices: climate change in Canada; Wilfred Laurier Press, 273 pages, ISBN 0-88920-442-X

Wegmüller, U., Werner, C., Wiesmann, A. and Frey O. 2019. GAMMA, Version 1.6, computer software, Gamma Remote Sensing, Gumligen, http://www.gamma-rs.ch [URL 2020]

Wolfe, S.A. 1997. Impact of increased aridity on sand dune activity in the Canadian Prairies. Journal of Arid Environments, Vol. 36, pp. 421-432

Wolfe, S.A. 2001. Eolian activity. In A synthesis of geological hazards in Canada; Brooks, G R (ed.); Geological Survey of Canada, Bulletin 548, pp. 231-240, 1 sheet

Young, H. and Moore, P. 1994. Composition and depositional environment of the silicaceous Odanah Member (Campanian) of the Pierre Shale in Manitoba. Geological Society of America, Special Papers, Vol. 287, pp. 175-196

APPENDIX 1

Overview Timetable for Field Investigations (2020-2025)

Project activity (collaborators)	2020-2021	2021-2022	2022-2023	2023-2024	2024-2025
Terrain mapping [A, B, C] surficial geology, geophysics (GSC, BGS, MGS)	Image acquisition; Cloud storage and processing Maintenance	Image acquisition; Desktop mapping; ERT; Benchmarking	Image acquisition; Desktop mapping; ERT; Bathymetry; Benchmarking	Image acquisition; Desktop mapping; ERT; Bathymetry; Benchmarking	Decommissioning; Image acquisition; Desktop mapping
GNSS [A, B, C] fixed and mobile (GSC, UA, USASK, MGS)	Data acquisition; Cloud storage and processing; Maintenance	Data acquisition; Cloud storage and processing; Interpretation; Maintenance	Data acquisition; Cloud storage and processing; Interpretation; Maintenance	Data acquisition; Cloud storage and processing; Interpretation; Maintenance	Decommissioning; Cloud storage and processing; Interpretation
UAV overflights [A, B, C] (GSC, UA, USASK)	Data and software acquisition; Cloud storage and processing	Data acquisition; Cloud storage and processing; Interpretation	Data acquisition; Cloud storage and processing; Interpretation	Data acquisition; Cloud storage and processing; Interpretation	Decommissioning; Cloud storage and processing; Interpretation
InSAR* [A, B, C] data, scenes (CN, CPR, 3v Geomatics, CCMEO)	Corner reflectors acquisition; Data acquisition; Cloud storage and processing	Corner reflector installation; Data acquisition; Cloud storage and processing; Interpretation	Data acquisition; Cloud storage and processing; Interpretation	Data acquisition; Cloud storage and processing; Interpretation	Decommissioning; Cloud storage and processing; Interpretation
Climate station data [A, B, C] climate variables (GSC, MGS, USASK)	Data acquisition Cloud storage and processing Maintenance	Component acquisitions; Climate station installation; Data acquisition; Cloud storage and processing; Interpretation; Maintenance	Climate station installation; Data acquisition; Cloud storage and processing; Interpretation; Maintenance	Data acquisition; Cloud storage and processing; Interpretation; Maintenance	Decommissioning; Cloud storage and processing; Interpretation
Boreholes and soils* [A, B, C] Matric suction, piezometers, SSI, SAA (GSC, UA, USASK, MGS)	Soil monitoring acquisitions; Interpretation; Maintenance	Borehole drilling*; Borehole installations; Downhole geophysics Data acquisition; Cloud storage and processing; Interpretation; Maintenance	Borehole installations; Data acquisition; Cloud storage and processing; Interpretation Maintenance	Borehole installations; Data acquisition; Cloud storage and processing; Maintenance	Decommissioning; Cloud storage and processing; Interpretation
Publications geoscience outreach (GSC, UA, USASK, MGS)	Conference abstracts Open file / Annual report Workshop Presentation Proceedings paper Book chapters Journal papers	Conference abstracts Proceedings paper Open file / Annual report Workshop Presentation	Conference abstracts Proceedings paper Open file / Annual report Workshop Presentation	Conference abstracts Journal paper Open file / Annual report Workshop Presentation	Conference abstracts Journal paper Geoscience Map Open file / Annual report Workshop Presentation

*Expected that partners will contribute in-kind funding in support for selected activities. Superscript A – project activities in the Thompson River valley. Superscript B – project activities in the Assiniboine-Qu'Appelle river valleys. Beyond 2022, other research sites may be included in the study. Superscript C – project activities elsewhere (e.g., Kelowna, Kitimat-Terrace-Prince Rupert).

APPENDIX 2

Work Plan (2020-2025)

Fiscal Year 2020/21 Research Activities (IMOU-5170) **Project outputs:** Conference abstracts, Open file / Annual report, Workshop presentation, Book chapters, Proceedings papers, Journal papers
ACTIVITY GROUP 1: Geohazard Mapping and Borehole Studies **Terrain mapping and fieldwork:** Logistical support for ground-truth fieldwork in Thompson River Valley (TRV) and Assiniboine River Valley (ARV); GNSS surveys; PRIME; Desktop mapping; Benchmarking DSMs (in-kind support by British Geological Survey - BGS, Manitoba Geological Survey - MGS) **Borehole and soil studies**: Procurement of soil sampling equipment and moisture sensors; Logistical support for fieldwork, workshops and conferences (in-kind support by CN, CP, University of Alberta - UA, University of Saskatchewan - USASK)
ACTIVITY GROUP 2: **Change detection with InSAR, GNSS, UAVs and Weather Stations** **InSAR monitoring**: Procurement of InSAR corner reflectors and supporting equipment for installation; Acquisition of (multispectral/hyperspectral) satellite imagery in TRV, processing, analyses and archiving; Logistical support for ground-truthing in TRV, workshops and conferences (in-kind support by 3vGEOMATICS - 3vG, Canada Centre for Mapping and Earth Observation - CCMEO) **GNSS monitoring**: Procurement of Geocube components from Ophelia (France) and GNSS components and software for in-house system; Logistical support for systems maintenance, fieldwork (TRV and ARV), workshops and conferences (in-kind support by CN, CP, UA, USASK, MGS) **UAV change detection**: Procurement of UAVs, software, components enabling high-resolution RGB, LiDAR and multispectral inventories; GigaPAN photogrammetry; Logistical supporting for fieldwork (TRV and ARV), workshops, conferences (in-kind support by CN, CP, UA, USASK, MGS) **Monitoring climate change variables**: Logistical support for routine maintenance of equipment, replacement and new units, replacing and augmentation of power sources, data storage enhancements with remote access to data transfer (TRV and ARV); logistical support for workshops and conferences (in-kind support by CN, CP, UA, USASK)

Fiscal Year 2021/22 Research Activities (IMOU-5170)

Project outputs: Conference abstracts, Open file / Annual report, Workshop presentation, Book chapters, Proceedings papers, Journal papers

ACTIVITY GROUP 1: Geohazard Mapping and Borehole Studies

Terrain mapping and fieldwork: Logistical support for ground-truth fieldwork in TRV, ARV, Okanagan valley (OKV) and Kitimat-Terrace-Prince Rupert (KTP); GNSS surveys; Sample analyses; Desktop mapping; ERT, Benchmarking; Cloud storage and processing (in-kind support by BGS, MGS)

Borehole studies and soil studies: Procurement of borehole inclinometers and piezometers for observation wells at CN and CP sites in TRV and ARV; Logistical support for workshops and conferences (in-kind support by CN, CP, UA, USASK)

ACTIVITY GROUP 2:
Change detection with InSAR, GNSS, UAVs and Weather Stations

InSAR monitoring: Processing, analyses, archiving and interpretation of satellite imagery in TRV, ARV, OKV and KTP; procurement of satellite imagery (multispectral) and InSAR corner reflectors; Logistical support for ground-truthing in TRV, ARV, OKV and KTP; Cloud storage and processing; Logistical support for workshops and conferences (in-kind support by 3vG, CCMEO)

GNSS monitoring: Data acquisition; Cloud storage and processing; Logistical support for systems maintenance, fieldwork (TRV, ARV, OKV and KTP); Logistical support for workshops and conferences (in-kind support by CN, CP, UA, USASK, MGS)

UAV change detection and Sky Canoe testing: Procurement of UAV software, components enabling NIR, LiDAR and multispectral inventories; Logistical supporting for fieldwork (TRV, ARV, OKV and KTP); Cloud storage and processing; Interpretation; logistical support for workshops and conferences (in-kind support by CN, CP, UA, USASK, MGS)

Monitoring climate change variables: Procurement of climate monitoring station (air pressure, temperature, rain gauge, snow sensor, anemometer and wind vane, insolation), moisture meters, piezometers, supporting hardware, software, data loggers, batteries, solar panels and data communication components; Logistical support for routine maintenance of equipment, replacement and new units, replacing and augmentation of power sources, data storage enhancements with remote access to data transfer (TRV, ARV, OKV and KTP); logistical support for workshops and conferences (in-kind support by CN, CP, UA, USASK)

Fiscal Year 2022/23 Research Activities (IMOU-5170) **Project outputs:** Conference abstracts, Open file / Annual report, Workshop presentation, Book chapters, Proceedings papers, Journal papers
ACTIVITY GROUP 1: Geohazard Mapping and Borehole Studies **Terrain mapping and fieldwork:** Logistical support for ground-truth fieldwork in TRV, ARV, OKV and KTP; GNSS surveys; sample analyses, desktop mapping; ERT, Seismic; Bathymetry; Benchmarking; Cloud storage and processing (in-kind support by BGS, MGS) **Borehole and soil studies**: Maintenance or borehole inclinometers and piezometers, installation, data acquisition, downhole geophysics, sample analyses, and monitoring of observation wells at CN and CP sites in TRV, ARV, OKV and KTP; Cloud storage and processing; Interpretation; Logistical support for workshops and conferences (in-kind support by CN, CP, UA, USASK)
ACTIVITY GROUP 2: **Change detection with InSAR, GNSS, UAVs and Weather Stations** **InSAR monitoring**: Processing, analyses, archiving and interpretation of satellite imagery in TRV and ARV; Logistical support for ground-truthing in TRV, ARV, OKV and KTP; cloud storage and processing; Logistical support for workshops and conferences (in-kind support by 3vG, CCMEO) **GNSS monitoring**: Data acquisition; Cloud storage and processing; Logistical support for systems maintenance, fieldwork (TRV, ARV, OKV and KTP); Logistical support for workshops and conferences (in-kind support by CN, CP, UA, USASK, MGS) **UAV change detection**: RGB, NIR, LiDAR and multispectral data acquisition; Logistical supporting for fieldwork (TRV, ARV, OKV and KTP); Cloud storage and processing; Interpretation; Logistical support for workshops and conferences (in-kind support by CN, CP, UA, USASK, MGS) **Monitoring climate change variables**: Installation of weather station (air pressure, temperature, rain gauge, snow sensor, anemometer and wind vane; insolation), moisture meters, piezometers, supporting hardware, software, data loggers, batteries, solar panels and data communication components; Logistical support for routine maintenance of equipment, replacement and new units, replacing and augmentation of power sources, data storage enhancements with remote access to data transfer (TRV, ARV, OKV and KTP); Cloud storage and processing; Interpretation; Logistical support for workshops and conferences (in-kind support by CN, CP, UA, USASK)

Fiscal Year 2023/24 Research Activities (IMOU-5170)

Project outputs: Conference abstracts, Open file / Annual report, Workshop presentation, Book chapters, Proceedings papers, Journal papers

ACTIVITY GROUP 1: Geohazard Mapping and Borehole Studies

Terrain mapping and fieldwork: Logistical support for ground-truth fieldwork in TRV, ARV, OKV and KTP; GNSS surveys; sample analyses, desktop mapping; ERT, Seismic; Bathymetry; Benchmarking; Cloud storage and processing (in-kind support by BGS, MGS)

Borehole and soil studies: Maintenance or borehole inclinometers and piezometers, data acquisition at CN and CP sites in TRV, ARV, OKV and KTP; Cloud storage and processing, Interpretation; Logistical support for workshops and conferences (in-kind support by CN, CP, UA, USASK)

**ACTIVITY GROUP 2:
Change detection with InSAR, GNSS, UAVs and Weather Stations**

InSAR monitoring: Processing, analyses, archiving and interpretation of satellite imagery in TRV and ARV; Logistical support for ground-truthing in TRV, ARV, OKV and KTP; Cloud storage and processing; Logistical support for workshops and conferences (in-kind support by 3vG, CCMEO)

GNSS monitoring: Data acquisition; cloud storage and processing; Logistical support for systems maintenance, fieldwork (TRV, ARV, OKV and KTP); Logistical support for workshops and conferences (in-kind support by CN, CP, UA, USASK, MGS)

UAV change detection: RGB, NIR, LiDAR and multispectral data acquisition; Logistical supporting for fieldwork (TRV, ARV, OKV and KTP); Cloud storage and processing; Interpretation; logistical support for workshops and conferences (in-kind support by CN, CP, UA, USASK, MGS)

Monitoring climate change variables: Data acquisition (air pressure, temperature, rain gauge, snow sensor, anemometer and wind vane, insolation, moisture meters, piezometers); logistical support for routine maintenance of equipment (TRV, ARV, OKV and KTP); Cloud storage and processing; Interpretation; Logistical support for workshops and conferences (in-kind support by CN, CP, UA, USASK, MGS)

Fiscal Year 2024/25 Research Activities (IMOU-5170)
Project outputs: Conference abstracts, Open file / Annual report, Workshop presentation, Book chapters, Proceedings papers, Journal papers
ACTIVITY GROUP 1: Geohazard Mapping and Borehole Studies **Terrain mapping and fieldwork:** Logistical support for decommissioning installations; Desktop mapping; Cloud storage and processing (in-kind support by BGS, MGS) **Borehole and soil studies**: Maintenance and decommissioning of borehole inclinometers and piezometers, data acquisition at CN and CP sites in TRV, ARV, OKV and KTP; Cloud storage and processing; Interpretation; logistical support for workshops and conferences (in-kind support by CN, CP, UA, USASK)
ACTIVITY GROUP 2: **Change detection with InSAR, GNSS, UAVs and Weather Stations** **InSAR monitoring**: Archiving and interpretation of satellite imagery in TRV and ARV; cloud storage and processing; logistical support for workshops and conferences (in-kind support by 3vG, CCMEO) **GNSS monitoring**: Logistical support for decommissioning GNSS installations (TRV, ARV, OKV and KTP); Cloud storage and processing; Logistical support for systems maintenance and decommissioning fieldwork (TRV, ARV, OKV and KTP); Logistical support for workshops and conferences (in-kind support by CN, CP, UA, USASK, MGS) **UAV change detection**: RGB, NIR, LiDAR and multispectral data acquisition; Logistical supporting for fieldwork (TRV, ARV, OKV and KTP); Cloud storage and processing; Interpretation; Logistical support for workshops and conferences (in-kind support by CN, CP, UA, USASK, MGS) **Monitoring climate change variables**: Logistical support for decommissioning weather stations, moisture meters, piezometers (TRV, ARV, OKV and KTP); Cloud storage and processing; Interpretation; Logistical support for workshops and conferences (in-kind support by CN, CP, UA, USASK, MGS)

APPENDIX 3

List of Key Acronyms in Open File Report

BC	British Columbia
BGS	British Geological Survey
BVLOS	Beyond Visual Line of Sight
CN	Canadian National Railways
CP	Canadian Pacific Railways
DEM	Digital Elevation Model
DInSAR	Differential Interferometric Synthetic Aperture Radar
DSM	Digital Surface Model
GCP	Ground Control Point
GPS	Global Positioning System
GSC	Geological Survey of Canada
ICL	International Consortium on Landslides
IMOU	Inter-Departmental Memorandum of Understanding
InSAR	Interferometric Synthetic Aperture Radar
IPL	International Program on Landslides
IUGS	International Union of Geological Sciences
LiDAR	Light Detection and Ranging
LoS	Line of Sight
MN	Manitoba
NRCAN	Natural Resources Canada
PRIME	Proactive Infrastructure Monitoring and Evaluation
RCM	Radarsat Constellation Mission
RGHRP	Railway Ground Hazard Research Program
RPAS	Remote Piloted Aircraft Systems
RPM	Remote Predictive Mapping
RS2	Radarsat 2
RTK-GNSS	Real Time Kinematic Global Navigation Satellite System
SAR	Synthetic Aperture Radar
S1	Sentinel 1

SFM	Structure from Motion
SK	Saskatchewan
SRTM	Shuttle Radar Topographic Mission
TC-IC	Transport Canada Innovation Centre
UA	University of Alberta
UAV	Unoccupied Aerial Vehicle
USASK	University of Saskatchewan
VTOL	Vertical Take Off and Landing